

Optimizing oncolytic adenoviruses for treatment of cholangiocarcinoma.

A research dissertation submitted by

Yi-Hsuan, Chen



A thesis submitted to the University of Birmingham for the degree of MRes in Cancer Sciences.

School of Cancer Research

College of Medical and Dental Sciences

University of Birmingham

Submitted: August 2014

This project was carried out at: University of Birmingham School of Cancer Research and Institute of Biomedical Research

Under the supervision of: Dr. Peter F. Searle and Dr. Simon C. Afford

UNIVERSITY OF
BIRMINGHAM

University of Birmingham Research Archive

e-theses repository

This unpublished thesis/dissertation is copyright of the author and/or third parties. The intellectual property rights of the author or third parties in respect of this work are as defined by The Copyright Designs and Patents Act 1988 or as modified by any successor legislation.

Any use made of information contained in this thesis/dissertation must be in accordance with that legislation and must be properly acknowledged. Further distribution or reproduction in any format is prohibited without the permission of the copyright holder.

Abstract

Oncolytic adenoviruses offer a promising new treatment for cancers, especially those which respond poorly to current therapies such as cholangiocarcinoma. However, for clinical use, high selectivity to cancers is required. Thus, I constructed two EGFP-reporter gene expressing viruses, hTERTp-E1AWT-EGFP and E2Fp-E1A Δ 24-EGFP to allow the comparison with an existing WTp-E1A Δ 24-EGFP virus. These viruses were compared for their ability to infect and replicate in two cholangiocarcinoma cell lines, CCLP1 and CCSW1 cells.

Flow cytometry was used to monitor EGFP expression by the replicating viruses. In these experiments, the virus WTp-E1A Δ 24 (virus B) reproducibly showed the greatest EGFP expression at equivalent multiplicity of infection. This replication efficacy was also confirmed in qPCR experiments measuring viral genome copy number. In cell viability assays, the hTERTp-E1AWT virus (virus A) was less potent than either E2Fp-E1A Δ 24 (virus C) or WTp-E1A Δ 24 (virus B), which had similar oncolytic potency.

I also compared the ability of replication-defective adenoviruses expressing EGFP and a range of alternative fibre proteins to infect the cholangiocarcinoma cell lines. Fibre proteins incorporating the knob domain from adenovirus type 3, or including the A20-RGD (arginine, glycine and aspartate)-containing peptide from foot and mouth disease virus, showed significantly improved infectivity. These data will assist in the development of improved oncolytic viruses for treatment of cholangiocarcinoma.

Acknowledgement

Special thanks goes to my supervisors: Peter F. Searle and Simon C. Afford for generous and patient guidance in many aspects, including experimental and written part of this project, Elizabeth Humphreys for kind assistances with laboratory techniques, Claire Shannon-Lowe for warm guidance with flow cytometry, Maha Ibrahim for generous support with microscopy, and my colleagues, Stamatis Karakonstantis and William Marshall for their help in this project.

Table of contents

1. Introduction	1
1.1 Brief introduction to Cholangiocarcinoma	1
Cholangiocarcinoma (bile duct cancer)	1
Hepatobiliary cancers.....	2
1.2 Brief introduction to Current treatment.....	2
Curative surgery resection	2
Transplantation	3
Radiotherapy.....	4
Chemotherapeutic system therapy.....	4
Targeted therapy.....	5
Summary and analysis of therapies	5
1.3 Novel treatment	5
Oncolytic virus.....	5
Oncolytic viruses induce immunogenic cell death	7
Types of oncolytic viruses	8
Adenovirus	12
CD40 ligand (CD40L/CD154).....	27
Aim of project	29
2. Materials and methods.....	30
2.1 Construct	30
Homologous recombination	30
Selective cassette: positive selection and negative selection	31
Digestion and ligation.....	33
2.2 Plasmid miniprep, bulkprep, gel purification	34
2.3 Cell culture.....	35
2.4 Adenovirus.....	37
2.4.1 Virus prep.....	38
2.4.2 Hexon staining (performed by Stamatis Karakonstantis)	39
2.4.3 Infection.....	40
2.4.4 Harvest (for FACs experiments).....	41
2.5 Flow cytometry.....	42
2.6 Quantitative polymerase chain reaction (qPCR)	42
2.7 MTT assay.....	43

2.8 Immunohistochemistry (performed by Elizabeth Humphreys, William Marshall, and Florence Chen)	44
2.9 Graph plotting and statistical analysis.....	46
3. Results	47
3.1 Gene construction of plasmid	47
3.2 Time-course experiment	52
3.3 Infection experiment (flow cytometry)	57
3.3.1 Replication competent (RC) viruses.....	57
3.3.2 Replication defective (RD) viruses	60
3.4 Infection experiment (qPCR)	65
3.5 Cell viability assay	68
3.5.1 Oncolytic effects of viruses in human cells (HEK293, CCLP, CCSW).....	68
3.5.2 Coinfection experiment	78
3.6 Immunohistochemistry (IHC)	81
4. Discussion-Is it a promising treatment?.....	93
96h time course experiment	95
Time course experiment	96
qPCR	97
MTT assays	98
MTT assays—CD40L virus co-infection.....	99
Immunohistochemistry (IHC)	102
Summary	102
Future work.....	103
Appendix.....	A1

1. Introduction

My project is about delivering oncolytic viruses for cholangiocarcinoma. In this introduction, I therefore begin with an overview of cholangiocarcinoma and its current treatments. I then provide an introduction to oncolytic viruses, and the types of modifications to them that were investigated in this project.

1.1 Brief introduction to Cholangiocarcinoma

Cholangiocarcinoma (bile duct cancer)

Bile ducts can be defined as the channels that transport bile from the liver to the duodenum: the upper part starting from the liver to the gallbladder is named the hepatic duct, while the one starting from the gallbladder and ending in duodenum is named the extra-hepatic (bile) duct. The former (hepatic duct) is generally recognized as part of the liver (contributing to hepatobiliary cancers); the latter is considered as part of gastrointestinal system (GI cancers).

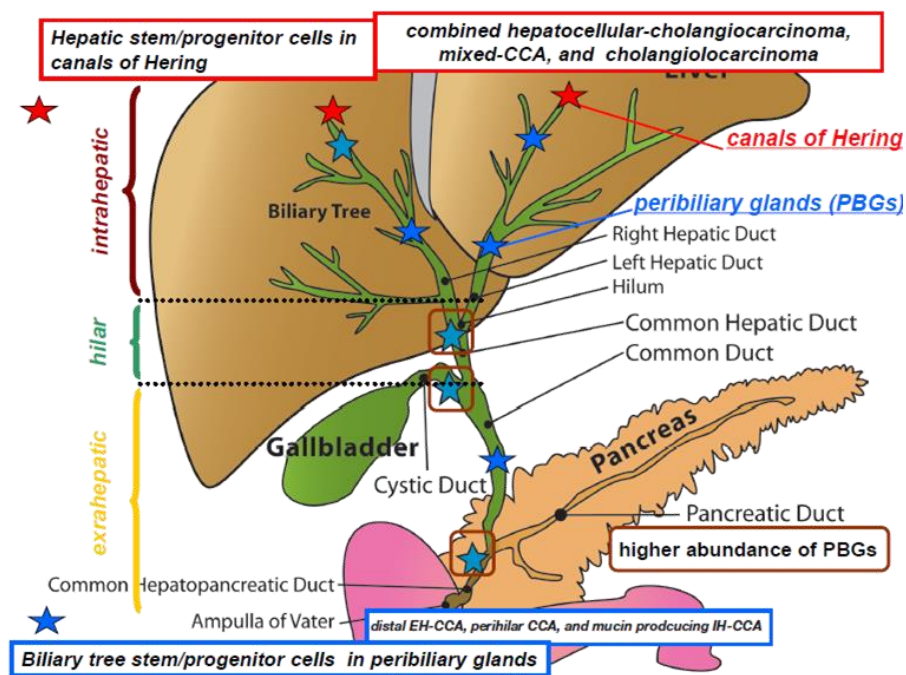


Figure 1. A schematic presentation of the anatomical structure of the liver, the gallbladder and the bile ducts. The bile ducts are basically divided into intrahepatic bile ducts, hilar bile ducts and extrahepatic bile ducts. The blue stars indicate the candidate stem cell niches in peribiliary glands (PBGs) which secrete the bile. The red star marks the candidate stem cell niches in the canals of hering/interlobular bile ducts (Cardinale et al., 2013).

Hepatobiliary cancers

Hepatobiliary Cancers are one of the top 10 commonest and deadliest cancers, which account for 5.8% among all the cancer types (World Cancer Research Fund International, WCRF). In the cases of hepatobiliary cancers, the commonest type is liver tumour (especially Hepatocellular carcinomas, HCC), and the second is bile duct cholangiocarcinoma (CC). Even though cholangiocarcinoma may be considered a relatively rare cancer, only accounting for about 3% of gastrointestinal cancers, it is the second commonest primary hepatic cancer.

Cholangiocarcinoma can be divided into 3 subclasses: **Intrahepatic cholangiocarcinoma** includes the biliary tree and right hepatic duct and left hepatic duct, **Hilar/perihilar cholangiocarcinoma** involves in hilum, common hepatic duct and part of cystic duct to gallbladder, and **Extrahepatic cholangiocarcinoma** that includes gallbladder and common bile duct.

1.2 Brief introduction to Current treatment

Curative surgery resection

Generally speaking, surgical resection represents the major curative treatment for cholangiocarcinoma, especially for the type of cholangiocarcinoma without primary sclerosing cholangitis (Malhi and Gores, 2006). For primary sclerosing cholangitis cholangiocarcinomas, liver transplantation is recommended. In the case of intrahepatic cholangiocarcinoma, surgical resection is recommended;

usually, the operation includes removing the part of the liver containing the cancerous bile ducts and a surrounding cancer-free margin. The 5 year survival rate of patients who accepted hepatic lobectomy or segmentectomy, ranges from 27% to 48% (Malhi and Gores, 2006). Technically, only half of them survive from cholangiocarcinoma. With the resection of 1st stage cholangiocarcinoma, the 5 years survival rate of intrahepatic cholangiocarcinoma is 31-63%. The mortality rate of resection is 5-10% in general, mainly due to infections or liver failure.

As a hope, the aim of using neo-adjuvant treatment is to increase resectability rates and decrease recurrence rate after resection. The neo-adjuvant treatments include chemotherapy, radiotherapy and radiochemotherapy.

Transplantation

Compared to extrahepatic cholangiocarcinoma and hilar cholangiocarcinoma, the transplantation treatment to intrahepatic cholangiocarcinoma is concomitant with a dramatic increase in disease recurrence rate, so this treatment cannot be recommended (Blechacz and Gores, 2008). However, there was a strategy described by De Vreede and his colleagues (De Vreede et al., 2000). They treated the extrahepatic cholangiocarcinoma patients with radiotherapy plus chemotherapy before liver transplantation, and this idea gained a huge success, which made recurrence rate decrease to 12% (from 51-59%) and 5 year survival rate increase up to 58-81% (from 23-26%). Hopefully, this strategy can be used in intrahepatic cholangiocarcinoma one day (De Vreede et al., 2000).

Radiotherapy

Radiotherapy is another technology for ablation of cancerous tissue, the applications including radiotherapy, radiofrequency ablation and transcatheter ablation. There are two major modalities for treatment of cholangiocarcinoma: one is external beam radiotherapy, and the other is intraluminal iridium 192 brachytherapy (Blechacz and Gores, 2008). Even though radiotherapy has proven effective for a minor group of cholangiocarcinoma patients, the radiation causes severe side effects, such as gastrointestinal bleeding, strictures, small bowel obstruction and hepatic decompensation. As a result, radiotherapy has only a minor role in treatment of cholangiocarcinoma (Blechacz and Gores, 2008).

Chemotherapeutic system therapy

Chemotherapy may be the first-line treatment for other types of cancer, but in cholangiocarcinoma, there are no qualified clinical studies to support the benefit of chemotherapies. Thus, the effect of chemotherapy in cholangiocarcinoma remains unclear. As one of the commonest studied chemotherapeutic agents 5-fluorouracil (5-FU) is introduced as mono-therapy or in combination with other agents such as doxorubicin, epirubicin, cisplatin, lomustine, mitomycin C, and paclitaxel. More and more new research focuses on gemcitabine, which gained approval for cholangiocarcinoma in 2006. It can be used as mono-therapeutic agent or combined with cisplatin, oxaliplatin, docetaxel, mitomycin C and 5-FU/leukovorin which is reported to provide a 60% response rate. However, there is not enough evidence to support gemcitabine as a good therapeutic agent (Blechacz and Gores, 2008).

Targeted therapy

Although a few agents have been proven efficient (Jimeno et al., 2005, Wiedmann et al., 2006), targeted therapy is still a treatment for the future. The potential treatments might include IL6, blocking of Mcl-1 expression and apoptosis-inducing ligand (TRAIL), but all of them are still in lab stage so far.

Summary and analysis of therapies

To sum up, for intrahepatic cholangiocarcinoma, the only cure or most efficient treatment is traditional surgical resection. However, to the patients with non-resectable cholangiocarcinoma, it is not good news at all. Although there are other alternative therapies, like radiotherapy, systemic chemotherapy, targeted chemotherapy, which may be the first-line treatments in other types of human cancer, they are not very efficient in cholangiocarcinoma. Hence, there is an urgent need to develop alternative treatments, and oncolytic viruses offer a promising new approach that merits investigation.

1.3 Novel treatment

Oncolytic virus

Oncolytic viruses are a type of gene therapy or virotherapy, which have recently attracted much interest as a promising cancer treatment, especially after the first oncolytic virotherapy (H101) was approved in China in 2005. In 2012, J. W. Choi et al summarized the reasons why oncolytic viruses offer an exciting novel approach. First of all, these viruses can be genetically manipulated, and they have the ability to trigger multiple anti-tumour pathways simultaneously. Second, oncolytic viruses use a totally different anti-tumour strategy, they can directly kill the cancer cells at the end of the lytic cycle and spread progeny

viruses to other uninfected tumour cells, killing the cell. Third, apart from direct oncolysis, oncolytic virus can also be “armed” with other anti-tumour molecules, this next generation oncolytic virus expanding the potential of anti-tumour treatments. Fourth, if the virus is well controlled or highly specific to tumour cells, there may be relatively minor side effects from oncolytic virotherapy. (Choi et al., 2012)

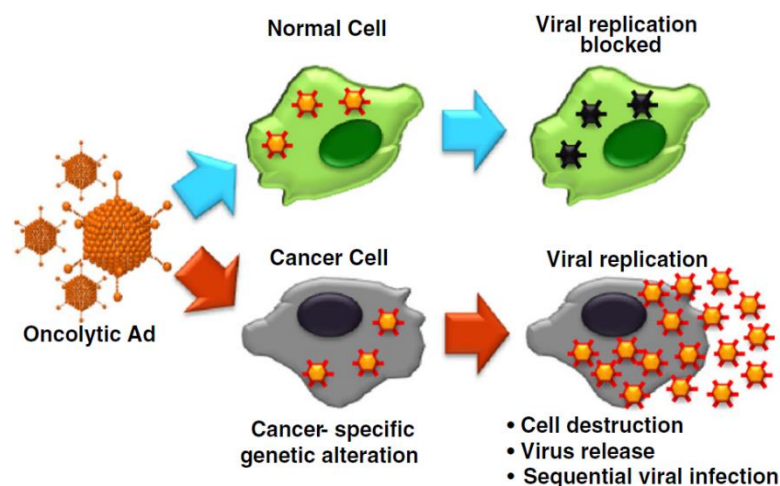


Figure 2. A scheme of the function for selective oncolytic adenovirus

Oncolytic viruses selectively replicate in cancer cells because of genetically engineered dependence on tumour cell functions. Even though the oncolytic viruses gain entry to normal cells, the viral replication is prevented (Choi et al., 2012).

There are three major anti-tumour mechanisms for oncolytic viruses. The first is direct oncolysis of cancer cells by the virus. This mechanism relies on the lytic cycle of the virus, which kills the host cell and releases progeny virus particles to infect surrounding tumour cells. In most cases, this pathway includes apoptosis, necrosis, pyroptosis and autophagic cell death (Bartlett et al., 2013). Second, oncolytic viruses affect the microenvironment around tumour cells, causing apoptosis and necrosis of non-virus infected cells by inhibiting angiogenesis and vasculature (Bartlett et al., 2013). Thirdly, oncolytic

viruses trigger innate and adaptive immune responses, including tumour-specific immune responses. This antitumour immunity increases the cytotoxicity to un-infected cancer cells not only in primary site but also in metastatic nodules (Bartlett et al., 2013).

Oncolytic viruses induce immunogenic cell death

Cell death may be immunogenic or non-immunogenic. Apoptosis was initially considered as non-immunogenic and non-inflammatory because there is no cytokine damage-associated molecular patterns (DAMPs) or inflammatory factor released. However, immunogenic forms of apoptosis, with release of DAMPs and inflammatory signals have subsequently been recognised. Other forms of immunogenic cell death (ICD) include autophagic cell death, necrosis, pyroptosis and secondary necrosis (Bartlett et al., 2013).

Necrosis, pyroptosis and autophagic cell death release pro-inflammatory cytokines. Necrosis results in DAMP release, and in autophagic cell death, the dying cell also releases DAMPs. Pyroptosis, induced by pathogens, has the ability to release cytokine and DAMPs, resulting in inflammation response (Bartlett et al., 2013).

Table 1. Types of immunogenic cell death (Bartlett et al., 2013)

Type of cell death	Immunogenicity
Apoptosis (type 1 cell death)	Some forms of apoptosis are non-immunologic, while others are immunogenic. The pre-apoptotic surface exposure of calreticulin (CRT) and heat shock protein (HSP) 70 and heat shock protein 90 may have a profound impact on the immune response. In addition, the release of high-mobility group protein B1 (HMGB1) during late apoptosis promotes antigen processing by dendritic cells (DC) and hence contributes to cytotoxic T-cell activation.
Autophagic cell death (ACD; type 2 cell death)	High. It may release DAMPs (HMGB1, ATP, and others) and elicit substantial inflammation.
Necrosis (type 3 cell death)	High. This causes release of DAMPs and elicits substantial inflammation and affects local environment.
Pyroptosis (or caspase 1-dependent cell death)	High. It is a highly inflammatory form of cell death due to cytokine release and escape of cytoplasmic contents (DAMPs). However, some pathogens encode immunosuppressive proteins.
Secondary necrosis	High. It is quite immunogenic due to necrosis occurring in apoptotic cells at the late stage.

Types of oncolytic viruses

There are four categories of oncolytic viruses: Firstly, viruses that are intrinsically tumour-selective. These viruses have natural anti-tumour ability, such as reovirus and Newcastle disease virus (NDV), both of which have been used in clinical trials (Lal et al., 2009, Reichard et al., 1992). The second category is the type which generates the selectivity and anti-tumour efficacy by deleting specific genes from virus. For instance, similar to the first approved H101 oncolytic virus in the world, Onyx-015 gained its selectivity by deleting the E1B 55k gene (Khuri et al., 2000).

Onyx-015 also has an E3B deletion which removes the gp19k gene which blocks MHC class-I antigen presentation on cell surface (Ries and Korn, 2002, Wold et al., 1994). Removing this gene accelerates the immune clearance of viruses and infected cells by cytotoxic T-lymphocytes (CTLs) (Scaria et al., 2000, Nemunaitis et al., 2007).

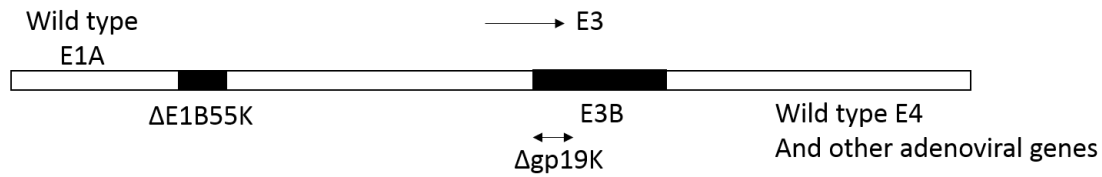


Figure 3. A scheme of Onyx-015 genome map

Onyx-015 virus contains two gene deletions; one is E1B55K, and the other is E3B. The deletion of E3B includes an important gp19K gene which deals with the antigen presentation on MHC class-I molecules. Removing this gene improves the host immune response to clear the virus and virus infected cells. This diagram is adapted from Zhan et al. (2005).

In order to explain the principle of E1B-55k deletion, we can start from the mechanism of p53. p53 is a tumour suppressor protein which is mutated in about 50% of all human cancers (Nemunaitis et al., 2000), while E1B-55k is an onco-protein. p53 can induce either cell cycle arrest at G1 phase through cyclin-dependent kinase inhibitor p21/WAF1/Cip1 (Nemunaitis et al., 2000), or cell apoptosis through *bax-1* pathway (Nemunaitis et al., 2000).

E1B-55k protein has multiple functions. One of them is to counteract an effect of E1A function which stabilizes p53 protein, which could induce cell apoptosis (Harada and Berk, 1999). E1B-55k can bind with p53 directly (Heise et al., 1997), inhibiting the transactivation function of p53 protein (Harada and Berk, 1999, O'Shea et al., 2004). In this case, E1B-55k protein acts as a general repressor of RNA polymerase II transcription, directly toward p53-activated promoters (Martin and Berk, 1998). E1B-55k inhibits transcription of these genes simply by binding with p53 protein, which regulates the general transcriptional machinery directly or through modification of chromatin (Martin and Berk, 1998). Thus, E1B-55k blocks E1A induced apoptosis by repressing p53 responsive promoters (Harada and Berk, 1999). E1B-55k protein also

shortens the half-life of p53 to reduce p53 protein expression levels (Harada and Berk, 1999). E1B-55k protein and E4-orf6 protein are the only two viral proteins required to destabilize p53 protein and accelerate p53 degradation (Harada and Berk, 1999, O'Shea et al., 2004).

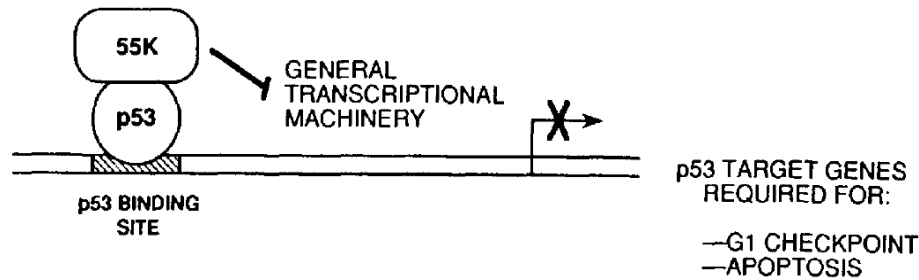


Figure 4. A scheme of E1B55k protein, p53 protein and p53 inducible gene regulation

p53 activated genes are required in G1 checkpoint during cell cycle and in apoptosis which needs p53 protein action as a transcription inducer. If E1B55k protein binds with p53 protein-p53 activated promoter complex, the transcriptional mechanism is blocked. Thus, normal human cells get the ability to overcome G1 checkpoint and inhibit apoptosis, leading to epithelial mesenchymal transition (Yew et al., 1994).

To sum up, E1B-55k protein is responsible for p53 binding and inactivation (Nemunaitis et al., 2000). Thus, an E1B-55k mutated virus is unable to suppress the function of p53 protein in normal cells, so that the oncolytic virus is unable to replicate in normal human cells (Nemunaitis et al., 2000). In contrast, cancer cells are lack of p53 protein, so that E1B-55k mutated virus prefers to replicate in cancer cells rather than in normal cells, in which the function of E1B-55k protein is not required (Harada and Berk, 1999). However, despite the appealing logic of this regulatory mechanism a later study concluded that it was another function of E1B-55k protein in the nuclear export of late viral RNAs that accounted for the tumour-selectivity of the Onyx-015 virus (O'Shea et al., 2004).

This type of oncolytic viruses is known as first generation of virotherapy. The strategy of this type of virus is deleting the required gene for the virus to replicate in normal cells but not in tumour cells. As a result, the virus gains its high selectivity to tumour cells (Khuri et al., 2000).

In this project, this class of virus was represented by adenoviruses with E1A Δ 24, in which the pRb binding site in the E1A protein (922nd to 947th bp of the Ad5 genome) was removed to increase the selectivity to tumour cells (Heise C, 2000).

The third type of oncolytic virus uses tumour cell-specific promoters to generate tumour selectivity in oncolytic virus, which is another of the strategies relevant to this project. The final approach to provide tumour-selectivity involves pseudotyped virus. Alterations of the fibre protein of adenovirus can allow binding to alternative receptors on the cell surface, which can provide a degree of tumour-selectivity of cell entry if the receptors are up-regulated on cancer cells. This strategy was also investigated in this project.

Table 2. Types and examples of oncolytic virus (Liu and Kirn, 2008)

Approach to selectivity	Examples and genetic alterations within virus	Genetic target(s) in tumors
Type 1: Inherently tumour-selective species	Newcastle Disease Virus (none) Reovirus (none)	IFN resistance Ras pathway
Type 2: Deletion of viral gene that is necessary for replication in normal cells, but expendable in tumour cells	Onyx-015 (E1B-55K-/E3B-deleted Ad) Delta-24 (E1A-CR2-deleted Ad) JX-594 (TK-deleted VV)	Loss of p53 pathway, late mRNA transport Loss of G1-S checkpoint control; loss of pRB function Proliferation
Type 3: Tumour-/tissue-specific promoter engineering to limit viral gene expression	CG7870 (E1A under rat probasin promoter, E1B under PSA promoter/enhancer Ad)	Prostate cancer
Type 4: Pseudotyped viruses	CAR/integrin-binding deleted Ad, replaced with tumour-targeting ligand	Tumour-specific receptor

Adenovirus

The adenovirus (AdV) has a non-enveloped icosahedral capsid of 100nm in diameter and a linear, double-stranded DNA genome about 36kb in length (Rosewell et al., 2011). The human adenovirus family has been divided into 6 classes, from A to F (Glasgow et al., 2006). Among all the serotypes of adenovirus, the most common type is serotype 5 (Ad5) of subgroup C which is widely used in gene therapies. The genome of Ad5 is flanked by cis-acting inverted terminal repeats (ITRs), and these ITRs are needed during viral DNA replication (Rosewell et al., 2011). Moreover, a cis-acting packaging signal (Ψ), located behind the left ITR, is required for packing viral genome into virion capsids (Rosewell et al., 2011).

Early transcription units are expressed before viral DNA replication, and E1A transcription unit is the first one to be transcribed after virus infection (Rosewell et al., 2011). E1A mRNA encodes two E1A proteins which function both to regulate viral transcription and stimulate the host cell to enter S phase (Rosewell et al., 2011). E1B transcription unit translates into two E1B proteins that are required to block host mRNA transportation, stimulate viral mRNA transportation, and block E1A-induced apoptosis (Rosewell et al., 2011).

The E2 region are divided into E2a and E2b sub-regions; E2a encodes 72kD DNA binding protein, whereas E2b translates into viral DNA polymerase and terminal protein precursor (pTP) (Rosewell et al., 2011). The E3 region is non-essential for adenovirus growth in cell culture; this region encodes seven proteins, and most are involved in evasion of host immune defences, such as cytotoxic T-lymphocytes (CTLs) mediated immune responses (Rosewell et al., 2011). The E4 region encodes more than six proteins, and their functions vary

from facilitating DNA replication, enhancing late gene expression, and decreasing host protein synthesis (Rosewell et al., 2011).

All the late mRNAs come from the same transcript expressed from the major late promoter (MLP), and most of these mRNAs encode structural proteins, including viral hexon, penton and fibre (Rosewell et al., 2011). A minor group of spliced RNAs encode additional protein (pIIIa, IVa2, VAI, VAII) with either structural or non-structural functions (Rosewell et al., 2011, Glasgow et al., 2006).

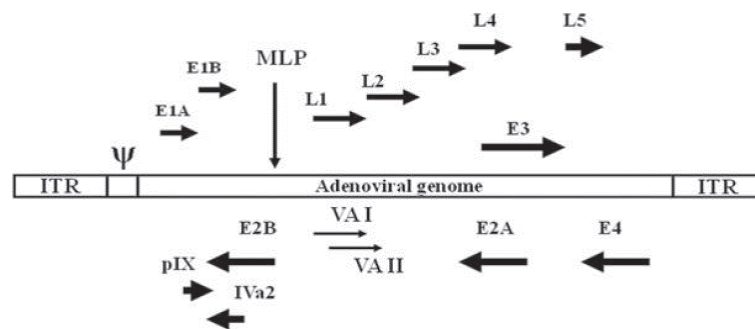


Figure 5. The transcription map of human adenovirus serotype 5 (Ad5)

The full length of 36kb genome is divided into several regions, including 4 early region transcription units (E1 to E4) and 5 alternatively spliced late mRNAs (L1 to L5) which are all initiated at the major late promoter (MLP). Four smaller mRNAs (pIX, IVa2, VAI, VAII) have been shown, which are formed during intermediate period of transcription. Inverted terminal repeats (ITRs), 103bp long, are located on both end of Ad5 genome, required for viral DNA replication. Packaging signal (Ψ) locates behind the left ITR, which is required for packing adenoviral genome into viral capsids (Rosewell et al., 2011)

The capsid of adenovirus is composed by three major structure proteins (hexons, pentons and fibres) and a couple of minor structure proteins (Glasgow et al., 2006). Hexon is the most abundant protein component which forms the shell of the protein capsid. Apart from supporting the shell structure, there is no other function for hexons (Glasgow et al., 2006). Five pentons form a penton

base platform at capsid vertices, where the fibre homotrimers attach (Glasgow et al., 2006). In a completed adenovirus, there are twelve penton base platforms and twelve fibre homotrimers. At the end of each fibre, there is a knob domain whereby the virus attaches to cellular receptors (Glasgow et al., 2006), initiating virus infection. After the initial attachment of knob domain to a cellular receptor on cell surface, receptor mediated endocytosis is triggered by the interaction between an Arg-Gly-Asp (RGD) motif in penton base and integrins ($\alpha\beta3$, $\alpha\beta5$, $\alpha\beta1$, $\alpha3\beta1$, $\alpha5\beta1$) on the cell surface (Glasgow et al., 2006), where penton base takes part in infection procedure. Adenovirus enters host cell by clathrin-coated vesicles which later incorporate into endosomes (Glasgow et al., 2006). The weak acid microenvironment of endosome partially disassembles the virus capsid, and the virus cores are released into cytosol and transported along microtubules to a nuclear pore. Only viral DNA enters the cell nucleus where the E1A and E1B regions are transcribed, initiating the replication cycle (Glasgow et al., 2006).

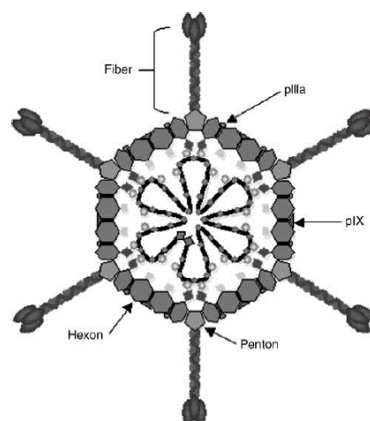


Figure 6. A schematic representation of general adenovirus structure

A wildtype adenovirus includes linear double stranded DNA core and a protein capsid. The viral capsid is composed by hexons, penton bases, fibres and some minor structural proteins (pIX and pIIIa have been shown). (Glasgow et al., 2006)

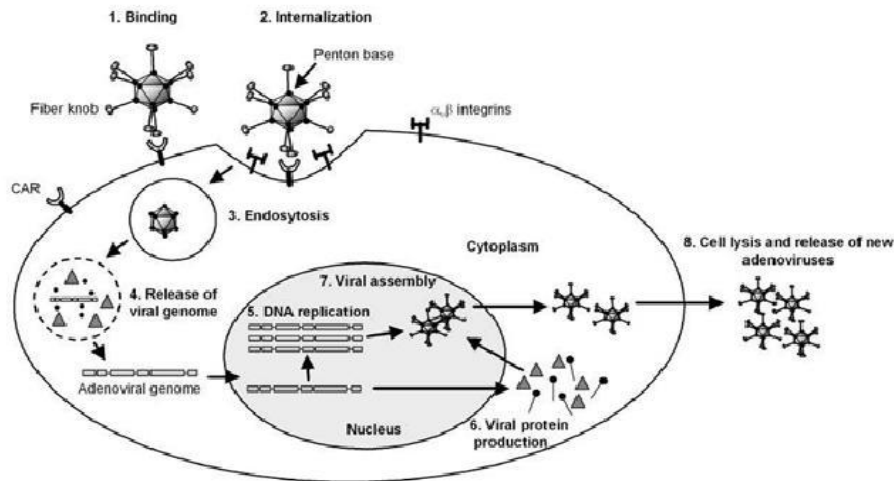


Figure 7. The endocytosis of adenovirus on cell surface

The adenovirus first binds to CAR fibre receptor on the plasma membrane of cell with Ad5 wild-type fibre. Then the integrin on human cells binds to the penton base, the base of fibre on viral capsid. This phenomenon is followed by forming of endosomes in the cytoplasm of host cells. The weak acidic microenvironment in endosome helps the degradation of the viral fibre, and the viral core releases towards host nucleus. As a consequence, viral core binds to the nuclear pore complex, and the viral genome is transmitted to the nucleus. After infection, the host cell enters lytic cycle to replicate adenoviruses. Adenoviral DNA is transcribed in nuclear; viral mRNA is translated and proteins are made in cytosol. At the end of lytic cycle, all viral proteins are transported to host cell nuclear to assembly progeny viruses. Then, these completed viruses are transported to cytosol again. Finally, these viruses lysed cell membrane and released to intercellular space, infecting surrounding cells. This Figure was adapted from ssg-adenovirus.co.uk.

Adenoviral Early 1A gene (E1AWT) and E1AΔ24

Adenoviral E1A region is the first transcribed gene after the virus entering human cells, which has the dual functions of pushing the cell into S phase, and activating the expression of the other viral early genes required for the viral lytic cycle (Choi et al., 2012). Altering the regulation of E1A transcription to making it express preferentially in tumour cells provides a mechanism to engineer tumour-selective into the virus. A small amount of E1A protein is enough for

virus replication, so a strictly-controlled promoter is more suitable than a strong promoter for oncolytic viruses (Choi et al., 2012).

Apart from varying the promoter used to express E1A, another strategy I involved in this project was to use the E1A Δ 24 mutant of E1A, which removes the pRb binding site from the E1A protein. Retinoblastoma protein is a tumour suppressor (Jakubczak et al., 2003), and a clinical report indicates that there is loss of retinoblastoma protein expression in 11.9% of intrahepatic cholangiocarcinoma (ICC) cases (Kang et al., 2002). However, it is likely that other cases would have alternations in cell signalling pathways leading to constitutive hyper-phosphorylation of pRb, which causes dissociation from E2F and negates the requirement for E1A to do this.

In normal cells in the G1 or G0 phase of the cell-cycle, pRb binds to the cellular E2F transcription factor, preventing it from activating the transcription of genes required for entry into S-phase. Following infection by WT adenovirus, the viral E1A protein preferentially binds the pRb, dissociating it from E2F and thus allowing E2F to activate transcription of the genes required for S-phase, which is necessary to allow viral replication. Thus, viruses with the E1A Δ 24 which removes the pRb binding site are unable to trigger S-phase entry, and are unable to replicate in normal cells (Frisch and Mymryk, 2002, Heise C, 2000, Jakubczak et al., 2003).

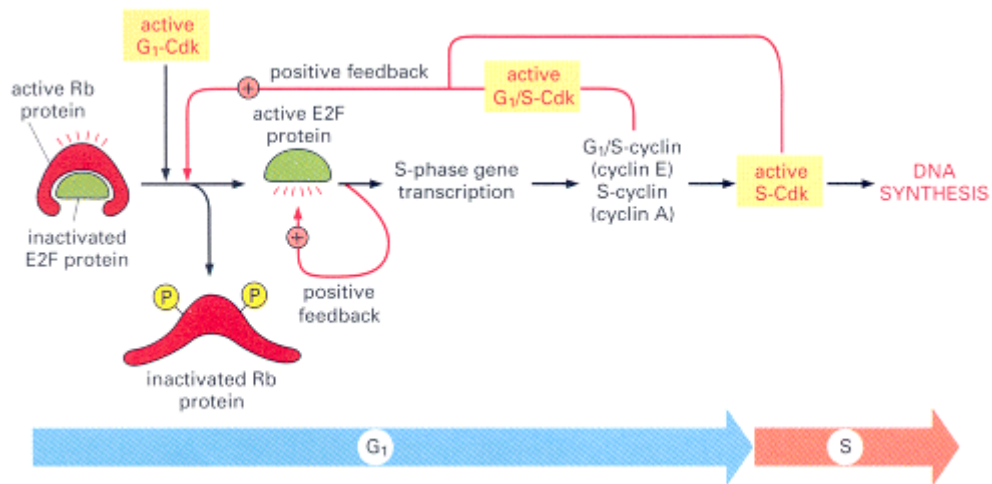


Figure 8. The regulation of retinoblastoma protein (pRb) in cell cycle

Active Rb inactivates E2F protein. G1 stage-cyclin dependent kinases (CDK) from cell cycle phosphorylate Rb, causing dissociation from E2F. E2F is now active and promotes transcription of genes required for progression of cell cycle into S stage. The brake, from Rb, is disengaged. This Figure was adapted from blogs.scientificamerican.com.

hTERT promoter (hTERTp)

Telomerase is the enzyme that extends telomeres. It is usually not expressed in human somatic cells, but this enzyme is highly activated in tumour cells. DNA polymerase cannot duplicate the whole chromatid to the end of chromosome on the lagging DNA strand, so that each time the chromosomal DNA is replicated, it becomes shorter at the ends.

Telomeres consist of many copies of a short repeat sequence (TTAGGG)_n in man, located at the ends of chromosomes, which prevent the loss of essential genes due to the incomplete replication of chromosome ends. In normal cells, telomerase is not activated, so the length of telomere declines with each mitotic cycle. Cells of young individuals have the longest telomeres, and the cells start to lose telomere length through progressive cell divisions. When telomeres

become shorter, the frequency of observing senescent cells increases, eventually leading to cell death. (Harley, 1991)

Hence, one of the markers of tumorigenesis is the activation of telomerase, which then allows an unlimited number of cell divisions. Telomerase is a RNA-dependent DNA polymerase, and the core enzyme consists of a structural RNA (named hTER in human cells) and a catalytic protein telomerase reverse transcriptase (hTERT) (Cong et al., 1999).

The hTERT promoter is GC-rich with no TATA or CAAT boxes but containing multiple binding sites for several transcriptional factors including MYC, MAX, upstream stimulating factor (USF), nuclear factor 1 (NF1), Ikaros 2 (IK2), activator protein 2 (AP2), activator protein 4 (AP4), stimulating protein 1 (Sp1) (Cong et al., 1999).

The minimal level of telomerase in normal somatic cells and its up-regulation in cancer cells have been shown to be at the level of transcription of the hTERT gene (Gunes et al., 2000). Several groups have therefore used the promoter of the hTERT gene to control expression of adenovirus genes essential for virus replication (Nemunaitis et al., 2010, Huang et al., 2003, Zou et al., 2004).

The hTERT promoter we used for the oncolytic virus construct is a 297bp long fragment from virus Ad5/3-hTERT-CD40L (also known as CGTG-401), kindly provided by Oncos Therapeutics (Pesonen et al., 2012). This virus has been tested in cancer patients, and it is proven well-tolerated and safe.

E2F1 promoter (E2F1p/E2Fp)

E2F is a family of transcriptional factors, including E2F1 to E2F6; each transcription factor has totally different role in regulating cell cycle and

controlling the expression of a variety of target genes (Stevaux and Dyson, 2002). E2F1 to E2F3 are transcription activators that interact with retinoblastoma protein (pRb) directly (van den Heuvel and Dyson, 2008, Stevaux and Dyson, 2002), while E2F4 and 5 are transcription repressors, which is able to work with pocket proteins (p107 and p130) (van den Heuvel and Dyson, 2008, Stevaux and Dyson, 2002). P107, p130 and pRb belong to the Retinoblastoma protein family, and p107, p130 have the function to regulate transitions between cell proliferation and terminal differentiation (Stevaux and Dyson, 2002). E2F6 does not associate with any of the retinoblastoma protein family, but it interacts with polycomb group proteins, acting as a gene transcription repressor (Stevaux and Dyson, 2002, Jakubczak et al., 2003).

Generally speaking, the E2F family is divided into activators (E2F1 to E2F3) and suppressors (E2F4, E2F5 work with pocket proteins) (Stevaux and Dyson, 2002). For activators, the E2F promoters are occupied in cell cycle late G1 phase or S phase, which promotes E2F target gene expression (Stevaux and Dyson, 2002). The E2F1 gene itself is also one of the E2F target genes, and it becomes hyper-expressed in tumour cells (Jakubczak et al., 2003). Hence, we use the promoter of E2F1 gene for the oncolytic virus construct made in this project. When host cell goes into late G1 phase or S phase, E2F1 forms a heterodimer by binding with a member of transcriptional factor DP family (usually TFDP1) (Jakubczak et al., 2003), and then this heterodimer binds to E2F binding motifs on promoters of target genes (Jakubczak et al., 2003); resulting in target gene activation. E2F and DP heterodimer can also bind to unphosphorylated Rb proteins, especially during G1 or G0 phases. Once this dimer binds to Rb protein, gene transcription

is inhibited (Jakubczak et al., 2003). Thus, E2F promoters are occupied by repressive E2F complexes (E2F4 to E2F6) in G0 and early G1 phase. When the cell enters late G1 phase, the repressor E2F complex is replaced by free activator E2Fs, followed by active gene transcription (Stevaux and Dyson, 2002).

In normal cells, pRb can bind to transcription factor E2F to inhibit the cell entering S phase. However, in human cancers, one of the most obvious changes is the loss of Rb protein binding to E2F family (due to loss or hyperphosphorylation of pRb), resulting in an increased amount of free E2F which directly activates the genes guided by E2F1 promoters. In other words, free E2F dramatically increases in most cancer cells relative to healthy cells, so the gene with an E2F1 promoter will be more activated in tumour cells rather than normal cells (Johnson et al., 2002), and that is the reason why we can use E2F1 regulated promoter (E2F1p) as a selective switch in oncolytic virus.

In my project, I use the E2F-regulated promoter from ICOVIR 15 which is an AdE2Fp-E1A Δ 24-RGD oncolytic virus (Rojas et al., 2010). In this engineered virus, eight E2F1 binding sites, arranged as four palindromes were inserted into the E1A promoter to inhibit E1A transcription cells with normal pRb function, while stimulating transcription in cells either lacking pRb, or with hyperphosphorylated pRb. This modification maintained most of the original structure of adenovirus genome including the function of E1A enhancer, producing an efficient, selective replication adenovirus in tumour cells without adding too much base pair (151bp only) or affecting its anti-tumour ability (Rojas et al., 2010).

When cancer cells are infected by ICOVIR 15, free E2F factors bind the E2F palindrome sites in the modified E1A promoter, triggering E1A Δ 24 transcription. The E1A protein further activates the transcription of other early genes, such as E2A, E2B, E2L and E4orf6/7 which amplify E1A transcription via positive feedback (Rojas et al., 2010). In normal cells, pRb binds to E2F, forming a complex to inhibit transcription. When the cell is infected by ICOVIR 15, this complex binds to the E2F1 promoter, docking histone deacetylase (HDAC) protein to the same promoter, preventing E2Fp-E1A Δ 24 transcription. WT E1A can bind to pRb, releasing E2F from E2F-pRb complex, whereas the E1A Δ 24 expressed by ICOVIR15 is unable to bind to pRb, preventing self-activation when E1A Δ 24 is expressed (Rojas et al., 2010).

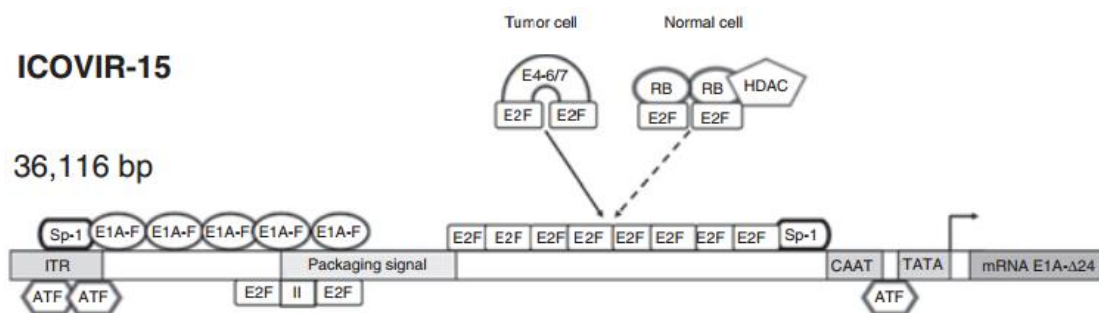


Figure 9. The modified E1A promoter of ICOVIR-15

In ICOVIR-15, eight E2F-1 binding sites were inserted into the E1A promoter. Given that there is plenty of free E2F factor in tumour cell, viral early gene E4-orf 6/7 binds to the E2F factor, forming a loop to self-activate E1A gene transcription. In normal cells, Rb protein is normally expressed so that E2F factor is trapped by Rb protein, and then HDAC binds to the complex to prevent transcription.

Sp-1, Sp-1 transcriptional factor; ITR, inverted terminal repeats; RB, retinoblastoma protein; II, enhancer element II; HDAC, histone de-acetylase; CAAT, TATA, binding sites for general transcription factors and RNA polymerase. (Rojas et al., 2010)

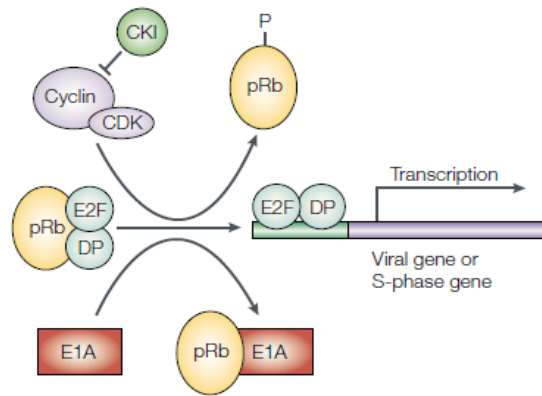


Figure 10. The transcriptional regulation between pRb, E2F, DP and WT E1A

Cyclin protein and cyclin dependent kinase (CDK) are regulated by cyclin kinase inhibitor (CKI). In normal cells in G0/G1 phase, pRb binds to E2F-DP complexes, inhibiting expression of S-phase genes. Stimulation of signalling pathways that lead to pRb phosphorylation cause dissociation from E2F-DP, allowing transcription of S-phase gene. Wild-type E1A has the ability to bind to pRb protein, causing release of E2F factor and DP, activating S-phase gene transcription. E1A Δ 24 loses its function to disassemble the pRb-E2F-DP complex, so blocking the ability of viruses with E1A Δ 24 from triggering S-phase entry in normal cells, and disallowing viral replication. pRb, retinoblastoma protein; E2F, E2F transcription factor; DP, Transcription factor Dp-1 (TFDP1). (Frisch and Mymryk, 2002)

The fibres of adenovirus

Fibre of adenovirus is composed of fibre protein homotrimers, and furthermore, these proteins are translated from L5 late mRNA (Glasgow et al., 2006). The fibres play a very important role during virus infection, binding to cellular receptors via the knob domain on the distal end of fibres (Glasgow et al., 2006). Then penton base platform of adenoviral capsid takes part in the infection procedure by host cell internalization; the interaction between integrins and penton base platforms promotes target cell to take up the virus by receptor mediated endocytosis (Glasgow et al., 2006).

Nonetheless, the receptor for a wild-type fibre of adenovirus 5, the coxsackievirus and adenovirus receptor (CAR) is widely-distributed in normal

tissue cells of human, even on the surface of erythrocytes. Hence, in a parallel project (executed by S. Karakonstantis), replication-defective adenovirus (using EGFP as reporter protein) were engineered with different fibres: Ad5/3, Ad5+RGD, Ad5/35, Ad5/FMD and also a wild-type control Ad5.

Native Ad5 Fiber

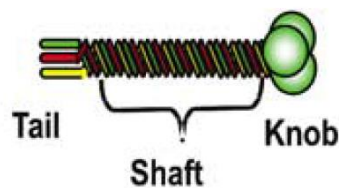


Figure 11. A schematic presentation of native adenovirus 5 fibre structure

The conserved N terminal tails contain the sequence to associate with penton base platform and nuclear localization signal. All viruses used in this project retained the same Ad5 fibre tail. A rod-like shaft of variable length in different serotypes contains beta sheets of a repeating fifteen amino acid motif, the number of beta sheets varying from 6 (Ad3) to 22 (Ad5). Tropism-modified viruses used in this project either substituted the knob domain of different adenoviruses, or inserted binding motifs into the HI-loop of the Ad5 fibre. The native Ad5 fibre knob has 188 residues. "Spike" is an overall term for virus fibre, including tail, shaft and knob. (Mathis et al., 2005)

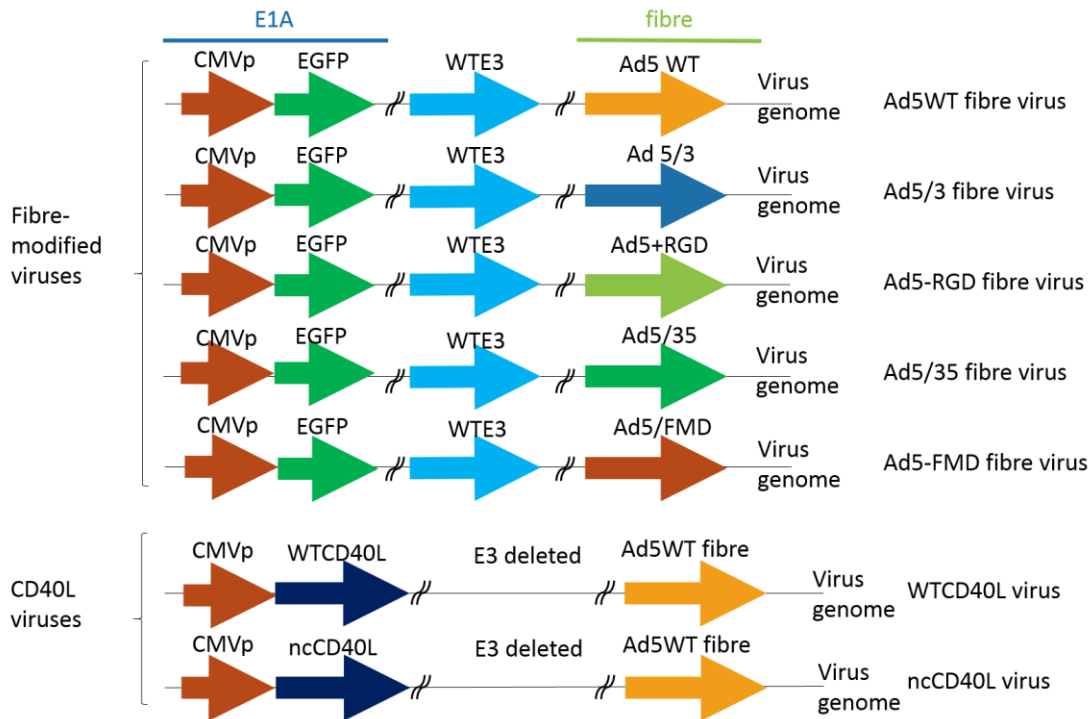


Figure 12. A schematic representation of replication defective viruses constructs used in this project

In this series of replication defective viruses, EGFP acts as a reporter protein. Among fibre modified viruses, these viruses only vary in the part of adenoviral fibres, the combination including WTAd5 fibre, Ad5/3 chimera fibre, Ad5-RGD motif insertion fibre, Ad5/35 chimera fibre and Ad5-FMD insertion fibre.

In the case of CD40L viruses, both wild-type CD40L and cleavable form (ncCD40L) which resists proteolytic shedding from the cell surface have been used.

Ad5-RGD motif fusion fibre

Arg-Gly-Asp (RGD) motif is a short peptide motif which specially binds to α_v integrin (Vigne et al., 1999). An RGD motif has been engineered into the HI loop of Ad5 fibre knob domain (Dmitriev et al., 1998), thereby allowing this adenovirus to use RGD-integrin interaction as an alternative CAR-independent cell entry pathway. Apart from RGD modified fibre, this team has tried many different chimera fibre, such as Ad5-FLAG chimera fibre (Krasnykh et al., 1998).

However, these combined fibres are not as efficient as Ad5-RGD fusion fibre, so we chose Ad5-RGD fibre as one of our targets.

Ad5-FMD motif fusion fibre

$\alpha_v\beta_6$ protein is an epithelial cell-specific integrin, that is strongly expressed in many carcinomas, the higher expression, the worse prognosis. For instance, 90% of oral squamous cell carcinomas express $\alpha_v\beta_6$ integrin, and its expression promotes tumour progression (Coughlan et al., 2009). Foot and mouth disease virus (FMDV) has the ability to form a strong interaction with $\alpha_v\beta_6$ integrin (Coughlan et al., 2009), and this is via viral structural protein (VP) in FMDV, which includes the A20FMDV2 peptide motif (which includes the familiar RGD motif), which confers specificity towards $\alpha_v\beta_6$ integrin (Coughlan et al., 2009). The A20FMDV2 peptide was inserted into the HI loop of Ad5 fibre knob domain, and interaction between this peptide and $\alpha_v\beta_6$ integrin has been proven highly stable and EDTA resistant (Coughlan et al., 2009). As a result, we took it as one of the candidates to regenerate a qualified comparison.

Ad5/3 chimera fibre

Although the majority of adenovirus serotypes make use of CAR as the primary receptor, a few use alternative receptor, like Ad3 and Ad35 (Shayakhmetov et al., 2000, Stevenson et al., 1995). Ad3 fibre binds to desmoglein 2 (DSG2), which was found to be up-regulated on a number of cancers (Wang et al., 2011). The binding efficiency of Ad3 fibre C terminal knob domain to DSG2 was as efficient as a full length fibre (Stevenson et al., 1995), so viruses have been generated that replace just the knob of Ad5 to generate a chimera fibre, which mediates entry via DSG2.

Ad5/35 chimera fibre

Ad35 was found to infect tumour cells with high efficiency through a CAR- and also α_v integrin-independent mechanism (Shayakhmetov et al., 2000). Ad35 virus enters cells via CD46 (Gaggar et al., 2003), which is also reported to be up-regulated in many cancers (Anderson et al., 2004). The reaction between Ad35 fibre and CD46 is measured as K_D (equilibrium dissociation constant) of 15.5 nM which is quite strong; in addition, the binding pocket of CD46 has been identified as Phe242, Arg279, Ser282, and Glu302 by Lieber's team in 2007 (Wang et al., 2007). This Ad35 fibre-CD46 molecular interaction has been well-studied, so Karakonstantis incorporated the shaft and knob domain from the Ad35 fibre (derived from a virus generated by Shayakhmetov et al. (2000)) into this series of replication-defective reporter viruses (Shayakhmetov et al., 2000).

Table 3. The modified adenovirus fibres used in this project

Fibre	Receptor	Description
Ad5-RGD motif fusion fibre	α_v integrin	Ad5-RGD fibre and α_v integrin pair utilizes α_v integrin as alternative cellular receptor which is totally CAR independent. Then the virus is absorbed by receptor-mediated endocytosis (Krasnykh et al., 1998).
Ad5-FMD motif fusion fibre	$\alpha_v\beta_6$ integrin	The adenovirus containing Ad5-FMD fusion fibre uses $\alpha_v\beta_6$ integrin to replace CAR as binding receptor, leading to internalization (Coughlan et al., 2009).
Ad5/3 chimera fibre	desmoglein 2 (DSG2)	The binding of adenovirus with Ad5/3 fibre and DSG-2 triggers transient opening of intercellular junctions, such as CD46 and Her2/neu receptors. This mechanism was observed during epithelial-to-mesenchymal transition (EMT) in epithelial cells, but the loss of intercellular junctions here indeed help for virus infection (Wang et al., 2011).
Ad5/35 chimera fibre	CD46	Adenovirus with Ad5/35 chimera fibre enters host cell by binding with CD46 receptors on cell surface, one CD46 receptor having space for two adenovirus (Wang et al., 2007).

CD40 ligand (CD40L/CD154)

CD40L is a type II transmembrane protein, which means that CD40L anchors itself on the membrane by the sequences on C-terminus. It is a member of the tumour necrosis factor (TNF) superfamily. CD40L is highly expressed on the surface of activated CD4+ T cells, and plays an important role in activating immune responses, by interacting with its receptor, CD40, which is expressed on many antigen-presenting cells (APC), such as macrophages and dendritic cells (DC). The interaction between CD40 and CD40L results in antigen presenting and cytokine release, leading to strong innate immune responses. In addition, the interaction between CD40 and CD40L improves the activation and enlargement of T cells, and they also increase interleukin-12 (IL-12) release. IL-12 plays a very important role in activating cytotoxic T cells for anti-tumour function.

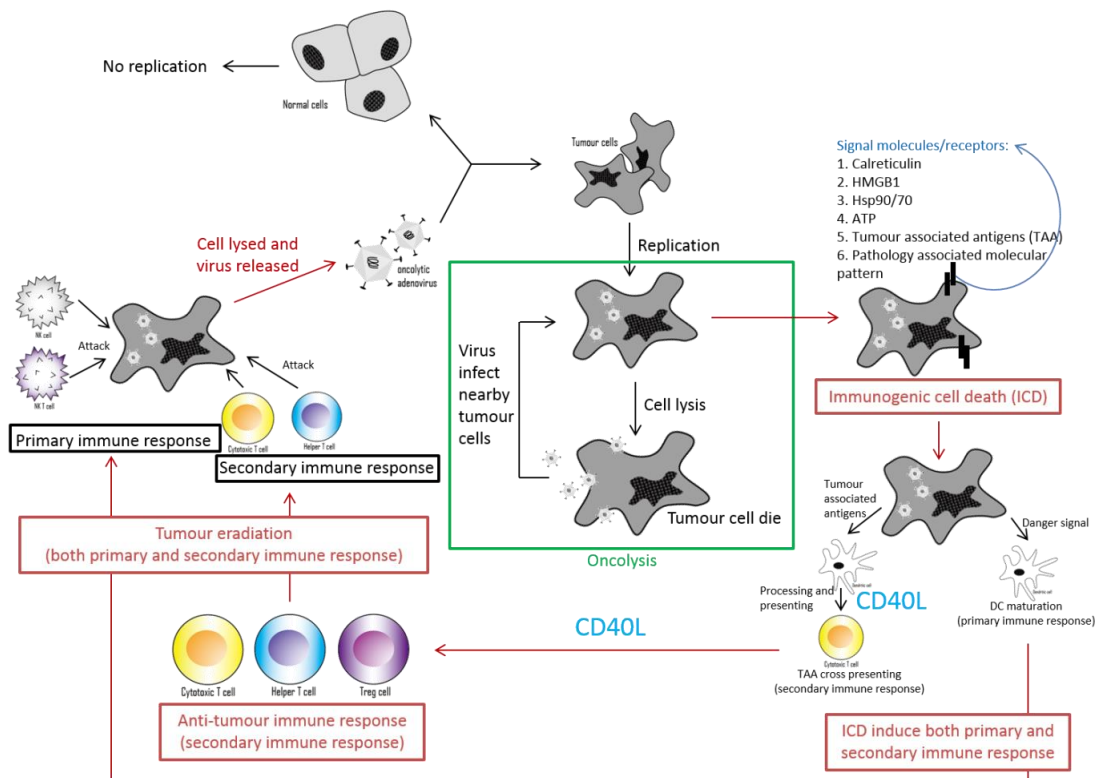


Figure 13. The working flow of oncolytic viruses via direct oncolysis and indirect via immune responses

The chart starts from oncolytic viruses. Oncolytic viruses replicate and kill the tumour cells by direct oncolysis, while this function is inhibited in normal cells. Moreover, the virus infected tumour cells also trigger immunogenic cell death and induce primary and secondary immune responses via CD40L. (Bartlett et al., 2013)

Even though there is no immune response in vitro, especially in cell lines, CD40L protein has been observed to promote apoptosis of CD40+ carcinoma cell lines (Eliopoulos and Young, 2004, Eliopoulos et al., 2000). The cholangiocarcinoma cell line used in this project is CD40+, providing an opportunity to investigate the potential added benefit of combining the pro-apoptotic effects of CD40L and oncolytic viruses.

Aim of project

Aim: To develop oncolytic adenoviruses optimised for treatment of cholangiocarcinoma

Objectives:

1. To engineer oncolytic adenoviruses (all with wild-type Ad5 fibre and an EGFP reporter gene) controlled by either the hTERT promoter, or an E2F1p-regulated promoter and E1A Δ 24, for comparison with an existing virus with only E1A Δ 24.
2. To test these viruses in cholangiocarcinoma (CC) cell lines, evaluating their replication efficiency and oncolysis.
3. To evaluate expression of alternative adenovirus receptors by immunohistochemistry (IHC) of histological sections of cholangiocarcinoma (CC) and surrounding liver tissue.
4. To compare the ability of adenovirus targeting via alternative fibre proteins to infect cholangiocarcinoma (CC) cell lines.
5. To test whether adenoviral expression of CD40L may enhance the efficacy of oncolytic adenovirus against cholangiocarcinoma (CC).

2. Materials and methods

2.1 Construct

Homologous recombination

Homologous recombination is a biological process that is widely exploited for designing DNA constructs. The constructs designed during this project were mainly based on the AdZ-5 vector, which contains the Ad5 vector genome with deleted E1 regions. This deletion makes the viral vector replication incompetent in cells. Moreover, this vector contains a selective cassette encoding the ampicillin resistant protein and the beta-galactosidase enzyme for blue/white screening, and the SacB gene for sucrose sensitivity. This selective cassette is located next to the CMV promoter and can be used as a marker when the targeted promoter-E1A fragment is recombined with the AdZ5 vector.

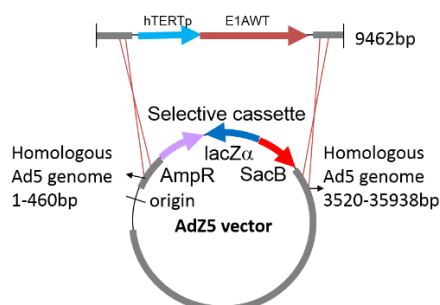


Figure 14. A schematic presentation of homologous recombination

The replication competent virus A (hTERTp-E1AWT) serves as an example. The desired DNA fragment (containing hTERTp and the 9462 bp E1AWT gene) was inserted into the AdZ5 vector via homologous recombination. The selective cassette was then replaced with the target gene; thus, a test of the absence of the ampicillin resistant protein, beta-galactosidase, and sucrose sensitivity is involved.

Selective cassette: positive selection and negative selection

The term ‘positive selection’ or ‘negative selection’ are named after the type of mutation completed by homologous recombination. If a vector gain the function of selective cassette (gain-of-function mutation), the screening corresponding to this type of mutation is named as ‘positive selection’. In contrast, once the vector loss the function of selective cassette (loss-of-function mutation), then the following screening is named ‘negative selection’.

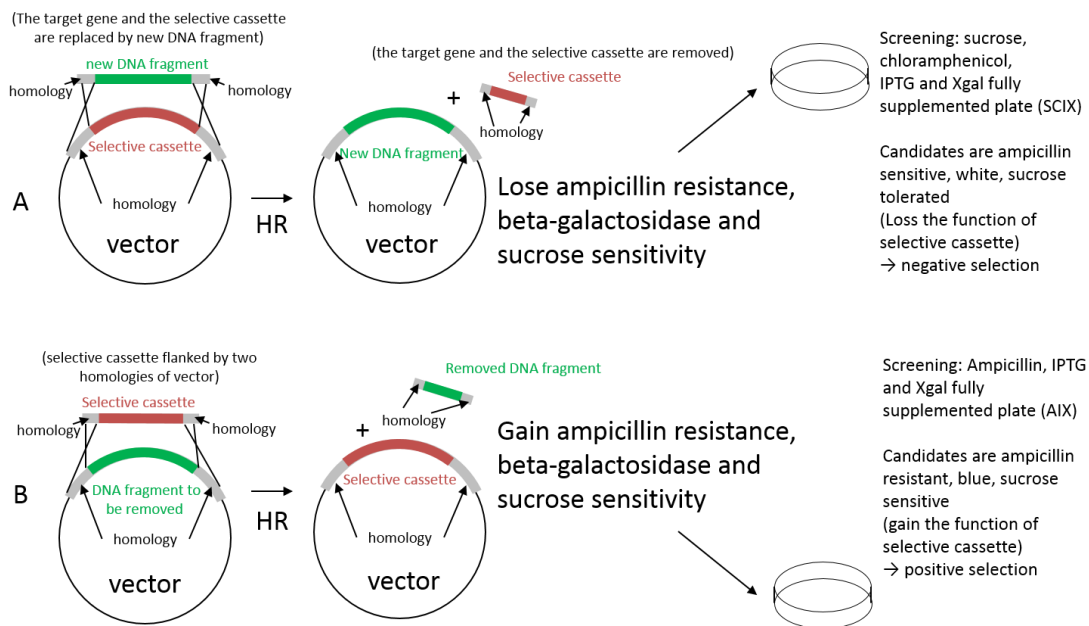


Figure 15. A schematic presentation of positive selection and negative selection

(A) Negative selection to insert a new DNA sequence (as used in this project first, to insert alternative promoter-E1 region fragments; and later, to insert EGFP into the E3 region): A vector contains the selective cassette and the target gene to be removed. The DNA fragment to be inserted contains regions of homology to vector sequences flanking the selection cassette. Through homologous recombination, the selective cassette and the target gene have been removed and replaced by the new DNA fragment, and the vector loses the function of selective cassette (ampicillin resistance, beta-galactosidase and sucrose sensitivity). For negative selection, the E.coli pool was spread on a SCIX plate (sucrose, chloramphenicol, IPTG and Xgal), to select for bacteria that have become resistant to sucrose. This could either be due to the intended loss of the selection cassette, in which case the beta-galactosidase is also lost and the colony appears white; or to mutation of the *sacB* gene, in which case the colony will probably retain beta-galactosidase expression, and so be blue. As additional confirmation of loss of the entire selection cassette, white colonies could be checked by re-streaking onto ampicillin plates. Bacteria that have lost the selection cassette via recombination should be sensitive to ampicillin, and so unable to grow on Amp plates. (B) Positive selection to insert the selection cassette (as used in this project to engineer the E3 region). To insert the selection cassette, it is flanked by short regions of homology with the vector, which will define the site of insertion. During homologous recombination, vector sequences between the homology regions are replaced by the selection cassette. Hence, the vector gains the function of ampicillin resistance, beta-galactosidase and Sac protein (sucrose sensitivity). Appropriate colonies are selected on AIX plates (ampicillin, IPTG and Xgal), where they should be blue. Sucrose sensitivity can be confirmed by re-streaking onto SCIX plates, where they should be unable to grow if they have acquired the entire, functional selection cassette. HR, homologous recombination.

Negative selection

The initial vector contained the selective cassette and the target gene to be removed, and then the selective cassette and the target gene were replaced by the new DNA fragment through homologous recombination. Thus, a positive

candidate was considered to be the one that had lost ampicillin resistance as well as beta-galactosidase activity and sucrose sensitivity.

Therefore, for negative selection, we used an SCIX (sucrose, chloramphenicol, IPTG, and Xgal) plate to screen such candidates. An ampicillin resistant test is usually performed to confirm after the screening of SCIX plates.

Positive selection

The other type of screening was named positive selection, which insert the selection cassette (as used in this project to engineer the E3 region) to new vector. To insert the selection cassette, the cassette was flanked by short regions of homology with the vector, called the site of insertion. During homologous recombination, vector sequences between the homology regions were replaced by the selection cassette so that the vector gained the function of ampicillin resistance, beta-galactosidase and Sac protein (sucrose sensitivity).

To screen the candidates, we used an ampicillin, IPTG, and Xgal (AIX) plate because the positive candidates should encode AmpR, SacB, and beta-galactosidase in theory. Following the AIX screening, a sucrose sensitivity test was usually carried out to confirm the mutation.

Digestion and ligation

Ligation is another widely used molecular biology technique for designing gene constructs. In this project, I only used it once to ligate a selective cassette into the E3 region. Basically, there are two types of ligations carried out after the initial restriction enzyme digestions: one is a sticky end ligation, and the other is a blunt end ligation. Generally speaking, sticky end ligation is more selective

than blunt end ligation. Furthermore, the doubly digested DNAs are more efficient than their singly digested counterparts, because the former inhibit self-ligation. During this project, I only used the enzyme MfeI to digest the targeted genes, which resulted into singly digested sticky end fragments. However, I used dephosphorylase to remove the 5' phosphate from the linearised DNA, thus inhibiting the vector self-ligation.

2.2 Plasmid miniprep, bulkprep, gel purification

One day before the miniprep or two days before the bulkprep, the bacteria were inoculated into the medium broth. This was followed by overnight incubation for two days. The first step in a miniprep protocol involved spinning down the bacteria. The pellet was then re-suspended in a glucose-enriched buffer and lysed in a lysozyme-containing buffer. The lysozyme activity was inhibited with an SDS-containing buffer; the SDS denatures the proteins as well as the genomic DNA, and the alkaline conditions of the buffer facilitate the plasmid release. The acetate buffer was then added to neutralize the alkaline buffer. The mixture was spun down to remove the denatured proteins as well as the genomic DNA. The supernatant was collected and precipitated using isopropanol in about 1h. The mixture was spun down again, and the pellet was incubated at 37°C (for 1 h or overnight) in RNase A containing the T₁₀₀E₅N₁₀₀ buffer. This step was followed by phenol/chloroform extraction for removing the contaminating proteins or RNAs. The sample obtained after extraction was expected to contain the plasmid DNA of interest. Finally, the sample was precipitated in 70% ethanol, spun down, and re-dissolved in the T₁₀E₁ buffer.

The plasmid bulkprep protocol includes all the steps in the miniprep protocol until the isopropanol precipitation. After the isopropanol precipitation, the mixture was spun down, and the pellet was dissolved in the T₅₀E₁₀ buffer. Then, CsCl and ethidium bromide (EtBr) were added to the solution, and the solution was centrifuged at 3000 rpm (about 660 g) to remove the debris. After adding Triton X-100, I carried out ultra-high speed centrifugation at 100,000 rpm (about 450,000 g) to generate a CsCl gradient. CsCl was used to generate the gradient, whereas EtBr was used to detect the DNA. Following centrifugation, the plasmid DNA band was collected and subjected to phenol/chloroform extraction. The semi-product was precipitated using 2 volumes of ethanol or 1 volume of isopropanol, and centrifuged once more at 3000 rpm (about 660 g). The pellet was then dissolved in the T₁₀E₁N₁₀₀ buffer and precipitated via centrifugation at 3000 rpm (about 660 g). Finally, the pellet was dissolved in the T₁₀E₁ buffer.

For general guidelines on gene cloning, plasmid miniprep, and bulkprep methodologies, please refer to Sambrook J, Fritsch EF, Maniatis T. *Molecular Cloning: A Laboratory Manual* 2nd edition: Cold Spring Harbor Laboratory Press, 1989.

For gel purification, we used a QIAquick Gel Extraction Kit, according to the manufacturer's instructions.

2.3 Cell culture

In this project, we used human embryonic kidney (HEK293) cells, human lung adenocarcinoma epithelial (A549) cells, and Cholangiocarcinoma (CCLP1 and CCSW1) cells. All the cell lines were obtained from the American Type Culture Collection (ATCC). We cultured the cell lines in Dulbecco's Modified Eagle's

medium (DMEM, Sigma-Aldrich Corporation) containing 10% Fetal Calf Serum (FCS), 1% L-glutamine, 1% penicillin/streptomycin, and grew them at 37°C in a 5% CO₂ incubator. Usually, we cultured the cell lines in a T75 flask containing 10 ml of the fully supplemented DMEM. All of the cell work was carried out in a laminar flow cabinet to ensure sterility.

After the cells became more than 90% confluent, they were sub-cultured. During cell culture, the older medium from the flasks was removed, and the new flasks were filled with 8 ml of the fully supplemented medium. After washing the adherent cells twice with 10 ml PBS (for removing cell debris, cell waste, etc.), 2 ml trypsin was added to detach the cells. When the cells were fully detached, 8 ml of the fully supplemented medium (with 10% FCS) was added to stop the process of trypsinization. Of the 10 ml solution, 2 ml was used for the sub-culture by transferring it into a new flask. The cells in the new flask became confluent in about 3 day. The number of cells used during sub-culture can be easily varied depending on the requirement (E.g., 5 ml, 3 ml, and 1 ml of the solution containing the cells can be used to attain confluency in one, two, and five days, respectively).

HEK293 cells are one of the most commonly used and well-studied cell lines containing the E1A and E1B regions of the adenovirus 5 DNA, well-known for their ability to support the rapid replication of adenoviruses, including that of the E1-deleted viruses, which are replication-defective in most cells. HEK293 cells originating from human embryonic kidney cells were grown in tissue culture and then transfected with the sheared adenovirus 5 DNA (Graham et al., 1977).

A549 is a human alveolar adenocarcinoma cell line derived from the surgically resected cancerous lung tissue of a 58 year old male patient (Giard et al., 1973). It was used for producing the oncolytic adenoviruses used in my project, to avoid the possible recombination with the adenoviral sequences in the HEK293 cells.

The CCLP1 and CCSW1 cell lines were derived from a hepatic adenocarcinoma (Shimizu et al., 1992). These two cell lines exhibit the morphologic features of a moderately differentiated adenocarcinoma. Tight junctional complexes that facilitate microvilli formation are present in both the CC cell lines. Both of these CC cell lines are tumorigenic in nude mice. Based on the cytogenetic analysis, both CCLP1 and CCSW1 possess highly aneuploid karyotypes with a couple of structural and numerical deviations. The CCSW1 cells are hypodiploid, with several chromosome losses and structural changes, whereas the CCLP1 are hyperdiploid, with multiple additional chromosomes (Shimizu et al., 1992). According to Shimizu Y et al., the doubling times for CCSW1 and CCLP1 in a growth medium containing 15% fetal bovine serum (FBS) is 72 h and 180 h, respectively. However, under the conditions used during cell culture (10% fetal calf serum (FCS) in DMEM), we found that the CCLP1 cells grow faster than the CCSW1 cells (data not shown).

2.4 Adenovirus

Infectious oncolytic adenoviruses were generated from plasmid constructs by calcium-phosphate mediated transfection into A549 cells in 25 cm² flasks. The progress of infections was monitored by observing EGFP expression via fluorescent microscopy. Cultures were harvested by shaking after 7 – 10 days,

centrifuging the cells and resuspending the cell pellet in 1 ml medium, which was subject to 3 freeze-thaw cycles (-80°C, 37°C) to release virus. The initial transfection stock of virus was expanded by infection of more A549 cells, initially using 100 µl to infect cells in a 6-well plate. This was followed by one or more further expansions in 75 cm² flasks, before a final large-scale virus prep, infecting A549 cells in typically 10 x 175cm² flasks.

2.4.1 Virus prep

When the cultures showed well-developed cytopathic effects (cpe; i.e. detachment of cells from the plate in grape-like clusters; yellowing of the medium), cells were harvested by shaking and transfer into 50 ml tubes. The cells were pelleted by centrifugation at 1600 rpm, then all cell pellets were resuspended and combined using 10 ml medium. Cells were disrupted by 3 freeze-thaw cycles (-80°C, 37°C), the debris pelleted by centrifugation at 4000 rpm for 10 minutes. After centrifuging, supernatant was separated using CsCl step gradients and ultra-speed centrifugation at 25,000 rpm for 2h in a Beckman SW40 rotor. Then, the band of complete virus was collected, exchanged into A195 buffer (Evans et al 2004) using a GE PD10 column, and divided into several tubes for further use.

To determine the virus concentration, a 50 µl aliquot was diluted 1:1 with 0.1% SDS, heat-inactivated at 56°C for 30 minutes, then used to determine DNA concentration. 1µg viral DNA corresponds to 2.57x10¹⁰ virus genomes (virus particles).

To confirm the correct genome structure of the virus, DNA was purified from a 0.5 ml aliquot of virus preps for analysis via restriction enzyme digestion This

0.5ml sample was mixed with 25 µl of 10% SDS, 10 µl of 0.5M EDTA, 5 µl of 5M NaCl and 2 µl of 10mg/ml proteinase K, and then the mixture was incubated in 37°C 1h or overnight. Therefore, a phenol/chloroform extraction was added to extract the viral DNAs, and then ethanol precipitation was introduced. Finally, the product of ethanol precipitation was dissolved in 100 µl of T₁₀E₁ buffer. Then, this viral DNA product was digested by appropriate restriction enzymes, and a separation of electrophoresis was added the complete procedure and reveal the result.

For the methodology of CsCl gradient, please refer to Mautner V. Methods for growth and purification of enteric adenovirus type 40. In: Wold WS, editor. Adenovirus Methods and Protocols. New Jersey: Humana Press, 1998:283-93.

2.4.2 Hexon staining (performed by Stamatis Karakonstantis)

The importance of this experiment will be more evident after looking at the differences between the multiplicity of infection and the infection unit.

Multiplicity of infection (MOI)

MOI provides a general description of the virus particles. We generally use MOI to set up experiments when the number of functional particles in the virus pool is unknown. Although MOI is convenient for manipulation, sometimes, it is not very accurate. Because the number of functional virus particles varies from group to group, this makes the comparison invalid.

Infection unit (IU)

In order to overcome the above situation, it is necessary to calculate the IU number. Hexon staining is an experiment for measuring the functional titre/µl of

the virus. This step is important because the quality of a virus prep can vary dramatically. We used a standard kit, called the Adeno X Rapid Titre Kit (Clontech), and followed the instructions in the user manual. We imaged some of the cells during the cell culture. A few cells were stained brown, indicating the expression of the viral hexon proteins. Each brown cell represents one virus infection unit (IU), thereby allowing the quantification of the IUs.

2.4.3 Infection

During infection, we usually decided a MOI (based on experimental testing). Before starting, and then on the infection day (day 0), we performed cell counting and calculated the appropriate virus dilutions prior to the infection, except in the case of the MTT assays. For the MTT assays, 96-well-plates were seeded with 1×10^5 or 5×10^4 cells/well one day before the infection. On the second day, we set up infection directly without counting again, and based the MOI on the number of cells plated. After calculating the MOIs, the appropriate virus dilutions were prepared in DMEM medium containing 2% FCS. We set up the infection in a smaller volume in order to increase the overall efficacy of the infection (e.g., 500 μ l for each well of a 6-well plate, 250 μ l per well for a 12-well plate, and 25 μ l per well for a 96-well plate). When everything was ready, the medium was removed from the 6-well plate or 12-well plate, and the virus was added to the medium, which was then incubated for 4 h (time-course experiments, infection experiments), 2 h (MTT assays), 90 min (qPCR experiments), or 1 h (RD virus infection experiments). After the initial incubation, the entire medium was removed, and the culture was washed twice with PBS. A new DMEM medium with 2% FCS was then added to the cell cultures. Media

containing 2% FCS are optimal for infections, whereas media containing 10% FCS are good for cell culture.

2.4.4 Harvest (for FACs experiments)

After adding the virus-containing infection medium, the time was recorded, and all the time points for harvesting were based on it. Basically, we used 24, 48, 72, and 96 h for The time course experiments were carried out for 24, 48, 72, and 96 h, whereas the infection experiments were carried out for 24 h in the case of HEK293 cells, and for 48 h in the case of the A549 and cholangiocarcinoma cells, respectively. To harvest the cells, the medium was removed, and the cell cultures were washed with PBS, followed by trypsinization using the TrypLE Express solution (Life Technologies). After all the cells had detached from the plate, a growth medium containing 2% FCS was added to inhibit the trypsin. The cell suspension was transferred to a 15 ml screw cap tube or to a 1.5 ml Eppendorf tube, depending on the liquid volume, and centrifuged at 1400 rpm (330–400 g) for 5 min. The supernatant was removed, and 100µl of PBS was added to suspend the cells. The cells were then transferred to a V-bottom 96-well plate. These were centrifuged again at 1400 rpm (330–400 g) for 5 min. Then, the supernatant was removed, and 100 µl of 2%PFA was added to fix the cells on ice for 20 min. The V-bottom 96-well plate was centrifuged at 1400 rpm 330–400 g for 5 min after a 20 min incubation. The supernatant was subsequently removed. The cells were washed with PBS, and were centrifuged again at 1400 rpm 330–400 g for 5 min. Eventually, the cells were stored in PBS containing 10% FCS. These cells were ready for flow cytometry analysis.

2.5 Flow cytometry

We used enhanced green fluorescent protein (EGFP) as the reporter gene in our viruses; therefore, when the virus entered the host cells and successfully replicated, the host cells were able to express GFP and appeared green in colour when exposed to light with a wavelength of 475 nm. Therefore, flow cytometry can be used to detect the intensity of GFP, so that the replication efficiencies of different viruses can be compared. We have two flow cytometers (Dako Cytomation CyAn ADP LX 7 Color (Dako Corporation, Birmingham, United Kingdom), and BD Accuri C6 cytometer (BD Bioscience, Birmingham, United Kingdom), with corresponding analysis softwares, Summit and BD Accuri C6, respectively. Most of the data in this project were analysed using the Dako CyAn cytometer, and a minor group of data was analysed using the BD Accuri C6 cytometer. The sample preparation for FACS is mentioned in the previous paragraph.

2.6 Quantitative polymerase chain reaction (qPCR)

We designed a set of qPCR experiments in order to confirm the findings of flow cytometry. After the classic procedure involving trypsinization of the cells and the subsequent inhibition of trypsin, a special cell DNA extraction kit was used for the qPCR-ready samples. This cell culture DNA extraction kit extracts the cell and virus DNA samples from the cell culture. For the CCLP1 cells, we used the DNeasy Blood & Tissue Kit from the Qiagen Corporation, and for the CCSW1 cells, we used the PureLink Genomic DNA Mini Kit from Invitrogen. We used two different kits in this experiment because of the limited availability of kits. Although we used two different kits to extract the DNA from the cell

culture, the same kit and same procedure was consistently used for each cell line. The results are therefore considered to be meaningful. After isolation, the DNA samples were stored in the freezer at -20°C until the qPCR procedure. Each sample was freeze-thawed and used only once.

For qPCR, we used the TaqMan Universal Master Mix 2x (Applied Biosystems) in place of Taq, along with Taq buffer, dNTPs, and water. The primers for the adenovirus targeted the hexon protein encoding gene on the capsid. They were as follows: forward primer, 5' CCACCCTTCTTTATGTTTTGTTTGA 3'; reverse primer, 5' GCAGGTACACGGTCTCGATGA 3'; and probe, 5' TCTTTGACGTGGTCCGTGTGCACC 3'. This set of primers can be used for detecting adenovirus type 1, 2, 5, and 6. The beta-2M primers used for detecting the cell genome copy number were designed by following the recommendations of a published study (Murray et al., 2003). The sequences were as follows: forward primer, 5' GGAATTGATTTGGGAGAG 3'; reverse primer, 5' CAGGTCCTGGCTCTACAA 3'; and probe, AGTGTGACTGGGCAGATCATCCAGCCTC. The total volume of each reaction was 20 µl, including 5 µl of the DNA sample, 10 µl TaqMan Universal Master Mix 2x, 0.1 µl each of the Barts F and R primers, 0.066 µl of the Barts probe, 0.4 µl each of the beta-2M F and R primers, and 0.2 µl of the beta-2M probe.

2.7 MTT assay

The MTT assay is one of the most commonly used cell viability assays. 3-(4,5-dimethylthiazol-2-yl)-2,5-diphenyltetrazolium bromide (MTT) is a yellow substrate that can enter the mitochondria and form purple crystals even in live cells. These crystals can be easily dissolved using Dimethyl sulfoxide (DMSO).

The colour change is measured at an absorbance of 490 nm absorbance using a spectrophotometer. Once the cells die, they get detached from the plate. Therefore, the dead cells can be easily removed when the old medium from the 96-well plate is removed before adding the MTT solution. Therefore, the dead cells do not get a chance to react with the MTT solution or to contribute to the purple signal. As a result, we can use the detected signals to compare the cell viability among various treatment groups.

When the plate was ready to assay, the MTT solution (10-fold diluted MTT in DMEM without phenol-red) was prepared before removing the medium. After removing the medium, the MTT solution was quickly added to prevent the cells from drying out. The plate with the MTT solution was then incubated inside a 37°C incubator supplied with 5% CO₂ for 2 h. Subsequently, the MTT solution was removed and the plate was dried inside a laminar flow hood for 30 min. DMSO was then added to the plate. On the morning of the second day, the plate was subjected to spectrophotometric determination (490 nm for 1 min). The uninfected and blank controls occupied the last three columns of the plate. The number obtained after reference subtraction was divided by the corresponding number obtained from the uninfected reference subtracted control, and then multiplied by 100%. Finally, the cell viability rate was calculated.

2.8 Immunohistochemistry (performed by Elizabeth Humphreys, William Marshall, and Florence Chen)

The analysis of receptor expression levels was based on the tissue samples resected from six patients with cholangiocarcinoma at the Queen Elisabeth

Hospital, with sample ID #4696, #4134, #3752, #3184, #2837, and #2544. After obtaining 15 slides from each patient, I performed tissue staining on these samples. After staining and mounting, I analysed the samples under a microscope. Tissue staining is one of the most commonly used histological methods to classify diseases and to identify specific molecules. In this set of experiments, we chose CD61, DSG2, CD46, integrin beta5, beta 8, alpha-v, alpha-v beta-6, CAR, CD40L, CK19, and CD40 molecules as our targets. The complete procedure included fixing and embedding the tissue, cutting and mounting the sections, deparaffinization, rehydration, staining, dehydration, and re-stabilization with the mounting dye.

For more details of immunohistochemistry, the procedure started from dewaxing and rehydrating the section by three clearanes, two ethanols and water in order. Then 3% H₂O₂ was added to block the endogenous peroxidase activity. The slide was then immersed into a pre-warmed, diluted citrate buffer, pH 6, to retrieve the antigens. The remaining solution was washed out with doubly distilled H₂O. Subsequently, 2.5% horse serum was added for blocking non-specific binding. This was followed by incubation and washing. The primary antibody was diluted in horse serum and then added to the slide. This was again followed by incubation and washing. The secondary impress peroxidase-conjugated antibody was added to the slide. This was followed by incubation and washing. The diluted DAB (substrate) was added to reveal the colour, and this step was followed by a wash step. The slides were placed into Mayers haematoxylin for background colouring. These slides were cleaned with water once again. After completing the procedure, the slides were then dehydrated

by reversing the order of dewax, water first, two ethanols, three clearenes.
Finally, the slides were mounted in DPX (permanent mount) and air dried.

2.9 Graph plotting and statistical analysis

Graph plotting: Sigma Plot version 12.5, Excel 2013, PowerPoint 2013

Statistics: SPSS version 20

3. Results

3.1 Gene construction of plasmid

The aim of this project was to compare oncolytic viruses controlled by hTERTp-E1A, E2Fp-E1A Δ 24, and only E1A Δ 24 in cholangiocarcinoma. Apart from the promoter and the E1A regions, the viruses were supposed to be identical. The starting materials included the Ad5/3-hTERT-E1A-CD40L adenovirus, kindly provided by Oncos Therapeutics (Pesonen et al., 2012), and the Ad5-E2F1p-E1A Δ 24-RGD fibre, obtained from ICOVIR 15 (Rojas et al., 2010). For an efficient comparison, it was necessary for the viruses to have the same Ad5WT fibre and the same E3/EGFP gene. Thus, the WTE3/EGFP region of the PS1334F1 plasmid and the Ad5 fibre of the AdZ5-CV5-WTE3-Ad5 fibre plasmid was introduced to different E1A promoter regions. The Ad5-WTp-E1A Δ 24-WTE3/EGFP-Ad5 fibre virus already existed, so it was not necessary to prepare this construct. The starting material for the Ad5-WTp-E1A Δ 24-E3/EGFP-Ad5 fibre virus was kindly provided by Turnell et al. (1999), and Dr. Peter F. Searle completed the construction before the experiment was initiated. For details regarding the genomes of the starting material, please refer to Heise C (2000).

Stage 1: Insertion of hTERTp-E1AWT and E2F1p-E1A Δ 24 into pAdZ5-CV5-E3+

The construct was generated using the Ad5/3-hTERTp-E1AWT-CD40L virus. First, *Sa*I restriction endonucleases (Sigma-Aldrich Corp.) were used to digest the viral DNA. After electrophoresis, isolation, and gel extraction, a purified hTERT promoter-E1A WT fragment was obtained. In stage 1, this fragment was recombined in SW102 bacteria containing pAdZ-CV5-E3+ (kindly provided by

Stanton et al. (2008)) to make a virus genome containing the hTERT promoter E1AWT with the wild-type E3 region and Ad5 fibre. A similar procedure was used for the E2F1p-E1A Δ 24 virus, using an Ad5-E2F1p-E1A Δ 24-RGD fibre plasmid as the starting material.

Negative selection was used to screen the candidates. Theoretically, recombination will result in loss of ampicillin resistance, sucrose sensitivity, and beta-galactosidase function. Thus, sucrose, chloramphenicol, isopropyl- β -D-thiogalactopyranoside (IPTG), and X-gal were added to plates for the selection procedure, and positive candidates that were sucrose resistant were identified as white colonies. Candidates were then tested on Amp plates for sensitivity.

Stage 2: Insertion of the selective cassette into the wild-type E3 region

In stage 2, the selective cassette was removed by MfeI restriction digestion from the PS1399N1 plasmid provided by Dr. Peter F. Searle, and the PS1327B6 plasmid was digested by MfeI to obtain a fragment with the Ad5 fibre and flanking E3 region. Then, these two fragments were ligated to form a circular plasmid for transformation to XL2-competent cells. Ligated products using both forward and reverse primers were obtained. Positive candidates stained blue in an X-gal-presenting environment, and were Amp-resistant and sucrose-sensitive. Sucrose sensitivity was usually used for negative screening. In sum, a selective plate contained Amp for the Amp resistance test, IPTG to determine beta-galactosidase expression, and X-gal for blue staining.

Stage 3: Replacement of the wild type E3 region by the E3/selective cassette fragment in the pAdZ5-hTERTp-E1AWT-E3+ and pAdZ5-E2F1p-E1AΔ24-E3+ plasmids

In stage 3, the two plasmids from stage 1 were recombined with the wild type E3-selective cassette fragments from stage 2. Then, two semi-products, hTERTp-E1AWT-E3/selective cassette-Ad5 fibre and E2F1p-E1AΔ24-E3/selective cassette-Ad5 fibre, were formed. In this stage, positive candidates were positively-selected by ampicillin-resistance, and IPTG, and X-gal were added to plates for the selection assay.

Stage 4: Replacement of the wild-type E3/selective cassette fragment with the wild type E3/EGFP region

In this stage, one of the two important starting materials, the wild-type E3/EGFP fragment had been constructed by Dr. Peter F. Searle in the PS1334F1 plasmid. This EGFP gene replaced two E3 genes, 6.7k and gp19k. The PS1334F1 plasmid was digested by the restriction enzyme *Pst*I, and electrophoresis, isolation, and gel purification of the target fragment. Finally, this fragment was ready to use.

The other initial material was obtained from the stage 3 procedure. In order to allow recombination of EGFP into the E3 region, the selective cassette was first inserted into the MfeI site in the E3 region, in the plasmid PS1327B6 containing the E3-containing, 5,665 bp *Hind*III fragment of Ad5 (stage 2). This was then recombined with the pAdZ5-hTERTp-E1AWT-E3+ and pAdZ5-E2F1p-E1AΔ24-E3+ plasmids (stage 3). At the end of stage 3, two semi-products, hTERTp-

E1AWT-E3/selective cassette-Ad5 fibre, and E2F1p-E1A Δ 24-E3/selective cassette-Ad5 fibre were ready to use.

Finally, in stage 4, the wild-type E3/selective cassette region was replaced in two plasmids by homologous recombination of the wild type E3/EGFP fragment, resulting in the final products. During this stage, positive candidates had loss of ampicillin resistance, sucrose sensitivity, and beta-galactosidase function. Sucrose, chloramphenicol, IPTG, and X-gal plates were used for screening. A positive candidate was defined as one that survived in the environment containing sucrose, and that was not able to hydrolyse X-gal resulting in a white colony.

The next step was bulk preparation, transfection, and production of viruses.

This procedure resulted in the production of three viruses, hTERTp-E1AWT-E3/EGFP-Ad5 fibre, WTp-E1A Δ 24-E3/EGFP-Ad5 fibre, and E2F1p-E1A Δ 24-E3/EGFP-Ad5 fibre, for use in infection experiments, cell viability assays, etc.

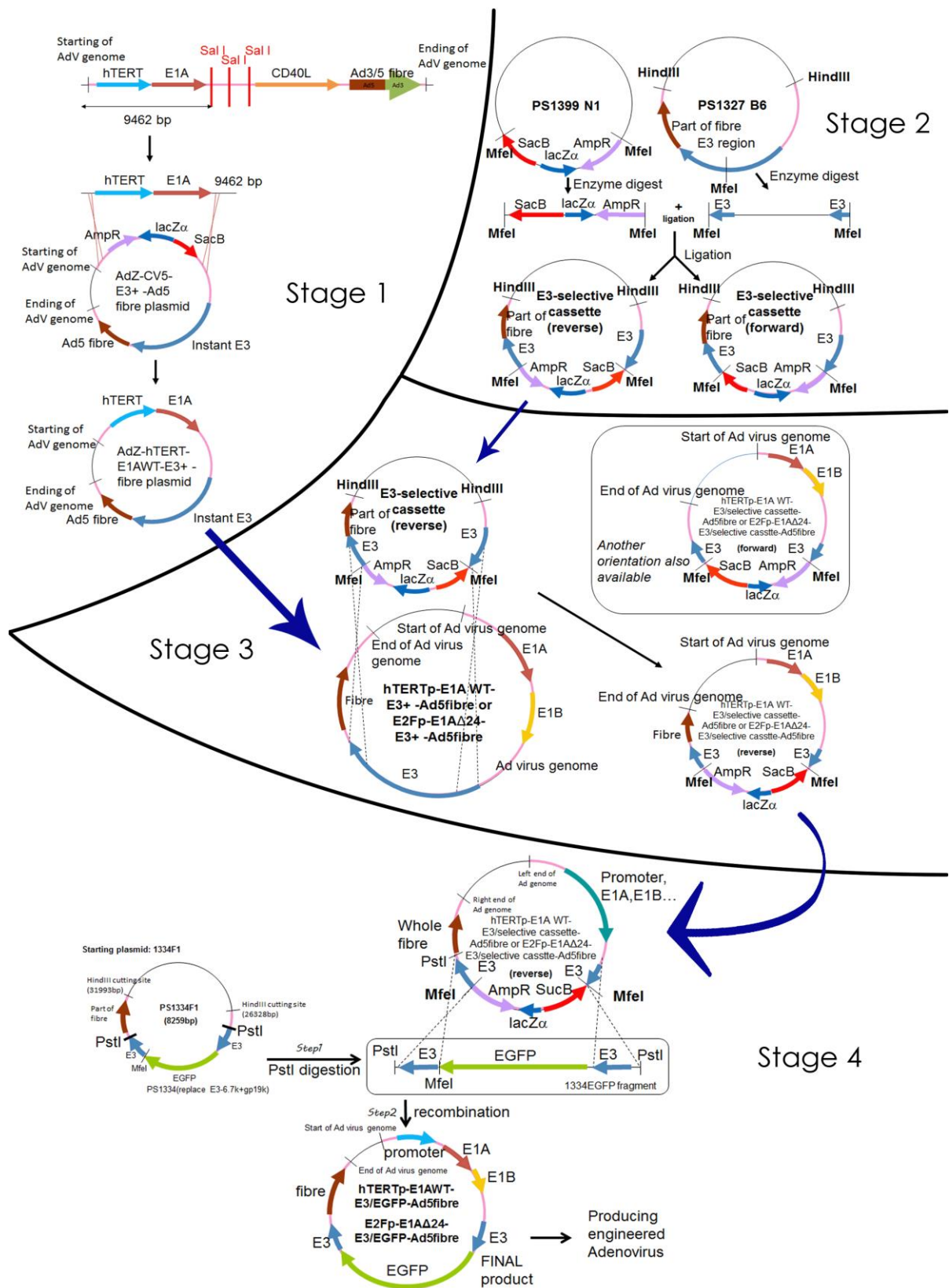


Figure 16. A schematic presentation of the construction strategy

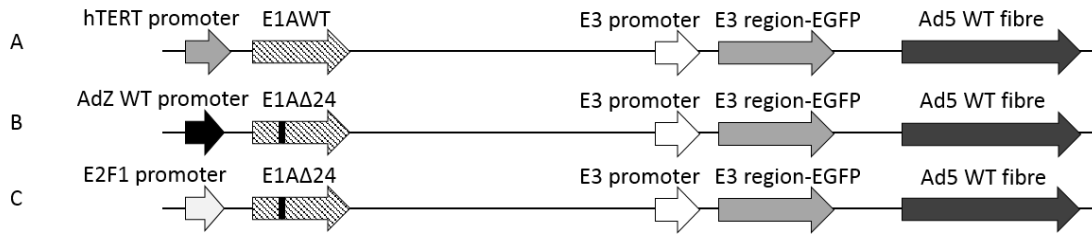


Figure 17. A schematic presentation of adenovirus constructs

(A) AdZ Adenovirus with hTERT promoter driving expression of wild-type E1A region (E1AWT). hTERT promoter, which is a promoter especially activated in telomerase over-expressing tumour cells, is intended to allow selective replication in tumour cells rather than healthy cells. We label it as virus A in the following sections. Adenovirus wild type promoter acts as a control here. (B) The selective replication of oncolytic adenovirus is dependent on E1A Δ 24. This virus is named as virus B in the following sections. (C) E2F1 promoter is selectively activated in transcription factor E2F over-expressing cell lines. E1A Δ 24 also replicates in tumour cells only. This virus is named as virus C in the following sections.

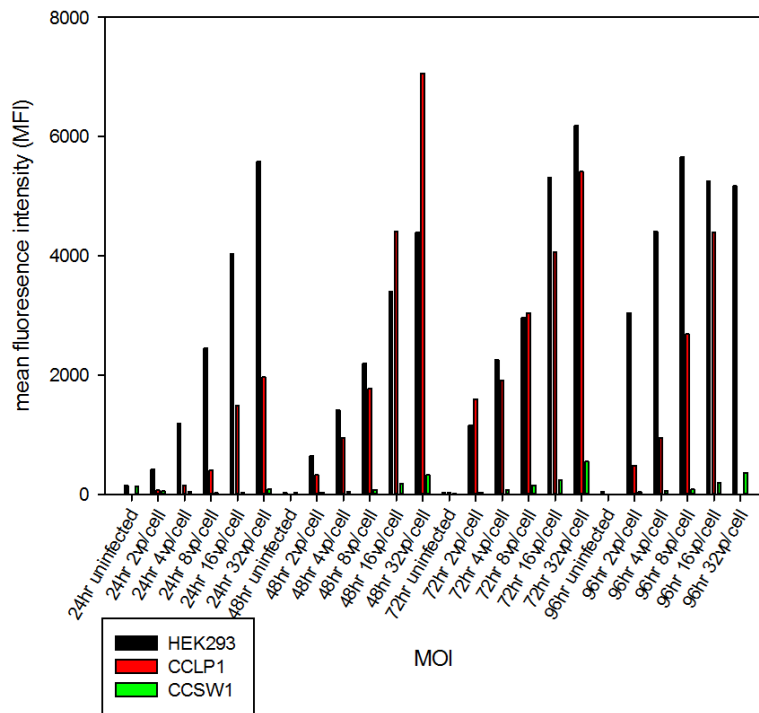
3.2 Time-course experiment

To determine the most effective viral multiplicity of infection (MOI) and the duration time of infection as well as to optimise the conditions for each cell line (HEK293, CCLP1, and CCSW1), we designed a series of time-course experiments.

For rapid screening of the effects of engineered promoter-E1A region viruses in different cells, we designed a set of time-course experiments to evaluate the best time-point and viral MOI for each cell line.

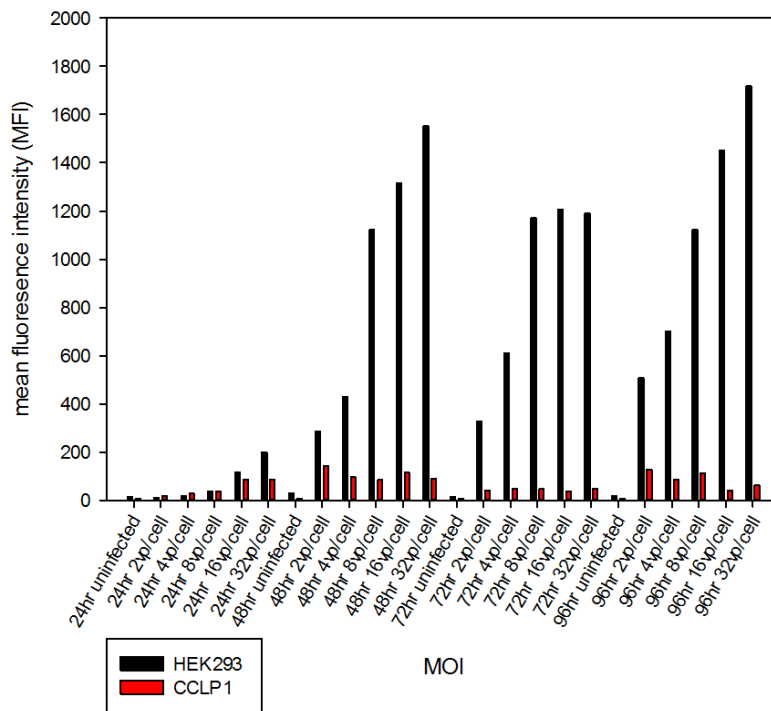
A

Mean fluorescence intensity of hTERTp-WTE1A virus (virus A) replicating in HEK293, CCLP1, CCSW1 cells by 96 hr



B

Mean fluorescence intensity of WTp-E1Adelta24 virus (virus B) replicating in HEK293 and CCLP1 cells by 96 hr



C

Mean fluorescence intensity of E2Fp-E1Adelta24 virus (virus C) replicating in HEK293, CCLP1, CCSW1 cells by 96 hr

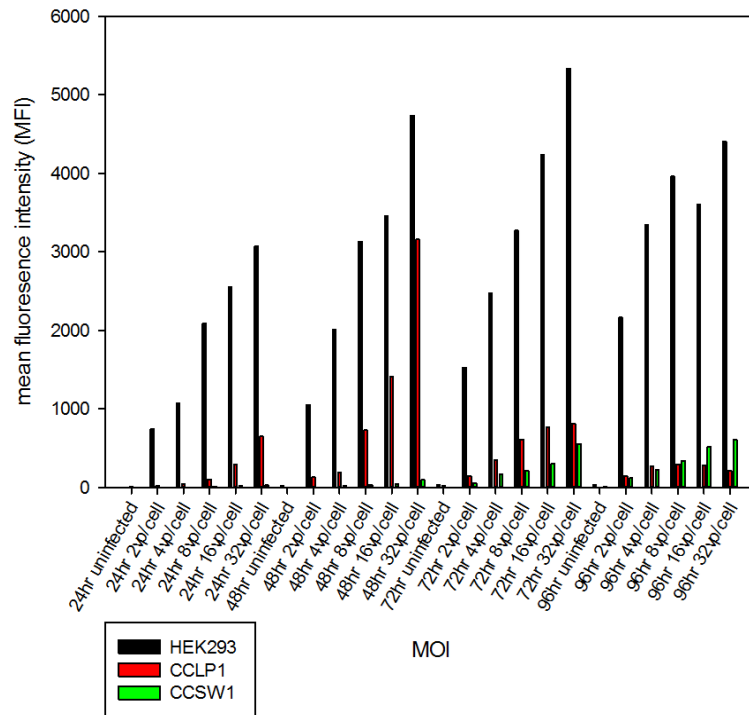


Figure 18. The trend of adenovirus replication in different cell lines within 96 h (MFI-vp/cell)

hTERT promoter-E1AWT virus (A), WT-promoter E1A 24bp-deleted virus (B), E2F-promoter E1A 24bp-deleted virus (C). HEK293, CCLP1 and CCSW1 cells were infected by replication competent viruses for 4h, and they were harvested at 24, 48, 72 and 96 h post-infection. FACS was applied to detect the signals of fluorescence.

The bar chart above suggests that the best time-point for harvesting HEK293 cells is 24 h and that a lower MOI of adenovirus (MOI = 2, 4, and 8) is sufficient to reveal the replication of viruses. On the other hand, the best harvesting time for CCLP cells is 48 h, during which the same dosage of virus can contribute to the most significant difference. In the case of CCSW cells, no significant difference was noted between each peak, either due to the low MOI (2–32) or because only very few CCSW cells were infected. Thus, increasing the MOI

and selecting the best MOI and harvesting time for CCSW cells seemed to be the best solution.

In Figure 19A, to confirm the best time for harvesting, a clear gap can be seen between the results for the uninfected group (control) and the infected group (MOI = 2, 4, 8, 16, and 32) within only 24 h. Therefore, 24 h can be considered as a sufficient duration for harvesting samples in HEK293 cells, and a lower MOI (2, 4, and 8) seemed sufficient to produce a significant result.

In Figure 19B, an overlap of the results for the uninfected group (control) and infected group (MOI = 2, 4, 8, 16, and 32) was noted at 24 h, suggesting that the CCLP cells take longer to show significantly different results.

A clear difference was noted at 48 h between the uninfected and infected groups (Figure 19C) for CCLP cells. For these cells, replication depended upon E1A expression by the viruses. Moreover, an initial lag for virus replication and EGFP expression was noted in CCLP cells compared to that in HEK293 cells.

No difference was noted between the results of the uninfected and infected groups for CCSW cells even after 48 h of the experiment (Figure 19D). In fact, even at 72 h and 96 h (data not shown), no clear-cut positive signal was noted. Therefore, a better solution was to increase the MOI to a higher level such as to 100, 300, and 1000 vp/cell, and of course, all MOI numbers I used in this project are tested in the same assays.

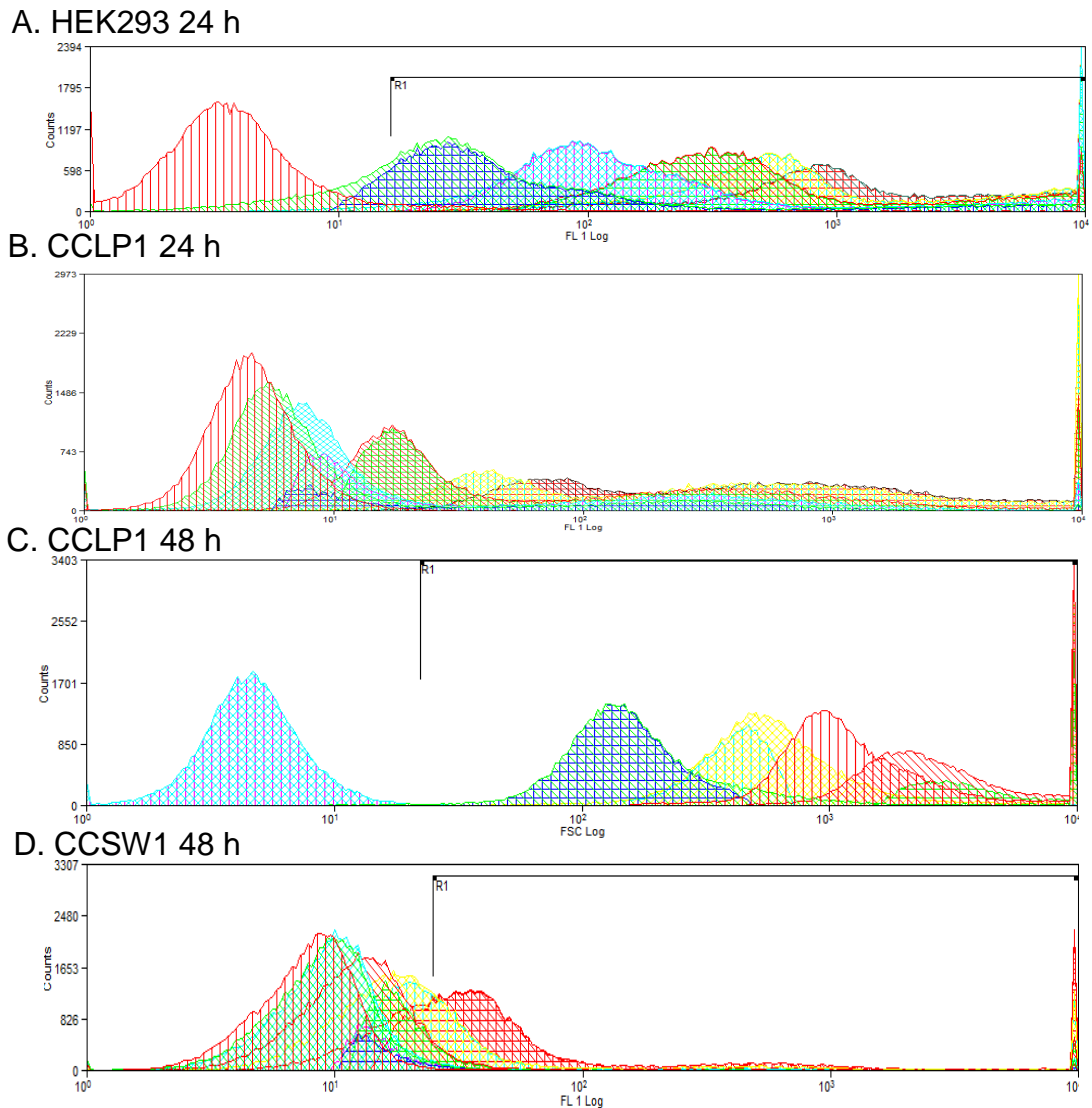


Figure 19. The histogram plot of replication-competent viruses in different cell lines within 96 h

(A) HEK293 cells 24 h (hTERTp-WTE1A virus A, red: control, blue: MOI = 2, light blue: MOI = 4, red and green: MOI = 8, green and yellow: MOI = 16, pink and blue: MOI = 32). (B) CCLP cells 24 h (hTERTp-WTE1A virus A, red: control, green: MOI = 2, light blue: MOI = 4, pink and green: MOI = 8, green and yellow: MOI = 16, pink and black: MOI = 32). (C) CCLP cells 48 h (hTERTp-WTE1A virus A, pink and light blue: control, green and blue: MOI = 2, light blue: MOI = 4, yellow: MOI = 8, red: MOI = 16, pink: MOI = 32). (D) CCSW cells 48 h (hTERTp-WTE1A virus A, red: control, green and light blue: MOI = 2, red with diagonals: MOI = 4, yellow and green: MOI = 8, red with stylish checks, diagonals: MOI = 16, pink and black: MOI = 32)

3.3 Infection experiment (flow cytometry)

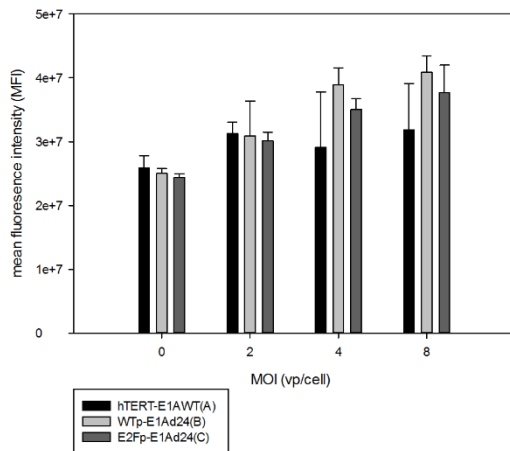
3.3.1 Replication competent (RC) viruses

After finalizing the time-point for harvesting and the suitable dosage for infection, we set up experiments to compare the differences among the effects of viruses in different cell lines.

Generally speaking, among all the data plotted by mean fluorescence intensity-MOI (vp/cell), the virus with WT promoter and E1A Δ 24 (B) had the best replication capability, and the virus with E2F promoter and E1A Δ 24 (C) was always the second, whilst the virus with hTERT promoter and WTE1A (A) replicated least well. However, since the quality of virus preparation differs, plotting by virus particle per cell may be not accurate. Thus, for most data, I also plotted the data by infection unit (IU), and sometimes the conclusion changed. To take human embryonic kidney 293 cells (HEK293) as an example, the WTp-E1A Δ 24 virus had the best replication capability in the Figures plotted by virus particle per cell (vp/cell), whereas the E2Fp-E1A Δ 24 virus replicated best as determined by infection unit (IU). Nonetheless, the intensity of GFP fluorescence of HEK293 cells was overall high. Hence, apart from the benefit of containing adenoviral E1A, E1B genes that helped virus replication, there might be some background signals in HEK293 cell. Since HEK293 cells were always harvested at 24 h, the increasing trend of viral replication might not be as dramatic as other cell lines. In the plot of infection units (IU), the E2Fp-E1A Δ 24 virus seemed the best, the WTp-E1A Δ 24 virus was second, and the hTERTp-E1A Δ 24 virus replicated least well (Figure 20).

A

Mean fluorescence intensity of hTERTp-WTE1A, WTp-E1Adelta24, E2Fp-E1Adelta24 virus replicating in HEK293 cells by 24 hr



B

Second order regression curve of Mean fluorescence intensity of hTERTp-WTE1A, WTp-E1Adelta24, E2Fp-E1Adelta24 virus replicating in HEK293 cells by 24 hr

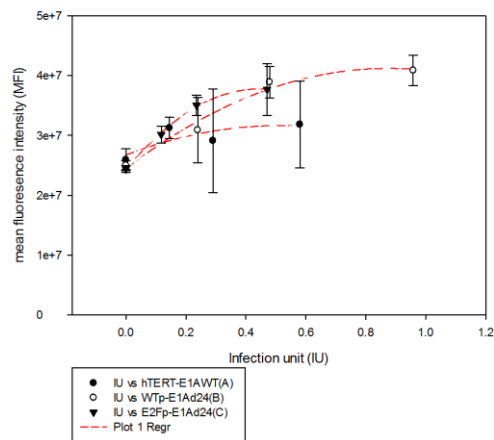


Figure 20. The replication curve of hTERT promoter-E1AWT virus, WT promoter-E1Ad Δ 24 virus, and E2F promoter-E1Ad Δ 24 virus in HEK293 cells

(A) The bar chart of hTERT promoter-E1AWT virus, WT promoter-E1Ad24 virus, and E2F promoter-E1Ad24 virus in HEK293 cells (MFI-vp/cell). (B) The replication curve was re-plotted based on MFI versus infection unit/cell. HEK293 cells were infected by replication competent viruses for 4 h, and they were harvested at 24h post-infection. FACS was applied to measure the fluorescence. The error bars are standard deviation of technical repeats of experiments.

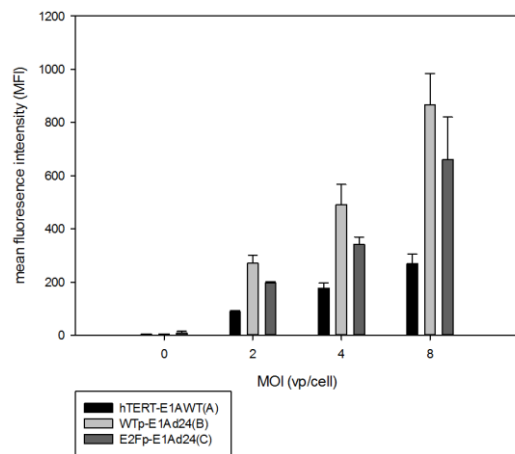
In CCLP-1, the MFI-MOI plot revealed that WTp-E1A Δ 24 virus (B) showed the best replication capability, followed by E2Fp-E1A Δ 24 virus (C), while virus A, with hTERT promoter and wild-type E1A, showed the worst infection capability (Figure 21).

However, the functional virus titer varies between virus preparations, and the same volume of virus stocks with same MOI may contain unequal functional titers; that is, the use of virus particles to measure the infection efficacy may not reflect the actual infection in cells. Hexon staining was performed to quantitate the infection unit (IU) of these viruses 1 or 2 days post-infection; in this assay, the amounts of viral hexon protein in HEK293 cells was determined, and IU

numbers were calculated. This assay allowed re-plotting of the data obtained as mean fluorescence intensity (MFI) versus IU/cell. The graph of this assay is presented in Figure 21B; based on this new plot, our interpretation changed to the following: E2Fp-E1A Δ 24 virus (C) showed the best replication ability, followed by WTp-E1A Δ 24 virus (B), and finally, hTERTp-WTE1A virus (A).

A

Mean fluorescence intensity of hTERTp-WTE1A, WTp-E1A Δ 24, E2Fp-E1A Δ 24 virus replicating in CCLP1 cells by 48 hr



B

Second order regression curve of Mean fluorescence intensity of hTERTp-WTE1A, WTp-E1A Δ 24, E2Fp-E1A Δ 24 virus replicating in CCLP1 cells by 48 hr

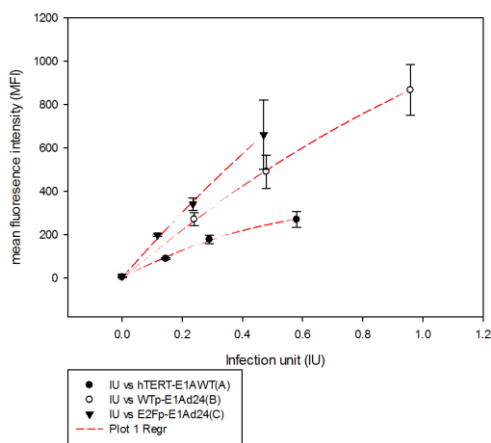


Figure 21. The replication curve of hTERT promoter-E1AWT virus, WT promoter-E1A Δ 24 virus, and E2F promoter-E1A Δ 24 virus in CCLP1 cells

(A) The bar chart of hTERT promoter-E1AWT virus, WT promoter-E1A Δ 24 virus, and E2F promoter-E1A Δ 24 virus in CCLP1 cells (MFI-vp/cell). (B) The replication curve was re-plotted based on MFI versus infection unit/cell. CCLP1 cells were infected by replication competent viruses for 4 h, and they were harvested at 48h post-infection. FACS was applied to measure the fluorescence signals. The error bars are standard deviation of technical repeats of experiments.

On the basis of the low infected rate of CCSW1 cells (supported by previous data), we decided to increase the MOI up to 100, 300 and 1000 vp/cell for infection experiment. No matter under 100, 300 or 1000vp/cell or plotted by vp/cell or IU/cell, the conclusion consisted. For CCSW1 cells, irrespective of plotting the results in vp/cell or IU/cell, WTp-E1A Δ 24 (B) virus showed the best

replication ability, followed by E2Fp-E1A Δ 24 virus (C), and, finally, hTERTp-E1AWT virus (A).

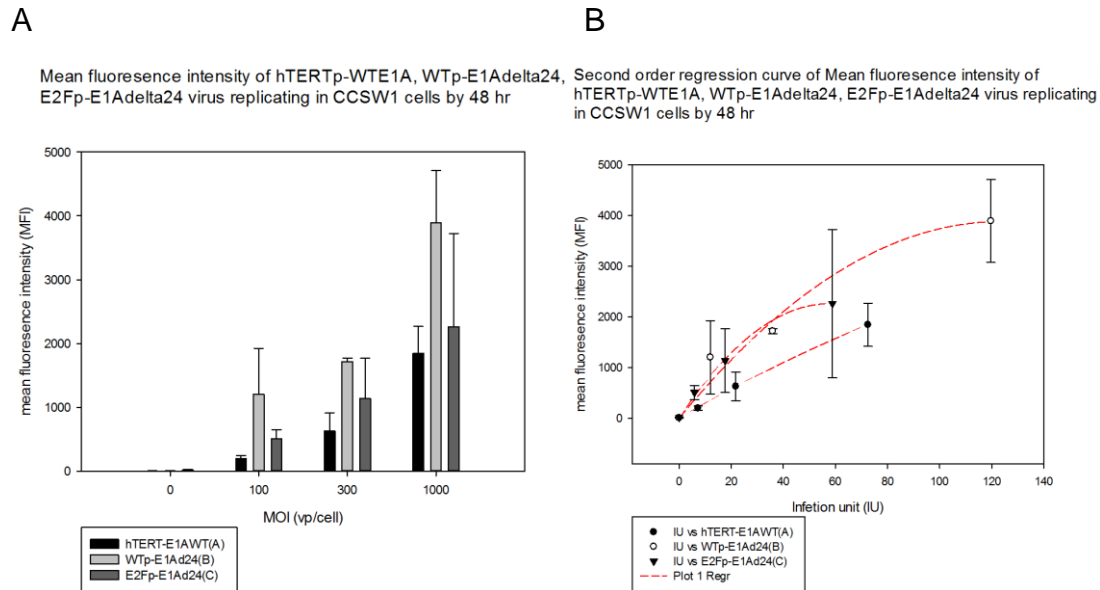


Figure 22. The replication curve of hTERT promoter-E1AWT virus, WT promoter-E1A Δ 24 virus, and E2F promoter-E1A Δ 24 virus in CCSW1 cells

(A) The bar chart of hTERT promoter-E1AWT virus, WT promoter-E1A Δ 24 virus, and E2F promoter-E1A Δ 24 virus in CCSW1 cells. This Figure was plotted based on MFI versus vp/cell. (B) For a more accurate interpretation and explanation regarding the replication efficacy, the Figure was re-plotted based on MFI versus infection unit. CCSW1 cells were infected by replication competent viruses for 4 h and harvested at 48h post-infection. FACS was applied to measure the fluorescence signals. The error bars are standard deviation of technical repeats of experiments.

3.3.2 Replication defective (RD) viruses

In addition to the replication-competent viruses, I also studied the replication-defective viruses in HEK293 and cholangiocarcinoma cells to test which fibre gave highest infection efficiency. In HEK293 cells, approximately 20% of cells showed a positive fluorescence signal at 24 h post-infection at MOI = 8 (Figure 23A). Because there was little variation between signals obtained in replicates with each virus, we therefore assumed that Ad5 wild-type fibre may have similar efficacy for virus infection as that with Ad5/3 chimera fibre and Ad5/FMD

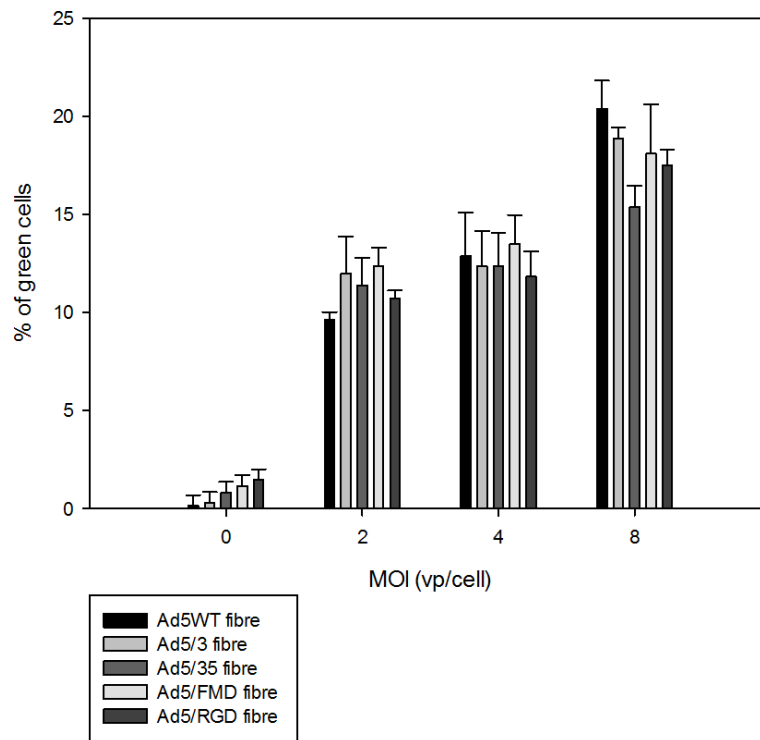
chimera fibre. The infection efficacy with Ad5 wild-type fibre was slightly better than that with Ad5/RGD chimera fibre in infecting HEK293 cells, while the Ad5/RGD chimera fibre gave marginally better infection efficacy than the Ad5/35 fibre. The results suggest that the Ad5 wild-type fibre could induce infection more efficiently than Ad5-RGD chimera fibre and Ad5/35 chimera fibre in normal human cells. Nonetheless, although there were small differences in rankings, basically there were no significant differences in infection efficiencies, which meant that HEK293 cells serve as a good negative control.

However, in the case of CCLP1 cells, because of the large and overlapping error bars obtained (Figure 23B), it was hard to deduce which of the fibres was more effective in facilitating infection of cholangiocarcinoma cells. It appears that virus with Ad5/RGD chimera fibre may be more efficient than the one with Ad5/3 chimera fibre and that the Ad5/3 chimera fibre virus may be more efficient than that with Ad5/35 chimera fibre. For viruses with Ad5 wild-type fibre and Ad5-FMD fibre, it was difficult to interpret the results because of the large error bars obtained.

In the case of CCSW1 cells, apart from viruses with Ad5/FMD chimera fibre and Ad5/3 chimera fibre, the ranking of the other viruses were not conclusive because of the low rate of infection. We used the same MOI for each cell line; as expected, HEK293 cells showed the fastest and highest infection efficiency. CCLP1 cells reacted slowly, but sensitively, to viruses. Thus, CCSW1 cells were not only non-sensitive but also slow responders to the viral infections. However, the valuable conclusion obtained was that Ad5/FMD chimera fibre and Ad5/3 chimera fibre are relatively efficient for infecting cholangiocarcinoma cells (Figure 23C), which is worth further optimizing for treatments.

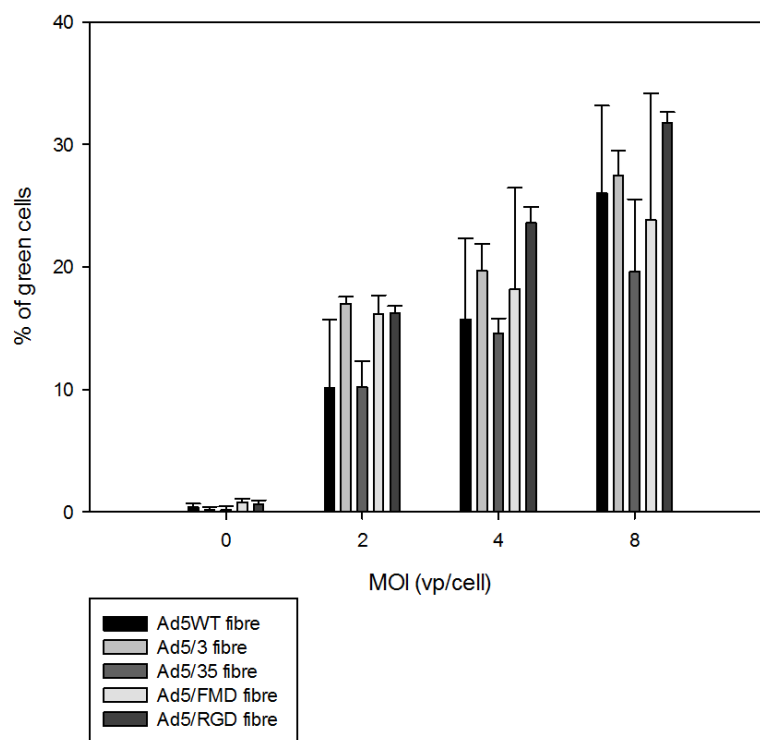
A

The infection efficacy of variable fibres in HEK293 cells



B

The infection efficacy of variable fibres in CCLP1 cells



C

The infection efficacy of variable fibres in CCSW1 cells

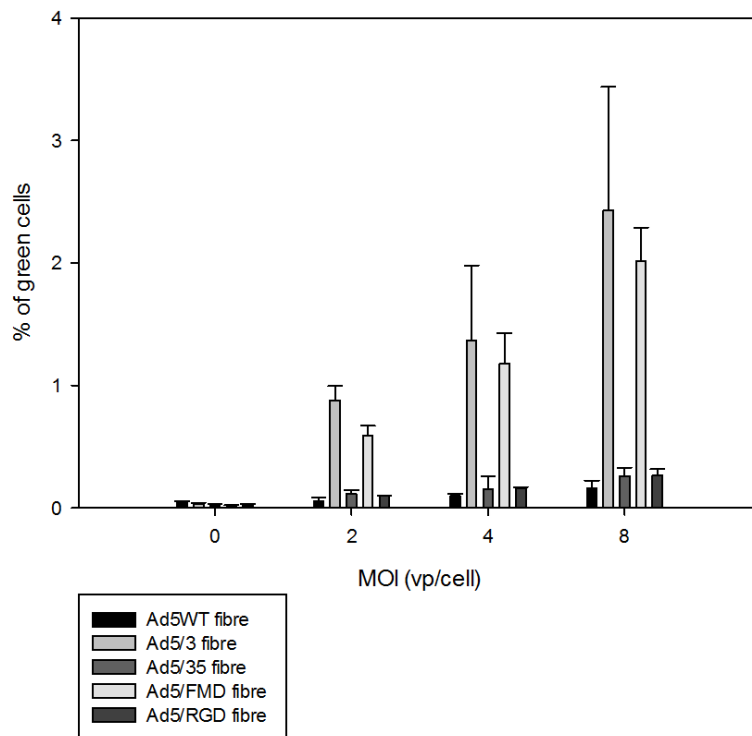


Figure 23. The percentage of fluorescence positive HEK293, CCLP1 and CCSW1 cells at 24 h or 48 h post-infection by fibre-modified viruses at 2, 4 and 8 vp/cell concentrations.

(A) The percentage of positive cells in HEK293 cells 24 h post-infection. (B) The percentage of positive cells in CCLP1 cells 48 h post-infection. (C) The percentage of positive cells in CCSW1 cells 48 h post-infection. HEK293, CCLP1 and CCSW1 cells were infected by fibre-modified viruses for 1 h and were harvested at 24 or 48h post-infection. FACS was applied to measure the fluorescence signals. The error bars are standard deviation of technical repeats of experiments.

To compare the infection efficiencies in CCSW1 cells, we increased the MOI to 100, 300, and 1000 vp/cell and subsequently measured fluorescence. The results showed large and overlapping error bars, making it difficult to reach a reliable conclusion. Under MOI=1000, there was no significant differences in infection efficacy because of the high virus/cell ratio. At 100 vp/cell, Ad5/35 chimera fibre is still the least efficient for viral host cell entry, and the higher MOI indeed promotes Ad5WT fibre virus infection. To sum up, the results

suggested that Ad5/3 chimera fibre was potentially most effective either under low or high MOI, followed by Ad5/FMD chimera fibre and Ad5WT fibre in CCSW1 cells. It was difficult to determine the sequence of effectiveness for other agents. Considering Ad5WT fibre as a control here, the results suggested that viruses containing Ad5/3 chimera fibre and Ad5/FMD chimera fibre were worth further optimizing.

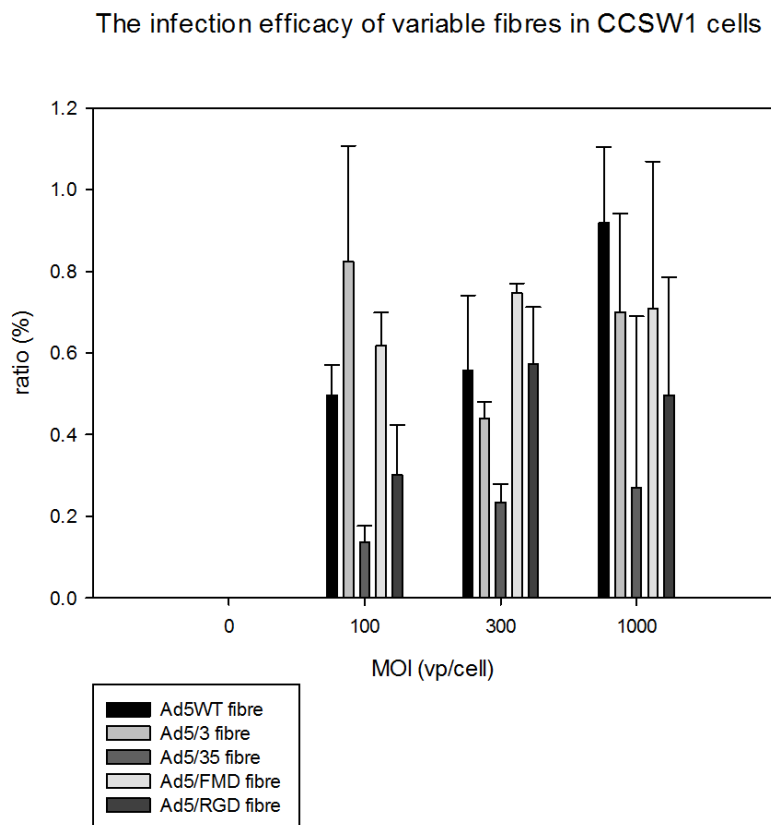


Figure 24. The mean fluorescence intensity ratio of CCSW1 cells at 48 h post-infection

CCSW1 cells were infected by fibre-modified viruses in 100, 300, and 1000 vp/cell for 1 h, and the samples were harvested 48 h post-infection. Then, FACS was used to measure the MFIs. The ratio was calculated from MFI of samples minus MFI of uninfected samples, divided by the MFI of uninfected samples. The error bars represent the standard deviations of technical repeats of this experiment.

3.4 Infection experiment (qPCR)

In the above experiments, the expression level of EGFP was used to indicate the relative level of virus replication in the cells. As a more accurate measurement of virus entry and replication, qPCR was used to quantitate the copy number of viral genomes per cell.

We selected MOI = 8 vp/cell to infect all the cells and then harvested the samples at 24 h, 48 h and 72 h. All three replication-competent viruses started replicating by 24 h (444–1560 DNA copy/cell) (Figure 25A). A large increase in the viral load was noted between 24 h and 48 h, while only a marginal increase was noted by 72 h. In contrast, the copy number of a replication-defective (E1-deleted) virus decreased to <1 copy/cell on days 1 and 2 (Figure 25B).

WT promoter-E1A Δ 24 virus (B) was the most effective virus to infect CCLP1 cells, followed by E2F promoter-E1A Δ 24 virus (C) and, finally, hTERT promoter-E1AWT virus (A). In general, WT promoter-E1A Δ 24 (B) and E2F promoter-E1A Δ 24 (C) viruses were more efficient than hTERT promoter-E1AWT virus (A), as ascertained in the flow cytometry experiments (Figure 21). We also found that, as compared to the control group and replication-defective virus (RD virus with wild-type fibre) (Figure 23 B), cells infected with the replication-competent viruses had 113, 972, and 519 adenoviral gene copy/cell, while cells infected with the replication-defective virus had only 0.5 copy/cell (Figure 25B).

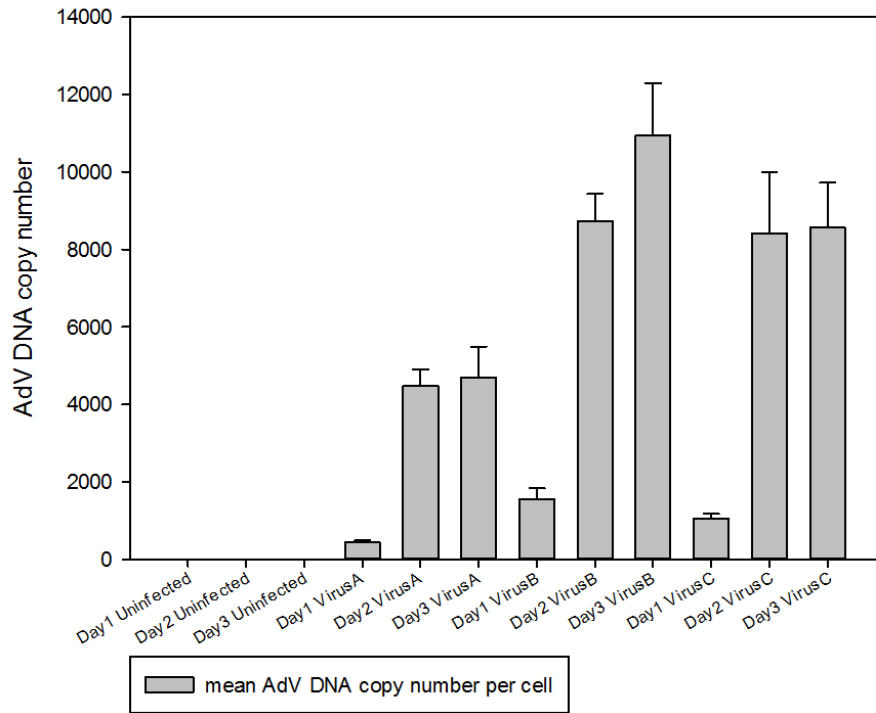
A similar experiment was performed using CCSW1 cells. However, as these cells were poorly infected, we used a higher MOI of 300 vp/cell. Surprisingly, viruses WTp-E1A Δ 24 (B) and E2Fp-E1A Δ 24 (C) reached 8440 and 5810

copy/cell at only 24 h post-infection, although the copy numbers decreased by 48 h and 72 h post-infection. Virus A reached 163 copy numbers/cell on day 1 (versus 444 copy numbers/cell in CCLP cells) and approximately 2500 copy numbers/cell on days 2 and 3.

Under a high MOI of 300, WT promoter-E1A Δ 24 virus (B) showed the most rapid infection, followed by E2F promoter-E1A Δ 24 virus (C) and hTERT promoter-E1AWT virus (A). As shown in Figure 18C, the copy number of hTERT promoter-E1AWT virus (A) RC viral gene increased in cells with time, while those of the WT promoter-E1A Δ 24 virus (B) and E2F promoter-E1A Δ 24 virus (C) decreased.

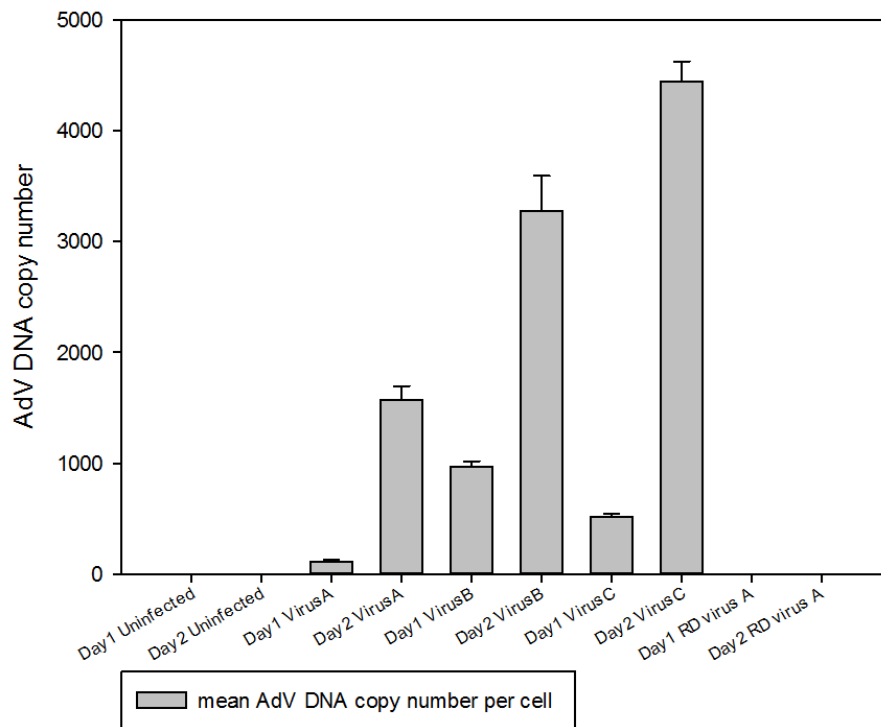
A

Adenovirus DNA copy number per CCLP cell in 72 hr



B

Adenovirus DNA copy number per CCLP cell in 48 hr



C

Adenovirus DNA copy number per CCSW cell in 72 hr

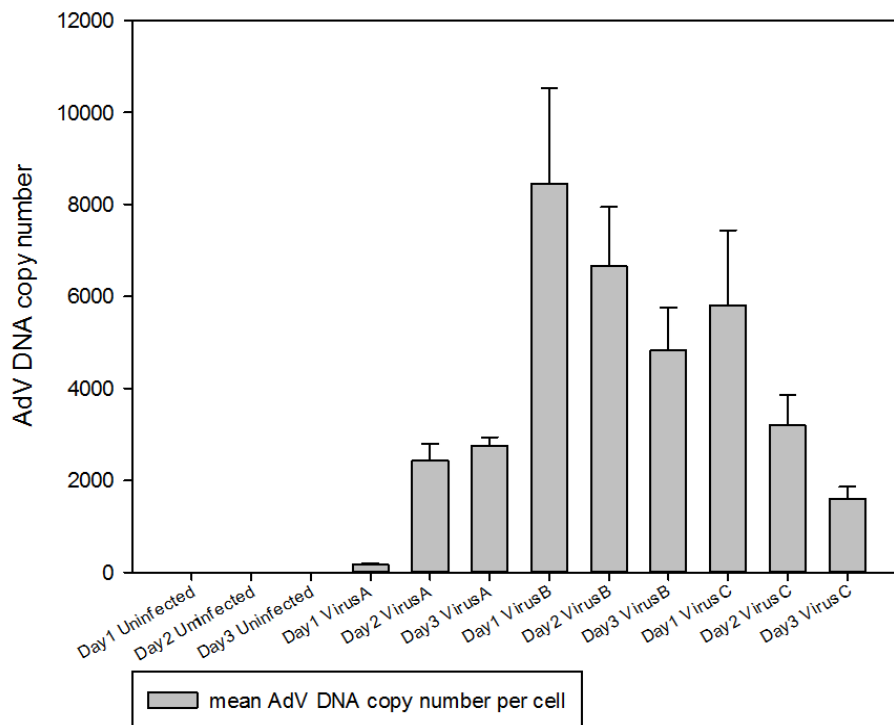


Figure 25. The adenovirus copy number per cell in cholangiocarcinoma cells on post-infection days 1, 2, and 3

(A) The bar chart represents the copy number of adenovirus genomes detected by qPCR in CCLP1 cells at 24 h and 48 h post-infection, and a replication-defective adenovirus was used as an internal control. (B) The copy number of adenovirus in CCLP1 cells at 24, 48, and 72 h. (C) The copy number of adenovirus in CCSW1 cells at 24, 48, and 72 h. CCLP1 and CCSW1 cells were infected by replication competent virus (hTERTp-E1AWT (A), WTP-E1A Δ 24 (B), E2Fp-E1A Δ 24 (C)) and replication defective virus A(Ad5WT fibre) for 90min, thereafter harvesting at 24, 48 and 72 h respectively. A kit was used to harvest the DNA sample, and these samples were quantified by qPCR. The error bars represent the standard deviation of technical repeats of this experiment

3.5 Cell viability assay

3.5.1 Oncolytic effects of viruses in human cells (HEK293, CCLP, CCSW)

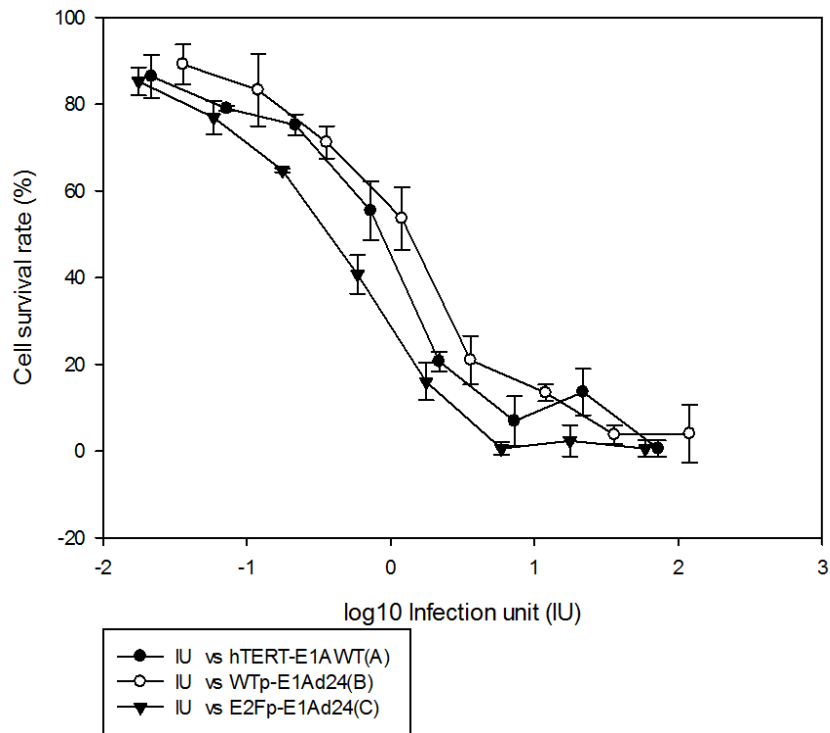
In the infection experiments using both flow cytometry and qPCR, the replication efficacy of the replication-competent (RC) adenoviruses was the

variable of interest. However, the efficacy of replication does not accurately represent the oncolytic effect of RC viruses. We therefore set up an experiment to compare oncolytic effect among RC viruses. One of the commonly used methods for this purpose is MTT assay; MTT (3-(4,5-dimethylthiazol-2-yl)-2,5-diphenyltetrazolium bromide) is a yellow tetrazolium dye that can enter the cell's mitochondria, and the NAD(P)H-dependent cellular oxidoreductases in the mitochondria can transform MTT (yellow) to formazan (purple). Because NAD(P)H flux is required in this pathway, cellular metabolic activity is highly related to the reduction of MTT substrates; highly active cells transform most of the tetrazole into the purple soluble formazan form. In contrast, cells with low metabolic rates produce little formazan, and hence the purple colour intensity is low. Thus, cell activity could be measured simply by using spectrophotometry.

For HEK293 cells, the time-point of 3 days was found to be appropriate. At the lowest MOI of 0.3, approximately 90% of the cells remained alive, while essentially no viable cells remained at the higher MOI of 100–1000. The scatter plot indicated a dose-dependent cell death curve. When the survival of cells was plotted against log₁₀ IU (Figure 26), the oncolytic effects of RC viruses rank in the following order: E2Fp-E1AΔ24 (C) ≥ hTERTp-E1AWT (A) ≥ WTp-E1AΔ24 (B). However, the differences in oncolytic effect with these RC viruses were very small. In addition, on day 6 the IC₅₀ (indicating that >50% of the cells were dead) of even the least-effective virus (WTp-E1AΔ24 (B)) decreased to 2 vp/cell (MOI, data not shown). Low viability overall meant that the data for day 9 were not very meaningful. Nevertheless, all the data for days 3, 6 and 9 were consistent regarding the ranking of viruses, i.e., E2Fp-E1AΔ24 (C) ≥ hTERTp-E1AWT (A) ≥ WTp-E1AΔ24 (B).

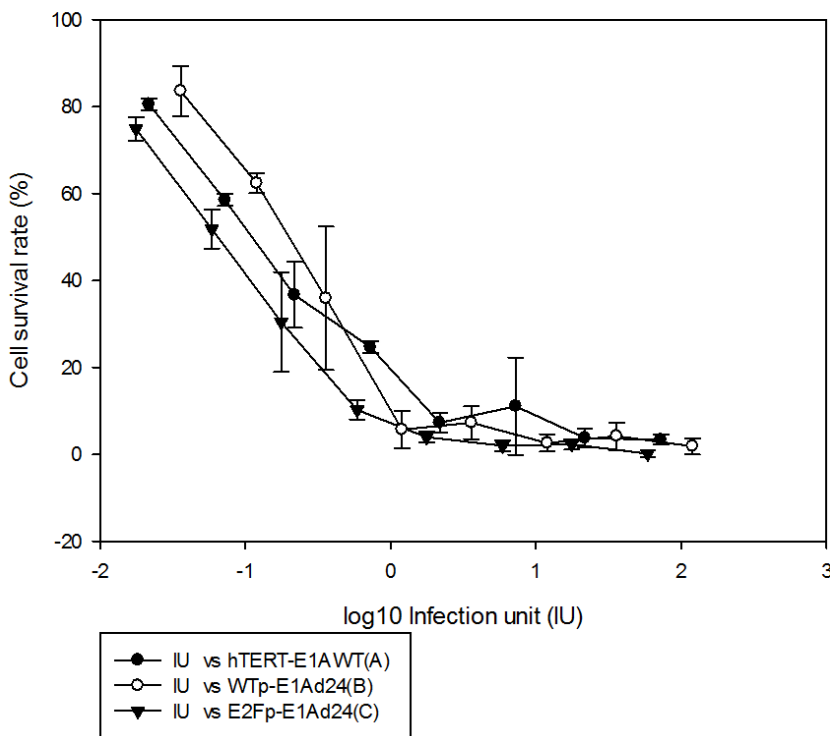
A

Survival Rate in HEK293 Cells by Day3



B

Survival Rate in HEK293 Cells by Day6



C

Survival Rate in HEK293 Cells by Day9

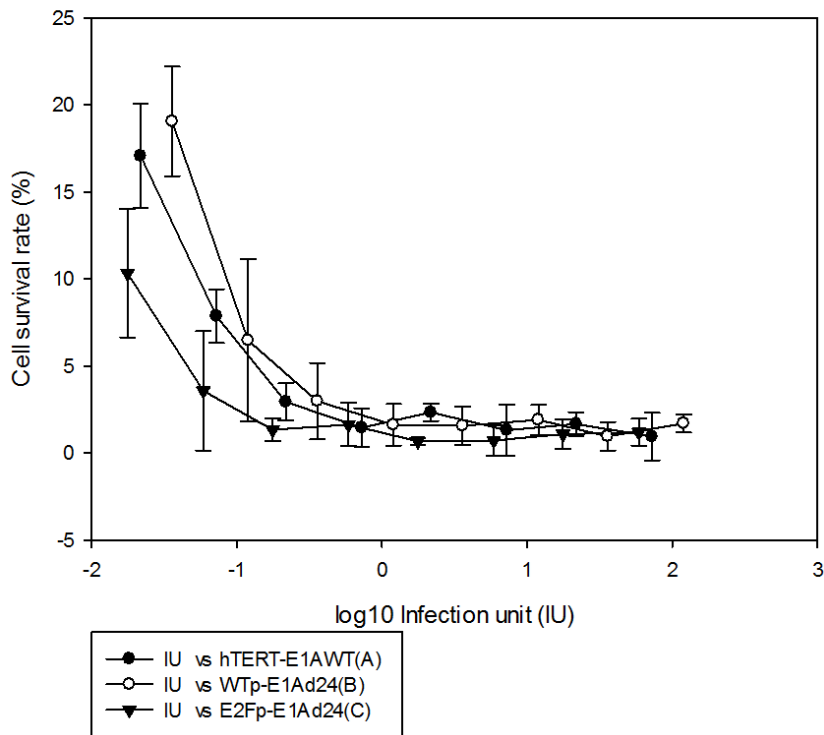


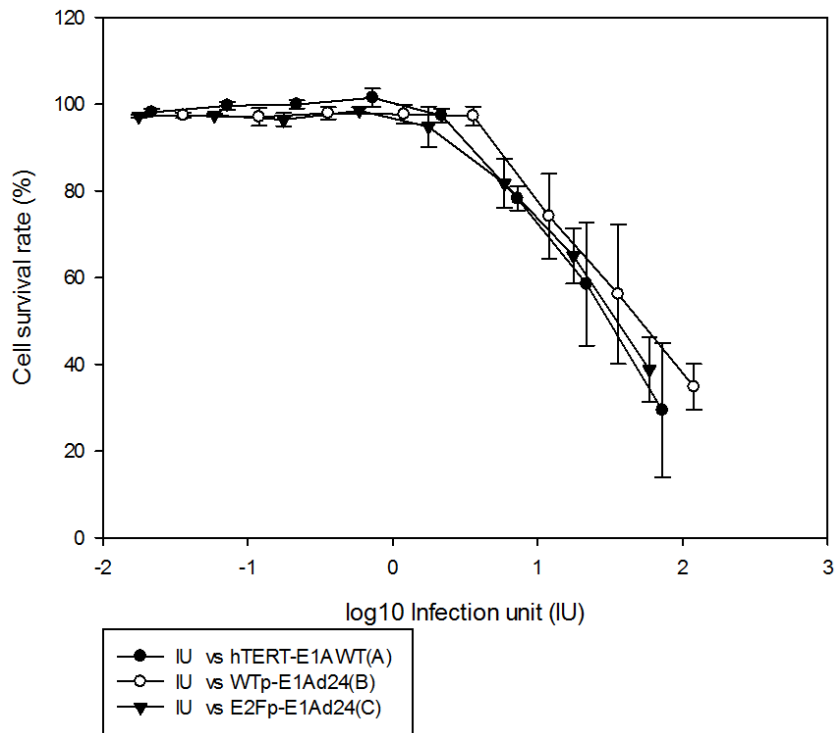
Figure 26. The cell survival rate of HEK293 cells on post-infection days (A) 3, (B) 6, and (C) 9. HEK293 cells were infected by replication competent viruses (hTERTp-E1AWT, WTp-E1AΔ24 and E2Fp-E1AΔ24) for 2h, followed by adding new medium and harvesting supernatant at days 3, 6 and 9 for MTT assay. The error bars are calculated from the technical repeats of the cell viability assay.

For CCLP1 cells, the plots were difficult to interpret (Figure 27). Although the day 3 curves were very close to each other, they could be interpreted as follows: hTERT promoter-E1AWT virus (A) was better than E2F promoter-E1AΔ24 virus (C) and both these viruses induced more oncolysis than WT promoter-E1AΔ24 virus (B). However, on day 6, although the curves overlapped, the virus ranking was determined to be A > C > B. On day 9, the ranking order changed: E2F promoter-E1AΔ24 virus (C) reduced cell viability most followed by hTERT promoter-E1AWT virus (A), and, finally, WT promoter-E1AΔ24 virus (B). Thus, hTERT promoter-E1AWT (A) virus was overall most efficient in inducing cell

death. As CCLP1 cell death was observed in MTT assays by day 3, it is reasonable that this would affect the results of the previous infection experiments (by flow cytometry and qPCR). In these experiments, dead cells were removed in the washing steps, and thus were not harvested and measured. The results of flow cytometry and qPCR experiments indicated that the WT promoter-E1A Δ 24 virus (B) functioned better than E2F promoter-E1A Δ 24 virus (C), and E2F promoter-E1A Δ 24 virus (C) replicated more efficiently than hTERT promoter-E1AWT virus (A). However, the MTT assay suggested the reverse, i.e., hTERT promoter-E1AWT virus (A) \geq E2F promoter-E1A Δ 24 virus (C) \geq WT promoter-E1A Δ 24 virus (B). These results suggest that the replication efficacy of RC viruses might not truly reflect the oncolytic effects of these viruses. If hTERT promoter-E1AWT virus (A) is indeed the best to induce cell death, it is reasonable there might be the less live cells remaining to test for infection efficiency. Thus, there may be no actual conflict between the two sets of results. However, since the curves are close to each other, cell viability assays could be repeated to get a clearer conclusion. In all, the MTT results demonstrated that hTERTp-E1AWT and E2Fp-E1A Δ 24 viruses induce more cell death in CCLP1 cells.

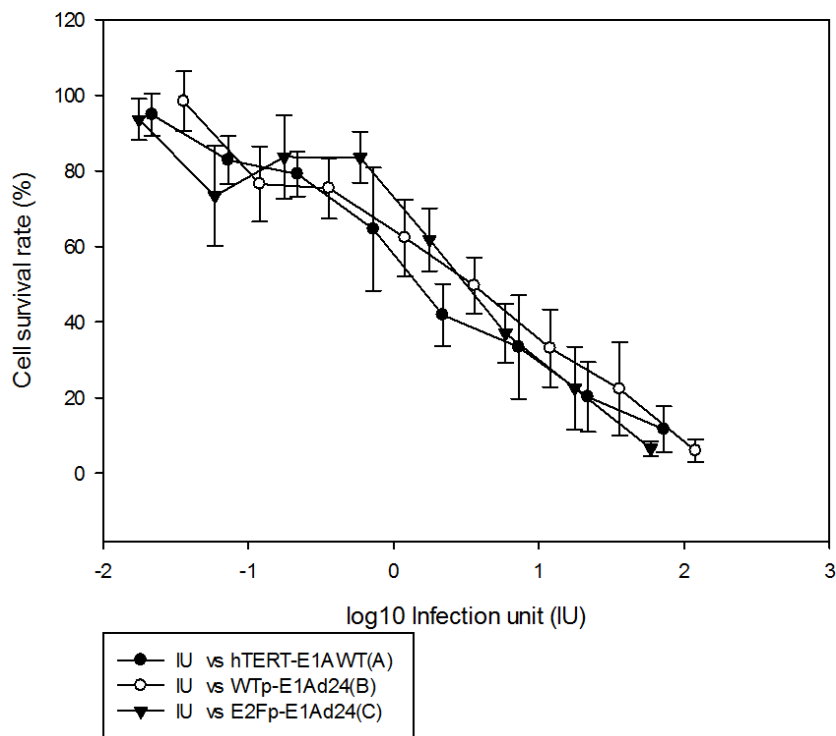
A

Survival Rate in CCLP1 Cells by Day3



B

Survival Rate in CCLP1 Cells by Day6



C

Survival Rate in CCLP1 Cells by Day9

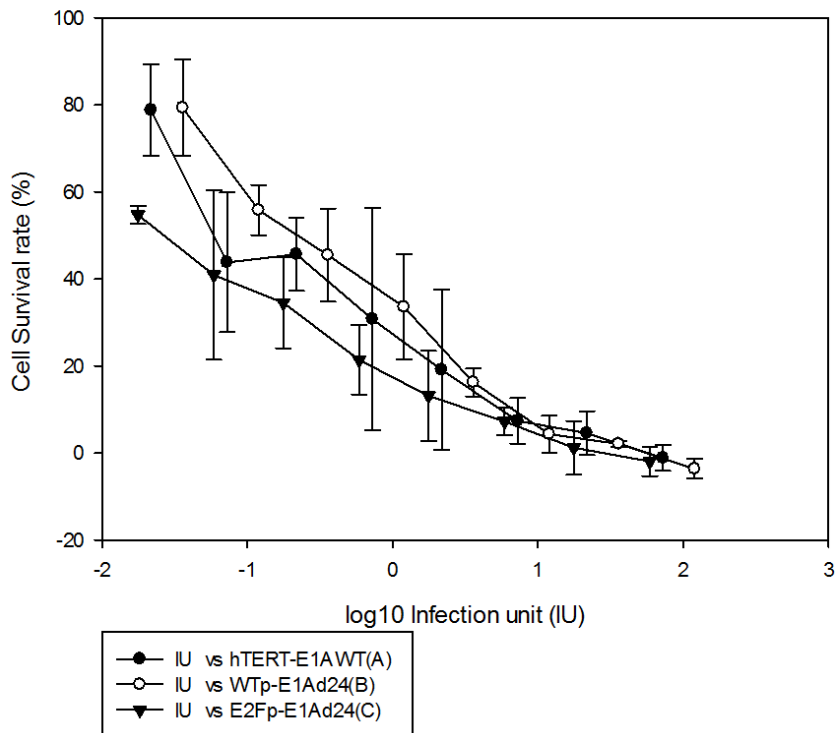
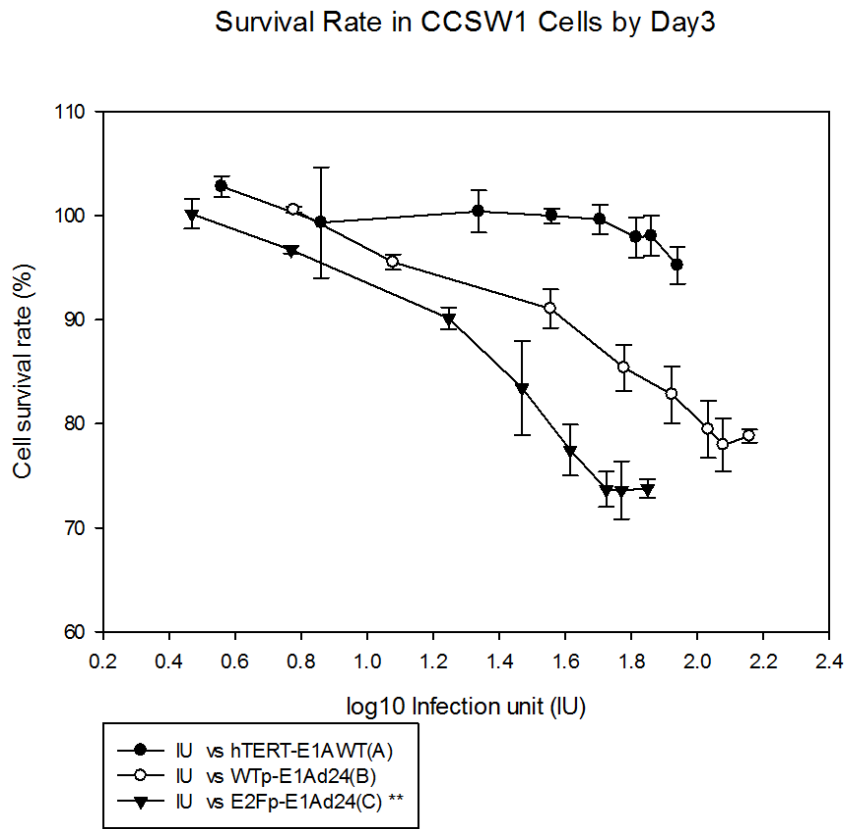


Figure 27. The cell survival rate of CCLP1 cells on post-infection days 3 (A), 6 (B) and 9 (C). CCLP1 cells were infected by replication competent viruses (hTERTp-E1AWT, WTp-E1AΔ24 and E2Fp-E1AΔ24) for 2h, followed by adding new medium and harvesting supernatant at days 3, 6 and 9 for MTT assay. The error bars are calculated from the technical repeats of cell viability assay.

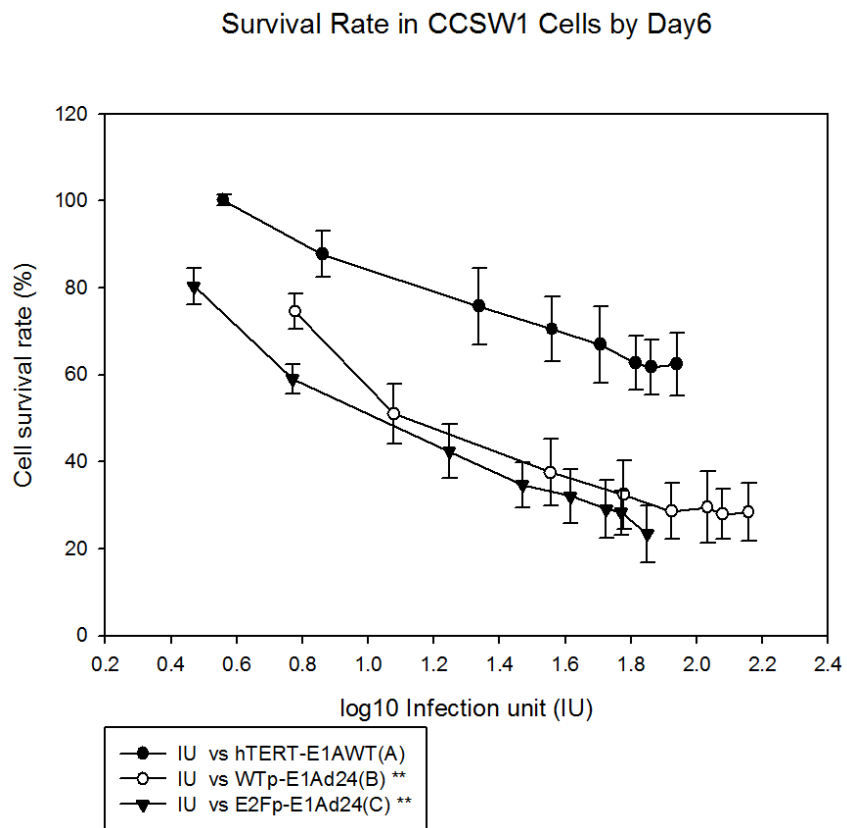
With respect to the viability of CCSW cells, the results shown in each of the plots indicated the following order of effectiveness: E2F promoter-E1AΔ24 virus (C) ≥ WT promoter-E1AΔ24 virus (B) > hTERT promoter-E1AWT virus (A) (Figure 28). Although the infection experiments assessed by flow cytometry and qPCR suggested that the order of effectiveness of the viruses was B > C > A, the order C ≥ B > A was consistent with the results of MTT assays. Therefore, the replication efficacy of RC viruses cannot truly represent the oncolytic effects of these viruses. In this case, it can be concluded that both WTp-E1AΔ24 and E2Fp-E1AΔ24 have better oncolytic function than hTERTp-E1AWT in CCSW1

cells. Although the hTERT promoter is more selective than the WT promoter, it did not increase oncolysis in CCSW1 cells. Furthermore, the hTERTp-E1AWT virus showed the weakest replication capacity in FACs and qPCR experiments (Figures 22 and 25C).

A



B



C

Survival Rate in CCSW1 Cells by Day9

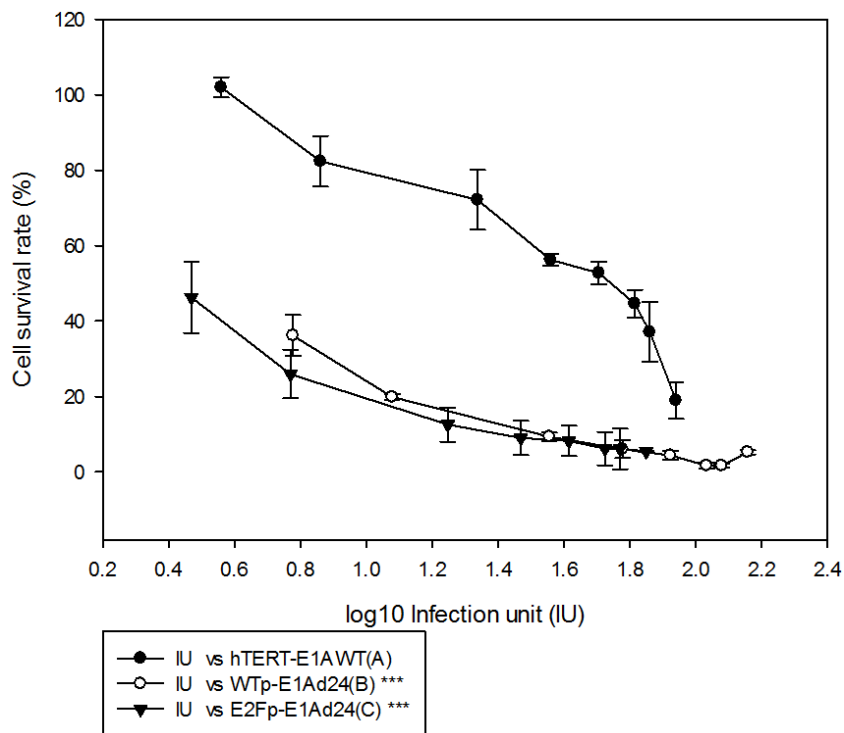


Figure 28. The survival rate of CCSW1 cells on post-infection (A) days 3, (B) day 6, and (C) day 9. (A) On day 3, the difference between cells infected with hTERT-E1AWT and E2Fp-E1AΔ24 was statistically highly significant (**), p-value = 0.009. (B) On day 6, the differences between cells infected with hTERT-E1AWT and WTp-E1AΔ24 and E2Fp-E1AΔ24 were both highly significant (**), p-value = 0.005. (C) On day 9, the differences between cells infected with hTERT-E1AWT and WTp-E1AΔ24 and E2Fp-E1AΔ24 were both extremely significant (***), p-value = 0.001.

CCSW1 cells were infected by replication competent viruses (hTERTp-E1AWT, WTp-E1AΔ24, and E2Fp-E1AΔ24) for 2 h, followed by the addition of new medium and harvesting at days 3, 6, and 9 (MTT assay). The error bars are calculated from the technical replicates of the cell viability assay.

Table 4. IC₅₀ of the cell viability assay (HEK293, CCLP1, CCSW1 cells)

IC50	A	B	C	IC50	A	B	C	IC50	A	B	C
293 DAY3	11.8781	11.30374	6.285639	CCLP DAY3	426.2707	424.6143	597.6268	CCSW DAY3	>1200	>1200	>1200
293 DAY6	1.533989	1.671525	1.100558	CCLP DAY6	20.26461	29.09556	53.36887	CCSW DAY6	>1200	108.6958	181.2974
293 DAY9	<0.3	<0.3	<0.3	CCLP DAY9	0.807824	1.854148	0.453285	CCSW DAY9	762.7191	<50	<50

* All the numbers above represent in MOI (vp/cell). The MOIs for HEK293 and CCLP1 cells in MTT assays range from 0.3 to 1000 vp/cell, while the MOI for CCSW1 cells ranges from 50 to 1200 vp/cell.

3.5.2 Coinfection experiment

Because of the multiple functions of CD40L that may influence the anti-tumour efficacy of oncolytic viruses, CD40L viruses were constructed to determine its effectiveness in viral infection. We compared the cooperative cytotoxicity using an MTT assay to detect the effect of the CD40L virus.

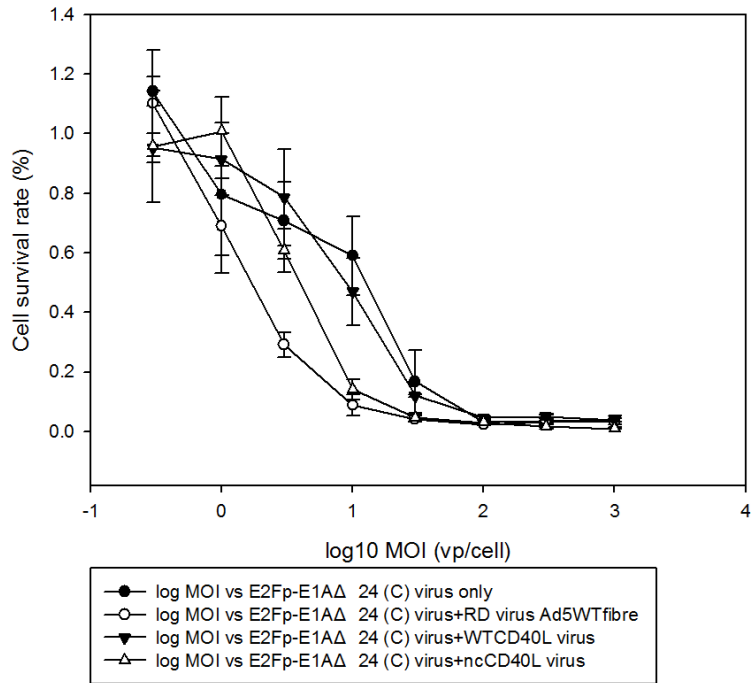
In the co-infection experiment, slight cytotoxicity of nc40L viruses toward CCLP cells was noted on day 6, with a cell survival rate of approximately 75–80% (Figure 29). In the experimental group, an oncolytic effect was identified for a combination of replication-competent virus C (E2Fp-E1AΔ24) and replication-defective viruses (CMVp-EGFP, CMVp-WT CD40L, CMVp-nc CD40L). All the viruses used in this experiment contained Ad5 WT fibres.

As expected, the oncolytic effect of replication-competent virus C (E2Fp-E1AΔ24) only (as an internal control) was found to be the weakest. However, unexpectedly, the combination of the E2Fp-E1AΔ24 virus (C) and CMVp-EGFP (the internal control) showed the best efficacy. In addition, ncCD40L showed better oncolytic effects than WTCD40L. It is thus possible that a certain percentage of the observed increases in oncolysis were due to the high cytotoxicity of the ncCD40L virus. However, we cannot ignore the fact that an interaction between replication-competent and replication-defective viruses indeed occurred. After adding additional replication-competent virus, the

replication-defective viruses (Ad5WT fibre, nc40L, and WT40L) exhibited an increased ability to replicate in cholangiocarcinoma cells. The nc40L virus results in a higher oncolytic effect than the WT40L virus, regardless of whether it is due to the cytotoxicity of the nc40L virus.

A

Replication-defective viruses gained the ability to replicate and oncolyze cancer cells by providing extra E1A, E1B viral proteins (encoded by replication competent virus C) - Coinfection Day 6



B

Replication-defective viruses only - Coinfection Day 6 control

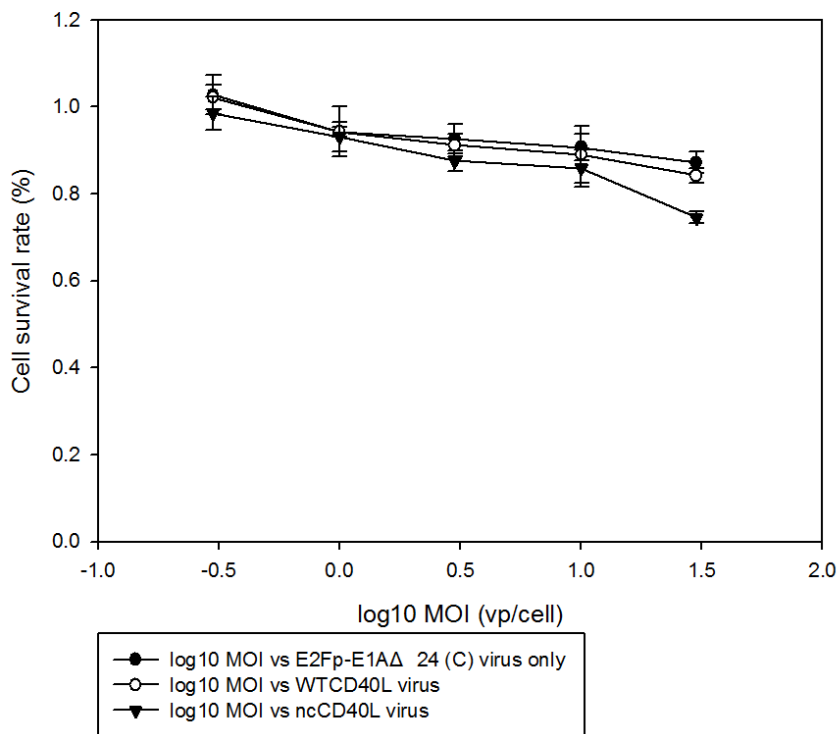


Figure 29. (A) The survival rate of CCLP1 cells co-infected by the replication-competent E2Fp-E1Ad24 virus and replication-defective viruses (CMVp-EGFP, CMVp-WTCD40L, ncCD40L) at day 6. (B) The cell-survival rate of replication-defective viruses only.

3.6 Immunohistochemistry (IHC)

Immunohistochemistry is an efficient approach to measure the expression level of specific targets in tumour tissues. This technique was used to detect potentially useful targets for oncolytic viruses in samples from cholangiocarcinoma patients.

A general description of this set of experiments is provided (Table 5).

Table 5. The number of slides used for the IHC analysis

Receptor	The number of slides used for analysis/total samples
$\beta 8$	4/6
CD40L	5/6
$\alpha \nu \beta 6$	5/6
$\beta 5$	5/6
$\alpha \nu$	6/6
CD46	5/6
CAR	4/6
DSG2	4/6
CD61	4/6
CD40	4/6
CK19	5/6
rbIgG	3/6
mlgG	4/6
gtIgG	2/6

Because of the limited number of cholangiocarcinoma patients, the collection of samples was difficult, and only 6 patients were included. However, the protein expression levels were evaluated based on these samples.

CK19 is a biomarker for the normal bile duct and is not expected to be expressed in liver tissue, but it is expected to have a strong signal in the normal bile duct. Our results met this expectation. Additionally, the cumulative bar chart (Figure 30) indicated that some CK19 proteins were expressed in

cholangiocytes. The expression pattern of the CK19 protein in samples derived from cholangiocarcinoma patients is shown in Appendix 5 (Figure A7-A).

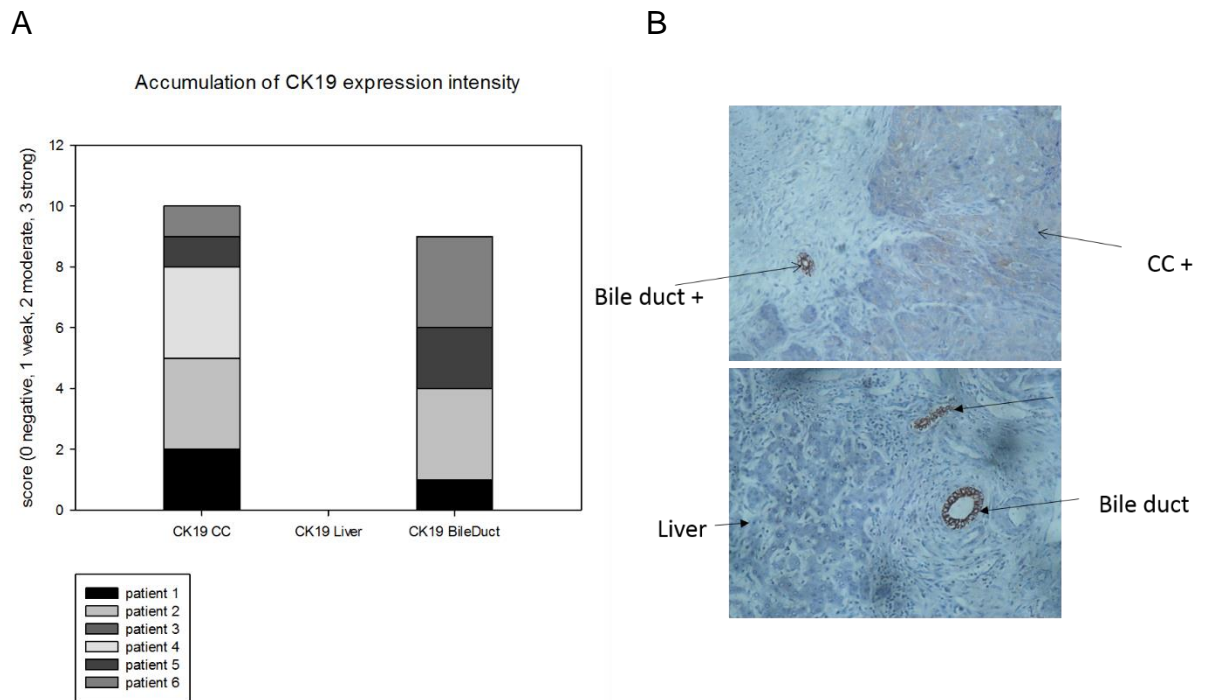


Figure 30. The average expression level of CK19.

CK19 is a biomarker for the normal bile duct, and was expected to be negative in liver tissue and strongly positive in bile ducts. CK19 protein was expressed in cholangiocytes. (A) This cumulative bar chart was plotted based on the intensity of signals in microscopy pictures (B). A strong signal in the bile duct, a negative signal in the normal liver, and a weak signal in cholangiocarcinomas were identified.

CARs are widely distributed throughout the human body; they were highly expressed in normal bile ducts, hepatocytes, and cholangiocytes. Hence, an oncolytic virus with Ad5WT fibres might not be a good candidate for selectively targeting tumour cells. As a result, in order to specifically target tumour cells, fibre-modified viruses are more suitable for virotherapy.

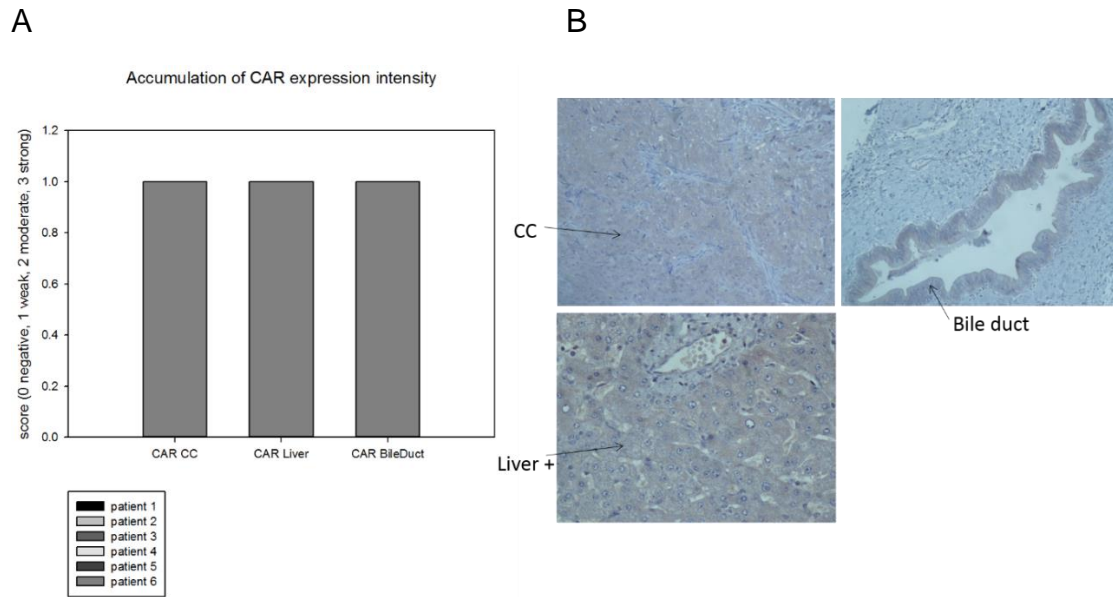


Figure 31. The cumulative expression level of CAR in samples derived from cholangiocarcinoma patients

CAR (coxsackievirus and adenovirus receptor) was expressed nearly equally in the normal bile duct, hepatocytes, and cholangiocytes. CAR is the receptor of coxsackievirus and adenovirus type 5, and the binding target of Ad5WT fibres. The expression pattern of CAR indicates the importance of modifying fibres of oncolytic viruses. (A) This cumulative bar chart was plotted based on the intensity of signals in microscopy pictures (B). A weak signal was detected in bile ducts, livers, and cholangiocarcinomas.

Integrin $\alpha\beta 6$, which is the binding target of Ad5-FMD viral fibres, was more highly expressed in cholangiocarcinomas than in normal bile ducts. However, it was also expressed in hepatocytes; thus, viruses with this fibre might require multiple selective strategies to efficiently infect cholangiocarcinomas rather than normal hepatocytes.

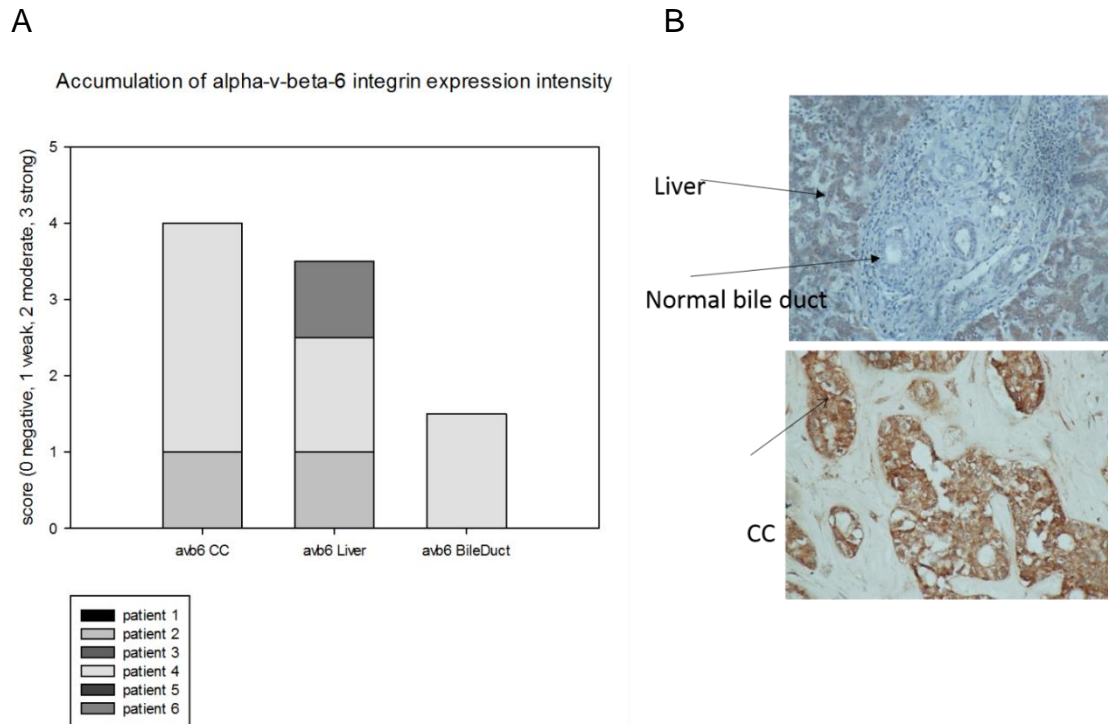


Figure 32. The cumulative expression level of integrin $\alpha\beta 6$ in samples derived from cholangiocarcinoma patients

(A) $\alpha\beta 6$ integrin is the receptor of Ad5-FMD fibre, which is highly expressed in cholangiocytes. Therefore, using Ad5-FMD fibres might be a good approach to increase the infection rate in tumour cells. However, $\alpha\beta 6$ integrin is also expressed in hepatocytes, which might be a challenge for Ad5-FMD fibre-modified viruses. This result indicates that Ad5-FMD fibres can be a good candidate when combined with other strategies. This cumulative bar chart was plotted based on the intensity of signals in microscopy pictures (B) A strong signal was identified in cholangiocytes, while hepatocytes and bile ducts were scored as moderate and negative, respectively. The expression pattern of $\alpha\beta 6$ integrin in cholangiocarcinoma patients is shown in Appendix 5 (Figure A7-C).

CD46 is the receptor for the Ad5/35 chimera fibre protein. However, it was weakly expressed in five out of six patients. The protein was better expressed in hepatocytes and normal bile ducts than in the cholangiocytes. Since the result of infection experiments of fibre-modified viruses (Figure 23) implies that Ad5/35 chimera fibre might not be specifically infective in cholangiocarcinoma

cell lines, it might be useful to treat other types of cancer cells. However, more samples and stains are necessary to get a more supportive conclusion.

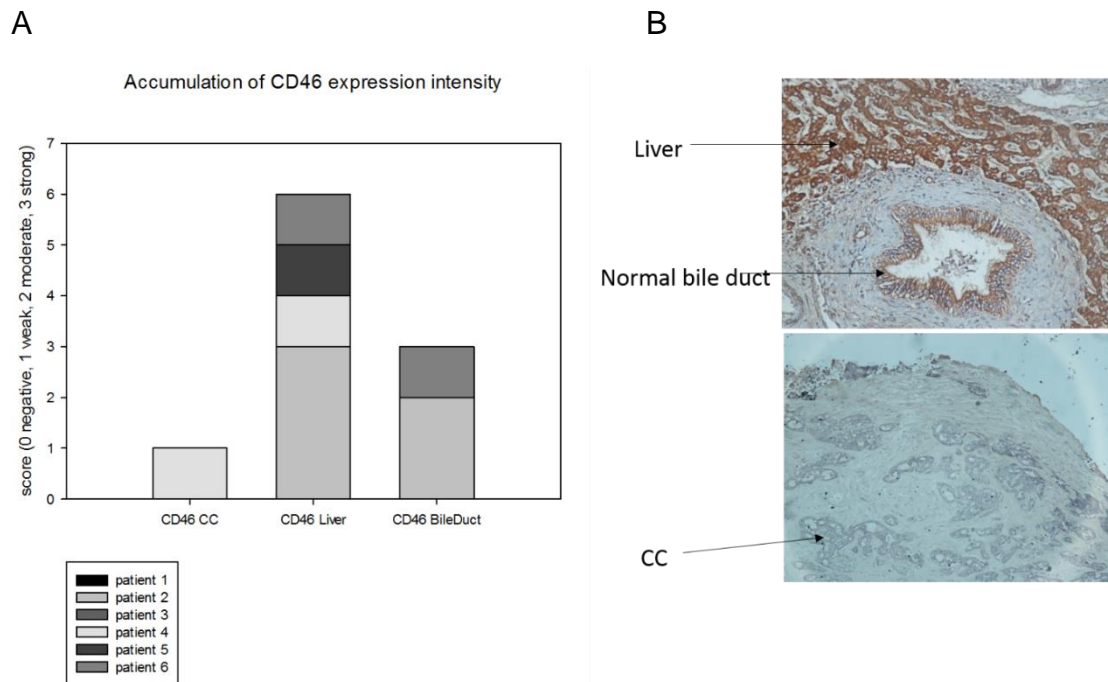


Figure 33. The cumulative expression level of integrin CD46 in samples derived from cholangiocarcinoma patients

(A) CD46 is the binding receptor to Ad5/35 chimera fibre. Nonetheless, it is poorly expressed in cholangiocytes. In contrast, it has a high expression level in hepatocytes, and the second highest expression in bile ducts. Because of the inefficient staining, a negative result in CCs might be obtained. Thus, repeated analyses are needed to determine a conclusive result. This cumulative bar chart was plotted based on the intensity of signals in microscopy pictures (B) A strong signal was identified in hepatocytes, a moderate signal in bile ducts, and no signal in cholangiocytes.

Desmoglein 2 (DSG2) is the binding target for Ad5/3 chimera fibre. The protein expression level in cholangiocytes was strong, whereas a moderate signal was detected for both hepatocytes and bile ducts. As a result, Ad5/3 fibre is promising for the treatment of cholangiocarcinoma. Nonetheless, the result was based on the analysis of only 4 out of 6 patients, and additional experiments are needed to confirm the finding.

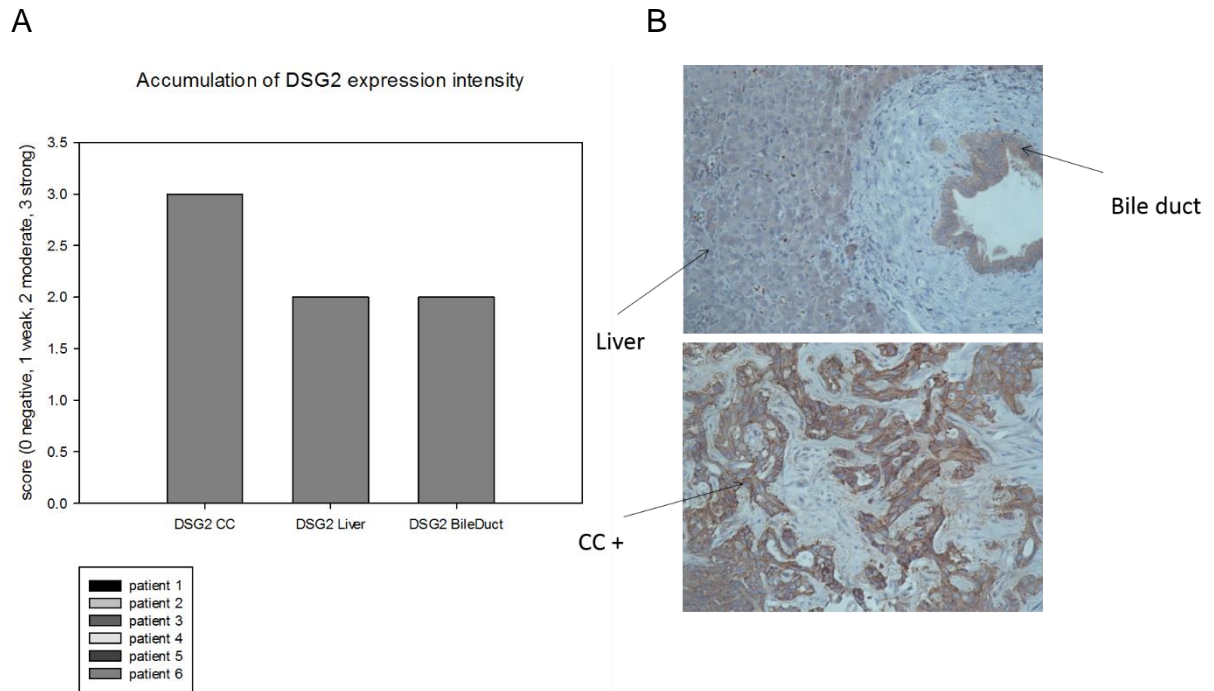
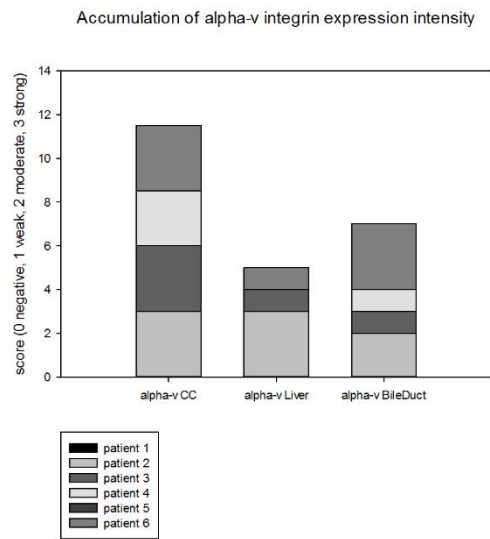


Figure 34. The cumulative expression level of integrin DSG2 in samples derived from cholangiocarcinoma patients

(A) DSG2 is the receptor of Ad5/3 fibre, which is strongly expressed in cholangiocytes, and moderate expressed in both hepatocytes and bile ducts. This cumulative bar chart was plotted based on the intensity of signals in microscopy images (B). In these microscopy images, a strong signal was identified in cholangiocytes, while both hepatocytes and bile ducts had moderate signals. The expression pattern of DSG2 in cholangiocarcinoma patients is shown in Appendix 5 (Figure A7-E).

αv integrin is the receptor of Ad5-RGD chimera fibre, which was strongly expressed in the cholangiocytes of 4 out of 6 patients. It was weakly to strongly expressed in hepatocytes and bile ducts. Since it is highly expressed in cholangiocytes, Ad5-RGD fibre has the potential to be a good target for selectively entering cells. Moreover, this integrin is also expressed in hepatocytes and bile ducts, but at a lower level. Strong signals were also detected in fibroblasts. Hence, the tumour selectivity is not sufficiently accurate using only Ad5-RGD fibre.

A



B

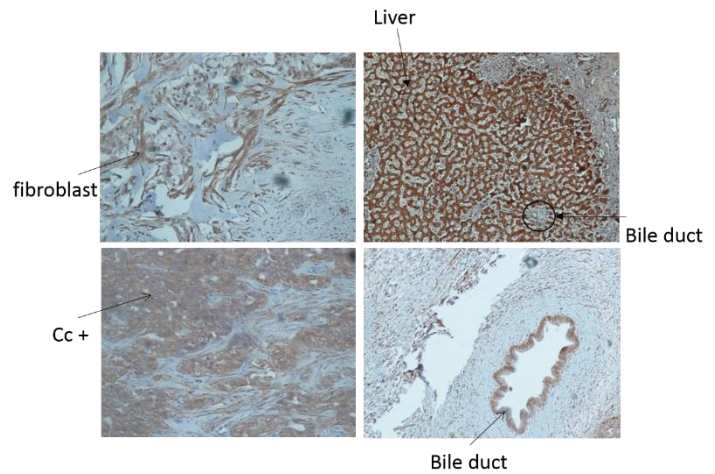


Figure 35. The cumulative expression level of αv integrin in samples derived from cholangiocarcinoma patients

(A) This integrin was highly expressed in most cholangiocytes (the samples from 3 patients had strong signal and 1 patient had a moderate expression level), and weak to strong signals were detected in hepatocytes (the samples from 2 patients were scored as weak, while 1 patient was observed as having strong expression) and bile ducts (the intensity varied from weak to strong). This bar chart was plotted based on the intensity of signals in microscopy images (B). The cholangiocytes, hepatocytes, bile ducts and fibroblasts all had strong expression.

CD40 itself has strong binding affinity to CD40L, and the oncolysis of CD40L virus is only activated in CD40+ cells. Fortunately, even though it was weak, CD40 was expressed in cholangiocarcinomas, so that cholangiocarcinomas were sensitive to CD40L viruses. However, CD40 was also expressed in normal tissues, so the specificity to tumour cells was not sufficient using only CD40L. It is necessary to consider other factors, such as promoters and the E1A viral protein.

From another point of view, NK (natural killer) cells contain CD40L and not CD40 (Carbone et al., 1997, Turner et al., 2001). As a result, once activated,

NK cells are able to clear all CD40+ tumours, such as cholangiocarcinomas. This can be another possible direction for cancer treatment.

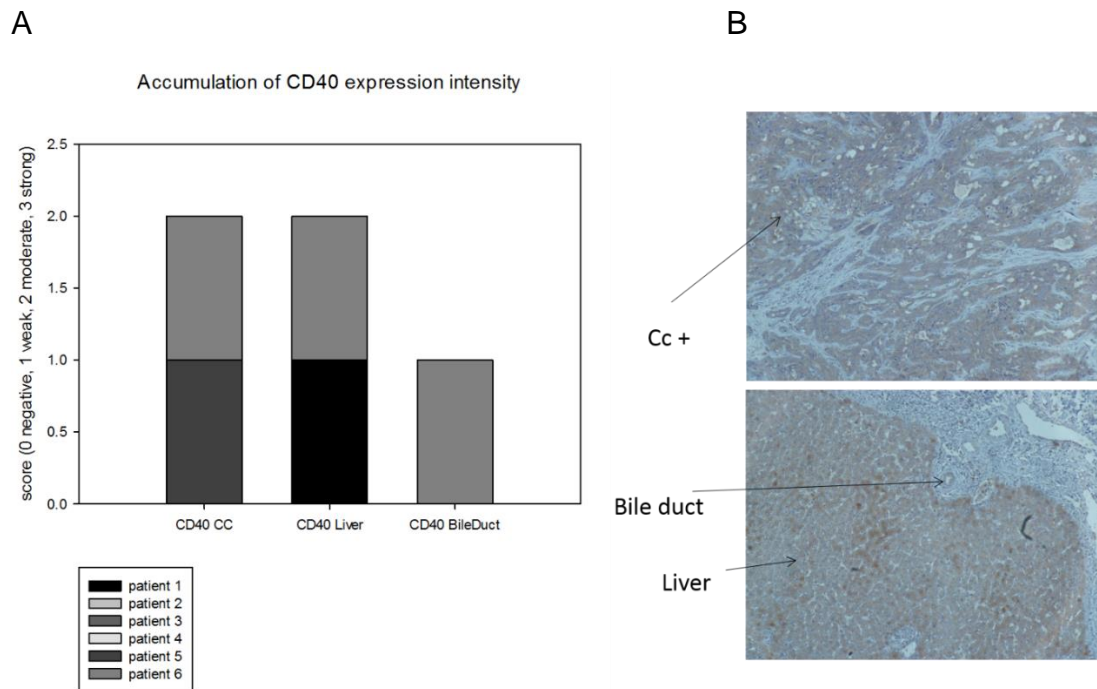


Figure 36. The cumulative expression level of CD40 in samples derived from cholangiocarcinoma patients

(A) CD40 is the receptor of CD40L, and the CD40L virus can only replicate in CD40+ cells. As shown in this chart, in samples from these two patients, the expression level of CD40 in cholangiocytes was equal to that in hepatocytes (weak, score 1); one patient had weak expression of CD40 in the bile duct. (B) The microscopy images were used for the analysis. A strong signal was scored as 3; a moderate expression was assigned a score of 2; a weak signal was given a score of 1; negative expression was marked as 0. These scores were interpreted using the bar chart on the left-hand side. The tissues (cholangiocarcinoma, liver, and bile duct) had weak expression.

CD40L plays an important role in the immune system, triggering both innate and adaptive immune responses; therefore, we chose it as one of our modifying targets. In the IHC experiment, the expression pattern of CD40L facilitated the design of the virus for further study. The bar chart (Figure 37) indicated that CD40L was highly expressed in cholangiocytes, suggesting a positive impact on virus treatment targeting cholangiocarcinomas. This suggests that it is

possible (either via virus or not) to induce an interaction between tumour cells and CD40+ immune cells (such as macrophages and dendritic cells) to increase cell cytotoxicity.

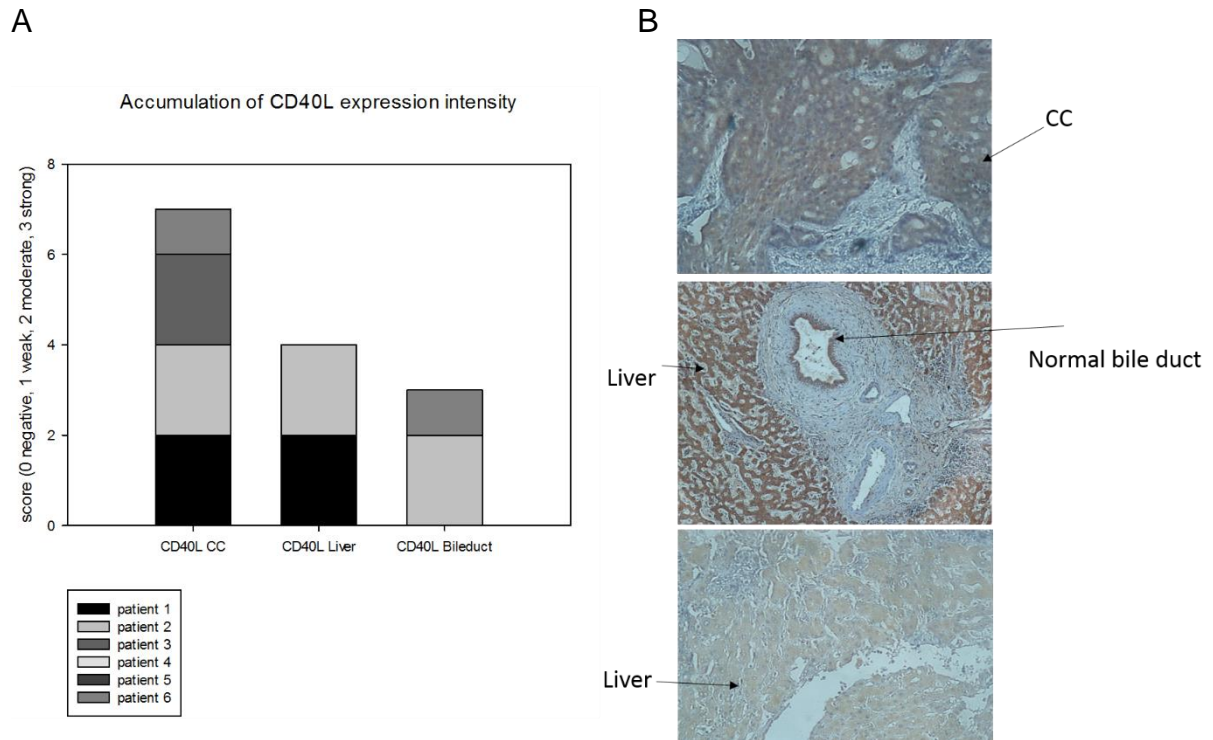


Figure 37. The cumulative expression level of CD40L in samples derived from cholangiocarcinoma patients

(A) CD40L is a very important inducer of both the innate and adaptive immune system, and its high expression in cholangiocytes is promising for cancer treatments. In this case, samples from 3 patients out of 6 had moderate expression in cholangiocytes, and one patient sample had weak expression in cholangiocytes. Two patient samples had moderate expression in hepatocytes. One patient sample had moderate expression in the bile duct, while another had weak expression in the bile duct. (B) The microscopy images show that the expression of CD40L in cholangiocytes was moderate (score 2). The expression level in the bile duct was moderate (score 2). The expression level in hepatocytes was scored as moderate and negative. The expression pattern of DSG2 in cholangiocarcinoma patients is shown in Appendix 5 (Figure A7-G).

The other receptors of integrins (integrin $\beta 5$, $\beta 8$, and CD61) are potential candidates for viral fibre targeting, and we expected that they would be

selectively expressed in cholangiocytes. However, $\beta 8$ and CD61 were not expressed. Alternatively, the negative results may be attributed to inefficient quantity of antibodies. An analysis of these two proteins was not possible. Nonetheless, integrin $\beta 5$ was strongly expressed in cholangiocytes, hepatocytes, and normal bile ducts, which was promising. This finding is worthy of further studies and may facilitate new virus development.

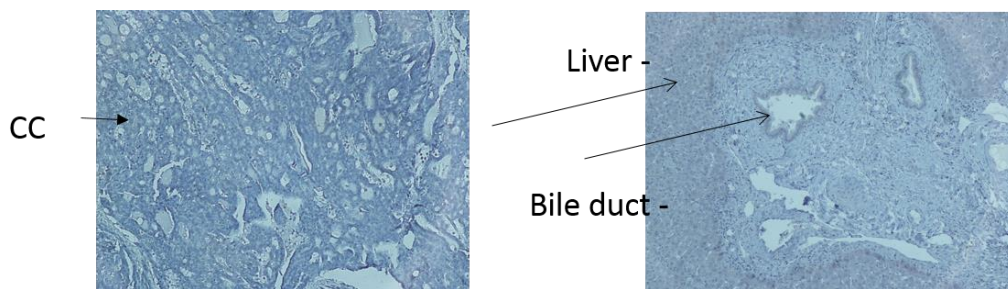


Figure 38. No expression of $\beta 8$ integrin in samples derived from cholangiocarcinoma patients

No expression was observed due to either a true lack of expression of this integrin or weak staining.

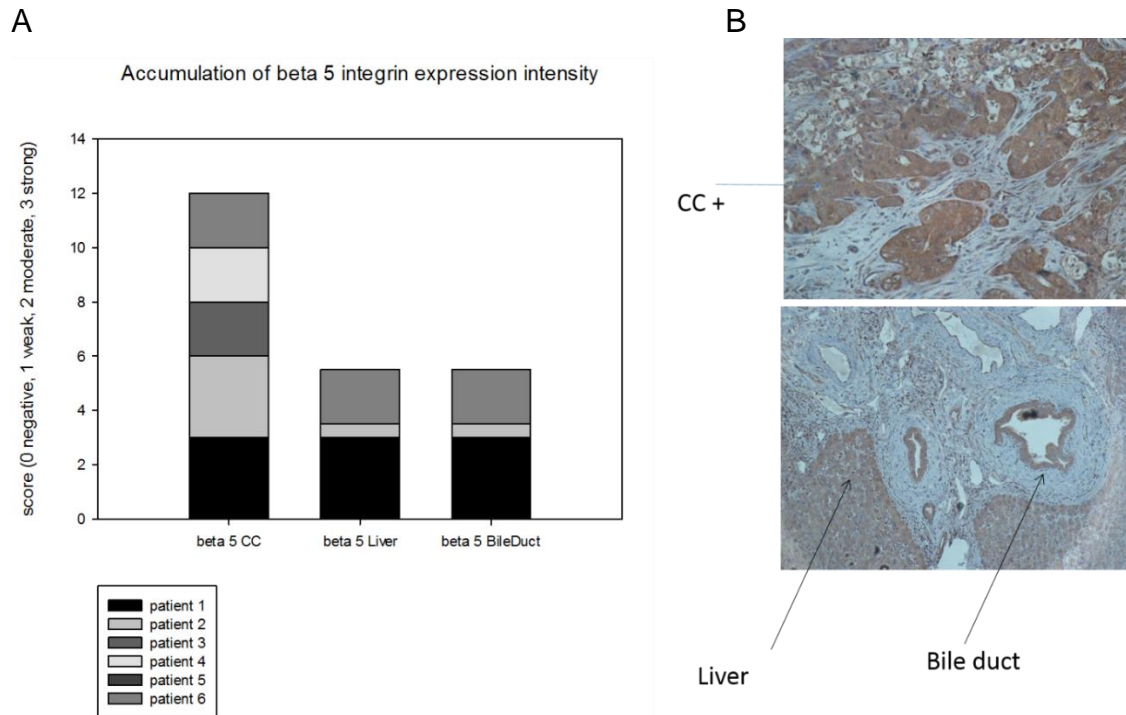


Figure 39. The cumulative expression level of $\beta 5$ integrin in samples derived from cholangiocarcinoma patients

(A) In the case of cholangiocytes, 2 out of 6 patients showed strong expression of this integrin, and 3 patients expressed it at a moderate level. Meanwhile, the hepatocytes and bile ducts expressed this integrin almost equally, at a level that was only half that of cholangiocytes. This cumulative bar chart was plotted on the basis of the intensity of signals in microscopy images (B) A very strong signal was identified in cholangiocytes, while both hepatocytes and bile ducts had moderate signals. The expression pattern of $\beta 5$ integrin in cholangiocarcinoma patients is shown in Appendix 5 (Figure A7-H).

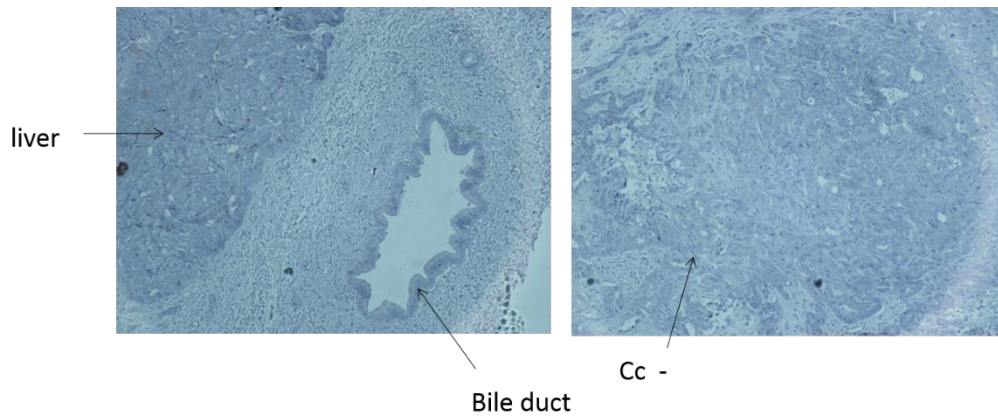


Figure 40. No expression of CD61 in samples from cholangiocarcinoma patients

All observations were negative. This was due to the low expression level of the protein or unpredicted errors in staining. No conclusive interpretation can be suggested.

4. Discussion-Is it a promising treatment?

On the basis of the data and findings so far, I am able to make the following conclusions. First of all replication competent viruses indeed replicated in cholangiocarcinoma cells, and viruses with WTP-E1A Δ 24 (B) and E2F1 promoter-E1A Δ 24 (C) were better than their counterpart with hTERTp-E1AWT (A). Second, for oncolytic effects, the cell viability assay revealed the ranking of C>B>A in CCSW cells, while the infectivity assays suggested the ranking of C>A>B in CCLP cells. Third, as expected RD viruses were unable to replicate without E1A genes. In addition, among fibre modified RD viruses, Ad5-RGD fibre conferred greater oncolytic effect than the Ad5/3 chimera and Ad5/35 chimera fibre in CCLP cells, while Ad5/3 fibre and Ad5-FMD fibre resulted in higher infection efficiency in CCSW cells. Fourth, it was unclear if CD40L virus would help to treat cholangiocarcinoma.

This results obtained in this project did lead to some clarification, for example which fibre was more efficient for infectivity, which promoter was better controlled, and the best construct design of adenoviruses. To sum up, I would prefer to use CCSW1 cells for further experiments because this cell line is a good model to show the significance between treatments with different viruses. Nonetheless, I would also test the treatments in another type of cholangiocarcinoma, CCLP1 cells. HEK293 cells were used in this study because we lacked a more relevant control.

Based on CCSW1 cells, WTP-E1A Δ 24 modified virus replicated the best as measured in qPCR and FACs experiments, followed by E2Fp-E1A Δ 24 virus although differences were small. This conclusion was also confirmed in cell

viability assays. However, the AdZWT promoter has no selectivity towards tumour cells, so that the E2F1 promoter would be a better choice in some cases. Nevertheless, the E2F1 promoter only works efficiently in Rb protein deficient tumours; unfortunately, the mutation rate in cholangiocarcinoma is not very high (11.9%, (Kang et al., 2002)). As a result, this promoter and this modified E1A region combination is potentially only useful in 11.9% of total cases. Hence, I will suggest E2Fp-E1A Δ 24 virus for Rb deficient cases, and WTP-E1A Δ 24 for the rest. In the case of fibres, Ad5-FMD and Ad5/3 chimera fibre viruses were the best candidates. To sum up, the case for a modified virus construct based on studies with CCSW1 cells has been built. E2Fp-E1A Δ 24 region with Ad5-FMD or Ad5/3 fibre would be used for pRb deficient cases, whereas WTP-E1A Δ 24 with Ad5-FMD or Ad5/3 fibre is suggested for non-Rb deficient cases. The efficacy of CD40L needs further study in CCSW1 cells because the experiments testing CD40L were only done in CCLP1 cells. However, a ncCD40L fragment might work better than WTCD40L (on the basis of the CCLP1 model). In addition, an intact E3 region might help to increase oncolytic effect, so the CD40L fragments should be inserted into other part of the virus genome rather than the E3 region.

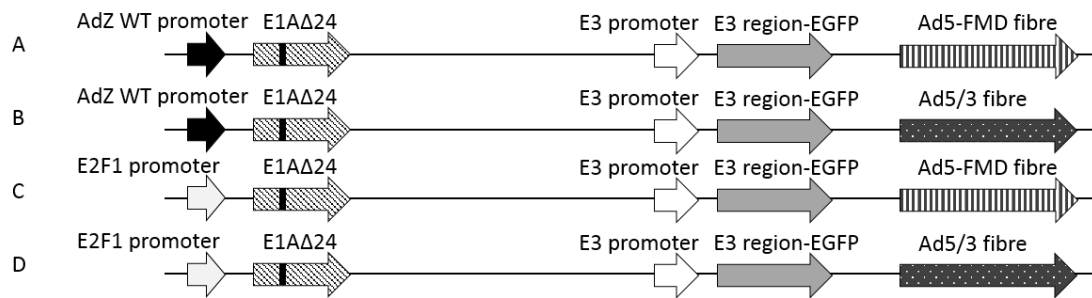


Figure 41. The schematic presentation of adenovirus design for CCSW1 model

Based on the conclusions of all the recent experiments, the design of a promising adenovirus is suggested. WT promoter-E1AΔ24 region combines with (A) Ad5-FMD and (B) Ad5/3 fibre. E2F1 promoter-E1AΔ24 region combines with (C) Ad5-FMD fibre and (D) Ad5/3 fibre. WTCD40L and ncCD40L can be inserted into anywhere rather than the E3 region, as oncolytic virus might have better effects with intact E3 region.

Reviewing all the finding so far, whether oncolytic virus would be a promising treatment is still under debate, but we can suggest an improved adenovirus based on the project results for further study (shown in Figure 34). Although a conclusive model can be proposed, there were some questions raised in this project which are worthy of further discussion below.

96h time course experiment

This series of experiments indeed indicated a suitable time-point to harvest virus and the suitable MOI to use for infection. Since the IUs of virus differed, I presented the data by MOIs. In cell viability assays, it seems that there is some cell death by day 3 or day 4 post-infection, so comparison of infectivity efficiency at 72 h and 96 h might be not very accurate since highly infected cells had died by then. Based on cell viability data, even MOI down to 0.3 vp/cell still caused nearly 10-20% cell death by day 3. In FACs time-course experiments, the MOIs used were 2, 4, 8, 16, 32 vp/cell, so the samples must be affected by cell death by day 3 and 4. That is why there were some inconsistencies in ranking different

viruses in the assays used, or dose-dependent effects which conflict with the data at 24 and 48 h time points. As a result, I suggest that for FACs experiments in future, harvesting should be done by 48h, and using a lower MOI like 2, 4, 8 vp/cell will be more appropriate.

Time course experiment

Among cytometry experiments, there was a problem about EGFP leakage. We noticed this problem when we found that there was almost 97% of green fluorescent cells even when cell lines were infected by 2vp/cell (MOI), and harvested at 24 h. This is an incredibly high infection rate. Based on statistical data, under MOI=2vp/cell, 13.534% of cells would be uninfected, 27.067% of cells would be infected by 1 virus and 59.399% cells would be infected by more than 1 virus. Thus, the observed result of 97% positive cells was much higher than expected. Thus, there must be some reasons to result in this consequence. One possible reason is EGFP leakage. Based on the A1-D Figure in the Appendix, there are some granules smaller than cells, so apparently leaking EGFP protein combined with cell debris or waste, or some other granules became coated with EGFP. However, the question is where do these granules come from?

In the experiment shown in appendix 1, which was A549 cells infected by virus hTERTp-E1AWT virus (A) and harvested at 48h, we can clearly identify a pronounced peak shift of the majority of the cells and some intensity out of the window, although at the MOI used most cells should be uninfected. The high proportion of apparently infected cells is unlikely to be due to secondary infection at this early time-point.

According to the experiment done by Stamatis Karakonstantis, he proved that the EGFP leakage came from the processing of the cells (the harvesting procedure has been described in methods), suggesting that the conditions used were too harsh; however, even when cells were harvested very gently, adding medium to inhibit trypsinization immediately the cells start to detach, we were unable to avoid this problem.

Based on the photograph recorded before harvesting (attached cells, black spots represent the fluorescent cell, appendix Figure A1-B), we indeed saw the dose-dependent effects with different MOI and not every attached cell infected. However, the flow cytometry indicated almost 100% viral infectivity in suspended cells. If only about 50% infectivity was found among attached cells, it is impossible to get 100% infected suspended cells. When I examined the harvested cells suspension by flow cytometry, I could see some small dots which were not cells, smaller in size but green as well. Potentially, these small, EGFP-positive vesicles might have associated with uninfected cells to give staining, but it is supposed to be low level of signal in the flow cytometry.

Because this made it impossible to set an appropriate gate for the positive cell population, we decided to use the MFI of the entire population to indicate level of EGFP expression in the samples.

qPCR

qPCR is an efficient technology to evaluate the oncolytic potency of replicating viruses, by directly measuring the virus DNA copy number in samples. From the bar charts of qPCR result (Figure 25), we were able to confirm the replication of RC virus, and the charts also indicated the trend and the ranking

of virus replication. WTP-E1A Δ 24 virus (C) always performed the best under similar MOIs, not only in CCLP1 cells but also in CCSW1 cells, and this result was consistent in all the experiments. However, for a more accurate presentation, I plotted the data to IUs which makes the ranking of viruses slightly different in each experiment.

In the experiment of qPCR in CCSW1 cells, the copy number of viruses in WTP-E1A Δ 24 virus (B) and E2F1p-E1A Δ 24 virus (C) infections seemed to decrease on day 2 and day 3, which is counter-intuitive.

This result can be considered with the data of Cell Viability Assays; the plot of Cell Viability Assays points out that when CCSW1 cells were infected by WT promoter-E1A Δ 24 virus (B) and E2F promoter-E1A Δ 24 virus (C) at a MOI=300vp/cell, about 10% of the cells died by day 3 (Figure 28A). Nonetheless, the cells which were infected by hTERT promoter-E1AWT virus (A) were still 100% alive on day 3. That is why the qPCR experiment shows an increasing potential of virus copy number in hTERT promoter-E1AWT virus (A) treated group, whereas the copy numbers in groups of WT promoter-E1A Δ 24 virus (B) and E2F promoter-E1A Δ 24 virus (C) show decreasing intensity due to the selective cell death of heavily infected cells.

MTT assays

Even though some plots (CCSW1 series) indeed provided some information, others did not indicate any differences in viral potency against CC, such as CCLP1 cells. These data show that the RC viruses have the ability to kill the cells, with lower doses being sufficient at longer times. In the experiments of CCLP1 cells, the error bars are too big to be relied on. In addition, the curves

were too close to each other so that it is hard to distinguish them. The data were unable to show the different potencies against CC between viruses; the curves only suggested a ranking of viruses because of the overlapping error bar. Hence, more experiments are required to confirm the findings obtained with MTT assays.

The level of cell killing at low MOI or with longer time points indicates that the speed of virus replication within the culture must be contributing to the oncolytic effects.

In addition, day 9 seems too late to harvest, and the plates of cells provide limited detail and information at this time. Hence, I suggest to change the time points used in this assay to days 3, 5 and 7, or to decrease the number of seeded cells/well (I seeded 1×10^5 cells/well in HEK293, CCLP1, 5×10^4 in CCSW1 cells/well).

MTT assays—CD40L virus co-infection

Based on the control of this experiment, generally there is no cytotoxicity in replication-defective virus infected cells, but some slight cell death was observed under high MOIs. Nonetheless, it is a good control. In the co-infection experiment, the survival of cells in the E2F1p-E1A Δ 24 RC virus (C) only group seems the highest as expected. However, the combination group of E2F1p-E1A Δ 24 RC virus (C) with the control RD-EFGP virus had the best cytotoxicity. In addition, co-infection of E2Fp-E1A Δ 24 virus with ncCD40L showed better oncolytic effects compared to a combination of E2Fp-E1A Δ 24 virus with WTCD40L, which is puzzling. One possibility is that CC cell lines do not express CD40 on cell surface, since CD40L cannot help oncolyse CD40- cells. To check

CD40 expression on the CC cell lines, we used primary antibody to detect CD40 and FITC conjugated secondary antibody (performed by Stamatis Karakonstantis). According to the result of receptor expression level on CCLP1 and CCSW1 cells, both CC cell lines express low levels of CD40 (Figure A2).

In order to answer this question, we can go back the viruses construct first (Figure 12). Fibre modified RD viruses contained the E3 region, while CD40L viruses had E3 deleted. E3 gene deletion might contribute to higher selectivity to tumour cells, but it may affect the replication of adenoviruses (Heise and Kirn, 2000). Among all the viral proteins in this table, E3 11.6 kD (Tollefson et al., 1996) and E4ORF4 proteins are directly related to cytotoxicity of oncolytic adenovirus. Once the whole E3 region was completely removed, this may delay the cell death of infected cells.

On the other hand, the E3 region also plays another role in alternative mechanisms to cell killing. Since E1A gene expression in the lytic cycle makes the cells sensitive to tumour necrosis factor (TNF)-mediated killing (Gooding, 1994), but this pathway is inhibited by E3 10.4/14.5 and 14.7 proteins. In theory, deleting these E3 10.4/14.5/14.7 protein encoded genes results in increasing TNF receptor expression *in vivo* and sensitizing cell to cytotoxic T cell cytotoxicity. Virus replicates inside the tumour cells, lysing them in the end of lytic cycle or inducing cell-mediated immune response to cancerous cells.

However, this pathway is unable to work in *in vitro* cell lines, so overall, the deletion of E3 region inhibits the function of E3 11.6 kD protein, but it is unable to induce cell-mediated immunity *in vitro*. As a result, E3 deletion may result in

a negative effect on *in vitro* assays. To overcome this obstacle, we can try to construct another virus containing CD40 ligands and E3 region so that the comparison between these viruses will be more meaningful.

Another possibility is the toxicity of GFP proteins (Liu et al., 1999) although it is supposed to be a minor issue in this experiment.

This co-infection experiment was not a good comparison; it contained multiple factors which might affect the results, like whether E3 region is deleted or not. Further experiments are required to confirm the findings. Because both CC cell lines were concluded to be minor-expressing CD40+ cells, I suggest to use another strongly expressing CD40+ and CD40- cell lines as internal controls for further CD40L virus experiments to identify and evaluate the worth of CD40L virus. Immunofluorescence cell staining technology (for cell line) is helpful to check the expression level of receptors on cell surface, so we can involve this system. To check the expression of CD40 first, and then we can use the result to test the functions of CD40L viruses.

Table 6. The potential mechanisms of antitumoral efficacy and its corresponding adenovirus genes (Heise and Kirn, 2000)

Mechanism	Examples of adenoviral genes modulating effect
I. Direct cytotoxicity due to viral proteins	E3 11.6kD, E4ORF4
II. Augmentation of antitumoral immunity CTL infiltration, killing tumor cell death, antigen release immunostimulatory cytokine induction antitumoral cytokine induction (e.g. TNF) enhanced sensitivity to cytokines (e.g. TNF)	E3 gp19kD* E3 11.6kD E3 10.4/14.5, 14.7kD* E3 10.4/14.5, 14.7kD* E1A
III. Sensitization to chemotherapy	Unknown (? E1A, others)
IV. Expression of exogenous therapeutic genes	N/A

*Viral protein inhibits antitumoral mechanism

Immunohistochemistry (IHC)

Apart from the processing of tissue staining, one of the strong disadvantage of this experiment is the limited sample numbers. Since I only had 6 samples to analyse, the statistics might not be accurate. In addition, all the patients might come from the same type of specific intra-cholangiocarcinomas, which makes the result biased towards particular unknown direction, leading to systematic errors. More IHC experiments are required to solidify the conclusions. In addition, there were a lot of errors during the processing of IHC, leading to non-specific result. Thus, more repeats are indeed required.

Summary

Although many questions remain to be answered in this project, two new viruses have been constructed, allowing for comparison of hTERTp-E1AWT with Ad5WTP-E1A Δ 24 and E2F1p-E1A Δ 24. In addition, all the viruses were active against CC. In this project, the replication efficacy and oncolytic effects of RC viruses were also evaluated.

Fibre modified- and CD40L viruses were also involved in this project, completing the overview of adenoviral treatment of cholangiocarcinoma. In the end, IHC experiments provided another point of view for virotherapy and

bridged the theoretical and technical aspects of this project. However, all the experiments were conducted *in vitro*, and further *in vivo* experimentation is required in order to determine the efficacy of this promising virus.

Future work

Suggested directions for future experimentation include

1. Construction of optimised adenovirus (suggested in Figure 41)
2. Evaluation of virus for replication efficacy and oncolytic effect, especially in CCSW1 cells
3. Involvement of CD40L virus in this model
4. Use of CCLP1 cells to confirm the results after building of the model in CCSW1 cells
5. Building of the virotherapy model for cholangiocarcinoma treatment
6. Perform *in vivo* experiments, such as animal experiments in order to test the toxicity, efficacy, and oncolysis of virus
7. Link to clinical trials, if possible

Reference

- ANDERSON, B. D., NAKAMURA, T., RUSSELL, S. J. & PENG, K. W. 2004. High CD46 receptor density determines preferential killing of tumor cells by oncolytic measles virus. *Cancer Res*, 64, 4919-26.
- BARTLETT, D. L., LIU, Z., SATHAIAH, M., RAVINDRANATHAN, R., GUO, Z., HE, Y. & GUO, Z. S. 2013. Oncolytic viruses as therapeutic cancer vaccines. *Mol Cancer*, 12, 103.
- BLECHACZ, B. R. & GORES, G. J. 2008. Cholangiocarcinoma. *Clin Liver Dis*, 12, 131-50, ix.
- CARBONE, E., RUGGIERO, G., TERRAZZANO, G., PALOMBA, C., MANZO, C., FONTANA, S., SPITS, H., KARRE, K. & ZAPPACOSTA, S. 1997. A new mechanism of NK cell cytotoxicity activation: the CD40-CD40 ligand interaction. *J Exp Med*, 185, 2053-60.
- CARDINALE, V., BRAGAZZI, M. C., CARPINO, G., TORRICE, A., FRAVETO, A., GENTILE, R., PASQUALINO, V., MELANDRO, F., ALIBERTI, C., BASTIANELLI, C., BRUNELLI, R., BERLOCO, P. B., GAUDIO, E. & ALVARO, D. 2013. Cholangiocarcinoma: increasing burden of classifications. *Hepatobiliary Surg Nutr*, 2, 272-80.
- CHOI, J. W., LEE, J. S., KIM, S. W. & YUN, C. O. 2012. Evolution of oncolytic adenovirus for cancer treatment. *Adv Drug Deliv Rev*, 64, 720-9.
- CONG, Y. S., WEN, J. & BACCHETTI, S. 1999. The human telomerase catalytic subunit hTERT: organization of the gene and characterization of the promoter. *Hum Mol Genet*, 8, 137-42.
- COUGHLAN, L., VALLATH, S., SAHA, A., FLAK, M., MCNEISH, I. A., VASSAUX, G., MARSHALL, J. F., HART, I. R. & THOMAS, G. J. 2009. In vivo retargeting of adenovirus type 5 to alphavbeta6 integrin results in reduced hepatotoxicity and improved tumor uptake following systemic delivery. *J Virol*, 83, 6416-28.
- DE VREEDE, I., STEERS, J. L., BURCH, P. A., ROSEN, C. B., GUNDERSON, L. L., HADDOCK, M. G., BURGART, L. & GORES, G. J. 2000. Prolonged disease-free survival after orthotopic liver transplantation plus adjuvant chemoradiation for cholangiocarcinoma. *Liver Transpl*, 6, 309-16.
- DMITRIEV, I., KRASNYKH, V., MILLER, C. R., WANG, M., KASHENTSEVA, E., MIKHEEVA, G., BELOUSOVA, N. & CURIEL, D. T. 1998. An adenovirus vector with genetically modified fibers demonstrates expanded tropism via utilization of a coxsackievirus and adenovirus receptor-independent cell entry mechanism. *J Virol*, 72, 9706-13.
- ELIOPOULOS, A. G., DAVIES, C., KNOX, P. G., GALLAGHER, N. J., AFFORD, S. C., ADAMS, D. H. & YOUNG, L. S. 2000. CD40 induces apoptosis in carcinoma cells through activation of cytotoxic ligands of the tumor necrosis factor superfamily. *Mol Cell Biol*, 20, 5503-15.
- ELIOPOULOS, A. G. & YOUNG, L. S. 2004. The role of the CD40 pathway in the pathogenesis and treatment of cancer. *Curr Opin Pharmacol*, 4, 360-7.
- FRISCH, S. M. & MYMRYK, J. S. 2002. Adenovirus-5 E1A: paradox and paradigm. *Nat Rev Mol Cell Biol*, 3, 441-52.
- GAGGAR, A., SHAYAKHMETOV, D. M. & LIEBER, A. 2003. CD46 is a cellular receptor for group B adenoviruses. *Nat Med*, 9, 1408-12.

- GIARD, D. J., AARONSON, S. A., TODARO, G. J., ARNSTEIN, P., KERSEY, J. H., DOSIK, H. & PARKS, W. P. 1973. In vitro cultivation of human tumors: establishment of cell lines derived from a series of solid tumors. *J Natl Cancer Inst*, 51, 1417-23.
- GLASGOW, J. N., EVERTS, M. & CUIEL, D. T. 2006. Transductional targeting of adenovirus vectors for gene therapy. *Cancer Gene Ther*, 13, 830-44.
- GOODING, L. R. 1994. Regulation of TNF-mediated cell death and inflammation by human adenoviruses. *Infect Agents Dis*, 3, 106-15.
- GRAHAM, F. L., SMILEY, J., RUSSELL, W. C. & NAIRN, R. 1977. Characteristics of a human cell line transformed by DNA from human adenovirus type 5. *J Gen Virol*, 36, 59-74.
- GUNES, C., LICHTSTEINER, S., VASSEROT, A. P. & ENGLERT, C. 2000. Expression of the hTERT gene is regulated at the level of transcriptional initiation and repressed by Mad1. *Cancer Res*, 60, 2116-21.
- HARADA, J. N. & BERK, A. J. 1999. p53-Independent and -dependent requirements for E1B-55K in adenovirus type 5 replication. *J Virol*, 73, 5333-44.
- HARLEY, C. B. 1991. Telomere loss: mitotic clock or genetic time bomb? *Mutat Res*, 256, 271-82.
- HEISE C, H. T., JOHNSON L, BROOKS G, SAMPSON-JOHANNES A, WILLIAMS A, HAWKINS L, KIRN D. 2000. An adenovirus E1A mutant that demonstrates potent and selective systemic anti-tumoral efficacy. *Nat Med*, 6, 1134-1139.
- HEISE, C. & KIRN, D. H. 2000. Replication-selective adenoviruses as oncolytic agents. *J Clin Invest*, 105, 847-51.
- HEISE, C., SAMPSON-JOHANNES, A., WILLIAMS, A., MCCORMICK, F., VON HOFF, D. D. & KIRN, D. H. 1997. ONYX-015, an E1B gene-attenuated adenovirus, causes tumor-specific cytolysis and antitumoral efficacy that can be augmented by standard chemotherapeutic agents. *Nat Med*, 3, 639-45.
- HUANG, T. G., SAVONTAUS, M. J., SHINOZAKI, K., SAUTER, B. V. & WOO, S. L. 2003. Telomerase-dependent oncolytic adenovirus for cancer treatment. *Gene Ther*, 10, 1241-7.
- JAKUBCZAK, J. L., RYAN, P., GORZIGLIA, M., CLARKE, L., HAWKINS, L. K., HAY, C., HUANG, Y., KALOSS, M., MARINOV, A., PHIPPS, S., PINKSTAFF, A., SHIRLEY, P., SKRIPCHENKO, Y., STEWART, D., FORRY-SCHAUDIES, S. & HALLENBECK, P. L. 2003. An oncolytic adenovirus selective for retinoblastoma tumor suppressor protein pathway-defective tumors: dependence on E1A, the E2F-1 promoter, and viral replication for selectivity and efficacy. *Cancer Res*, 63, 1490-9.
- JIMENO, A., RUBIO-VIQUEIRA, B., AMADOR, M. L., OPPENHEIMER, D., BOUROUD, N., KULESZA, P., SEBASTIANI, V., MAITRA, A. & HIDALGO, M. 2005. Epidermal growth factor receptor dynamics influences response to epidermal growth factor receptor targeted agents. *Cancer Res*, 65, 3003-10.
- JOHNSON, L., SHEN, A., BOYLE, L., KUNICH, J., PANDEY, K., LEMMON, M., HERMISTON, T., GIEDLIN, M., MCCORMICK, F. & FATTAEY, A. 2002. Selectively replicating adenoviruses targeting deregulated E2F activity are potent, systemic antitumor agents. *Cancer Cell*, 1, 325-37.

- KANG, Y. K., KIM, W. H. & JANG, J. J. 2002. Expression of G1-S modulators (p53, p16, p27, cyclin D1, Rb) and Smad4/Dpc4 in intrahepatic cholangiocarcinoma. *Hum Pathol*, 33, 877-83.
- KHURI, F. R., NEMUNAITIS, J., GANLY, I., ARSENEAU, J., TANNOCK, I. F., ROMEL, L., GORE, M., IRONSIDE, J., MACDOUGALL, R. H., HEISE, C., RANDLEV, B., GILLENWATER, A. M., BRUSO, P., KAYE, S. B., HONG, W. K. & KIRN, D. H. 2000. a controlled trial of intratumoral ONYX-015, a selectively-replicating adenovirus, in combination with cisplatin and 5-fluorouracil in patients with recurrent head and neck cancer. *Nat Med*, 6, 879-85.
- KRASNYKH, V., DMITRIEV, I., MIKHEEVA, G., MILLER, C. R., BELOUSOVA, N. & CURIEL, D. T. 1998. Characterization of an adenovirus vector containing a heterologous peptide epitope in the HI loop of the fiber knob. *J Virol*, 72, 1844-52.
- LAL, R., HARRIS, D., POSTEL-VINAY, S. & DE BONO, J. 2009. Reovirus: Rationale and clinical trial update. *Curr Opin Mol Ther*, 11, 532-9.
- LIU, H. S., JAN, M. S., CHOU, C. K., CHEN, P. H. & KE, N. J. 1999. Is green fluorescent protein toxic to the living cells? *Biochem Biophys Res Commun*, 260, 712-7.
- LIU, T. C. & KIRN, D. 2008. Gene therapy progress and prospects cancer: oncolytic viruses. *Gene Ther*, 15, 877-84.
- MALHI, H. & GORES, G. J. 2006. Review article: the modern diagnosis and therapy of cholangiocarcinoma. *Aliment Pharmacol Ther*, 23, 1287-96.
- MARTIN, M. E. & BERK, A. J. 1998. Adenovirus E1B 55K represses p53 activation in vitro. *J Virol*, 72, 3146-54.
- MATHIS, J. M., STOFF-KHALILI, M. A. & CURIEL, D. T. 2005. Oncolytic adenoviruses - selective retargeting to tumor cells. *Oncogene*, 24, 7775-91.
- MURRAY, P. G., LISSAUER, D., JUNYING, J., DAVIES, G., MOORE, S., BELL, A., TIMMS, J., ROWLANDS, D., MCCONKEY, C., REYNOLDS, G. M., GHATAURA, S., ENGLAND, D., CAROLL, R. & YOUNG, L. S. 2003. Reactivity with A monoclonal antibody to Epstein-Barr virus (EBV) nuclear antigen 1 defines a subset of aggressive breast cancers in the absence of the EBV genome. *Cancer Res*, 63, 2338-43.
- NEMUNAITIS, J., GANLY, I., KHURI, F., ARSENEAU, J., KUHN, J., MCCARTY, T., LANDERS, S., MAPLES, P., ROMEL, L., RANDLEV, B., REID, T., KAYE, S. & KIRN, D. 2000. Selective replication and oncolysis in p53 mutant tumors with ONYX-015, an E1B-55kD gene-deleted adenovirus, in patients with advanced head and neck cancer: a phase II trial. *Cancer Res*, 60, 6359-66.
- NEMUNAITIS, J., SENZER, N., SARMIENTO, S., ZHANG, Y. A., ARZAGA, R., SANDS, B., MAPLES, P. & TONG, A. W. 2007. A phase I trial of intravenous infusion of ONYX-015 and enbrel in solid tumor patients. *Cancer Gene Ther*, 14, 885-93.
- NEMUNAITIS, J., TONG, A. W., NEMUNAITIS, M., SENZER, N., PHADKE, A. P., BEDELL, C., ADAMS, N., ZHANG, Y. A., MAPLES, P. B., CHEN, S., PAPPEN, B., BURKE, J., ICHIMARU, D., URATA, Y. & FUJIWARA, T. 2010. A phase I study of telomerase-specific replication competent oncolytic adenovirus (telomelysin) for various solid tumors. *Mol Ther*, 18, 429-34.

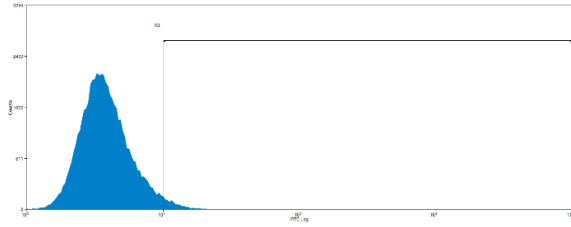
- O'SHEA, C. C., JOHNSON, L., BAGUS, B., CHOI, S., NICHOLAS, C., SHEN, A., BOYLE, L., PANDEY, K., SORIA, C., KUNICH, J., SHEN, Y., HABETS, G., GINZINGER, D. & MCCORMICK, F. 2004. Late viral RNA export, rather than p53 inactivation, determines ONYX-015 tumor selectivity. *Cancer Cell*, 6, 611-23.
- PESONEN, S., DIACONU, I., KANGASNIEMI, L., RANKI, T., KANERVA, A., PESONEN, S. K., GERDEMANN, U., LEEN, A. M., KAIREMO, K., OKSANEN, M., HAAVISTO, E., HOLM, S. L., KARIOJA-KALLIO, A., KAUPPINEN, S., PARTANEN, K. P., LAASONEN, L., JOENSUU, T., ALANKO, T., CERULLO, V. & HEMMINKI, A. 2012. Oncolytic immunotherapy of advanced solid tumors with a CD40L-expressing replicating adenovirus: assessment of safety and immunologic responses in patients. *Cancer Res*, 72, 1621-31.
- REICHARD, K. W., LORENCE, R. M., CASCINO, C. J., PEEPLES, M. E., WALTER, R. J., FERNANDO, M. B., REYES, H. M. & GREAGER, J. A. 1992. Newcastle disease virus selectively kills human tumor cells. *J Surg Res*, 52, 448-53.
- RIES, S. & KORN, W. M. 2002. ONYX-015: mechanisms of action and clinical potential of a replication-selective adenovirus. *Br J Cancer*, 86, 5-11.
- ROJAS, J. J., GUEDAN, S., SEARLE, P. F., MARTINEZ-QUINTANILLA, J., GIL-HOYOS, R., ALCAYAGA-MIRANDA, F., CASCALLO, M. & ALEMANY, R. 2010. Minimal RB-responsive E1A promoter modification to attain potency, selectivity, and transgene-arming capacity in oncolytic adenoviruses. *Mol Ther*, 18, 1960-71.
- ROSEWELL, A., VETRINI, F. & NG, P. 2011. Helper-Dependent Adenoviral Vectors. *J Genet Syndr Gene Ther*, Suppl 5.
- SCARIA, A., GREGORY, R. J. & WADSWORTH, S. C. 2000. Adenoviral vectors capable of facilitating increased persistence of transgene expression. Google Patents.
- SHAYAKHMETOV, D. M., PAPAYANNOPOULOU, T., STAMATOYANNOPOULOS, G. & LIEBER, A. 2000. Efficient gene transfer into human CD34(+) cells by a retargeted adenovirus vector. *J Virol*, 74, 2567-83.
- SHIMIZU, Y., DEMETRIS, A. J., GOLLIN, S. M., STORTO, P. D., BEDFORD, H. M., ALTARAC, S., IWATSUKI, S., HERBERMAN, R. B. & WHITESIDE, T. L. 1992. Two new human cholangiocarcinoma cell lines and their cytogenetics and responses to growth factors, hormones, cytokines or immunologic effector cells. *Int J Cancer*, 52, 252-60.
- STANTON, R. J., MCSHARRY, B. P., ARMSTRONG, M., TOMASEC, P. & WILKINSON, G. W. 2008. Re-engineering adenovirus vector systems to enable high-throughput analyses of gene function. *Biotechniques*, 45, 659-62, 664-8.
- STEVAUX, O. & DYSON, N. J. 2002. A revised picture of the E2F transcriptional network and RB function. *Curr Opin Cell Biol*, 14, 684-91.
- STEVENSON, S. C., ROLLENCE, M., WHITE, B., WEAVER, L. & MCCLELLAND, A. 1995. Human adenovirus serotypes 3 and 5 bind to two different cellular receptors via the fiber head domain. *J Virol*, 69, 2850-7.
- TOLLEFSON, A. E., RYERSE, J. S., SCARIA, A., HERMISTON, T. W. & WOLD, W. S. 1996. The E3-11.6-kDa adenovirus death protein (ADP) is

- required for efficient cell death: characterization of cells infected with adp mutants. *Virology*, 220, 152-62.
- TURNELL, A. S., GRAND, R. J. & GALLIMORE, P. H. 1999. The replicative capacities of large E1B-null group A and group C adenoviruses are independent of host cell p53 status. *J Virol*, 73, 2074-83.
- TURNER, J. G., RAKHMILEVICH, A. L., BURDELYA, L., NEAL, Z., IMBODEN, M., SONDEL, P. M. & YU, H. 2001. Anti-CD40 antibody induces antitumor and antimetastatic effects: the role of NK cells. *J Immunol*, 166, 89-94.
- VAN DEN HEUVEL, S. & DYSON, N. J. 2008. Conserved functions of the pRB and E2F families. *Nat Rev Mol Cell Biol*, 9, 713-24.
- VIGNE, E., MAHFOUZ, I., DEDIEU, J. F., BRIE, A., PERRICAUDET, M. & YEH, P. 1999. RGD inclusion in the hexon monomer provides adenovirus type 5-based vectors with a fiber knob-independent pathway for infection. *J Virol*, 73, 5156-61.
- WANG, H., LI, Z. Y., LIU, Y., PERSSON, J., BEYER, I., MOLLER, T., KOYUNCU, D., DRESCHER, M. R., STRAUSS, R., ZHANG, X. B., WAHL, J. K., 3RD, URBAN, N., DRESCHER, C., HEMMINKI, A., FENDER, P. & LIEBER, A. 2011. Desmoglein 2 is a receptor for adenovirus serotypes 3, 7, 11 and 14. *Nat Med*, 17, 96-104.
- WANG, H., LIAW, Y. C., STONE, D., KALYUZHNIY, O., AMIRASLANOV, I., TUVE, S., VERLINDE, C. L., SHAYAKHMETOV, D., STEHLE, T., ROFFLER, S. & LIEBER, A. 2007. Identification of CD46 binding sites within the adenovirus serotype 35 fiber knob. *J Virol*, 81, 12785-92.
- WIEDMANN, M., FEISTHAMMEL, J., BLUTHNER, T., TANNAPFEL, A., KAMENZ, T., KLUGE, A., MOSSNER, J. & CACA, K. 2006. Novel targeted approaches to treating biliary tract cancer: the dual epidermal growth factor receptor and ErbB-2 tyrosine kinase inhibitor NVP-AEE788 is more efficient than the epidermal growth factor receptor inhibitors gefitinib and erlotinib. *Anticancer Drugs*, 17, 783-95.
- WOLD, W. S., HERMISTON, T. W. & TOLLEFSON, A. E. 1994. Adenovirus proteins that subvert host defenses. *Trends Microbiol*, 2, 437-43.
- YEW, P. R., LIU, X. & BERK, A. J. 1994. Adenovirus E1B oncoprotein tethers a transcriptional repression domain to p53. *Genes Dev*, 8, 190-202.
- ZHAN, J., GAO, Y., WANG, W., SHEN, A., ASPELUND, A., YOUNG, M., LAQUERRE, S., POST, L. & SHEN, Y. 2005. Tumor-specific intravenous gene delivery using oncolytic adenoviruses. *Cancer Gene Ther*, 12, 19-25.
- ZOU, W., LUO, C., ZHANG, Z., LIU, J., GU, J., PEI, Z., QIAN, C. & LIU, X. 2004. A novel oncolytic adenovirus targeting to telomerase activity in tumor cells with potent. *Oncogene*, 23, 457-64.

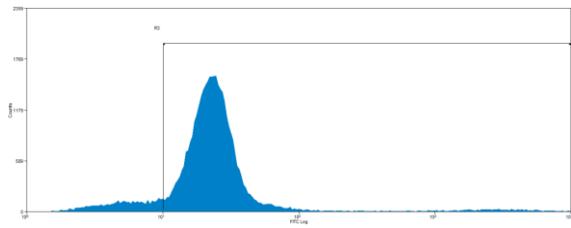
Appendix

1. Flow cytometry experiments

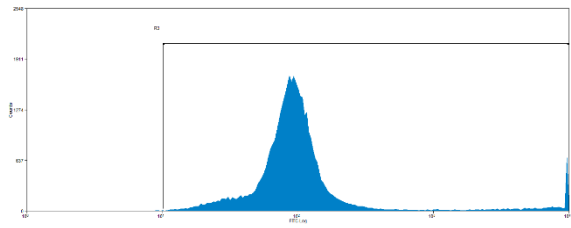
A.



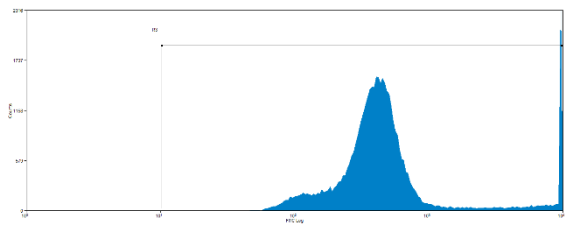
Un-infected control



MOI=2vp/cell (0.145 IU/cell)



MOI=4vp/cell (0.29 IU/cell)



MOI=8vp/cell (0.58 IU/cell)

B.

A549 RC virus ACE 48hr



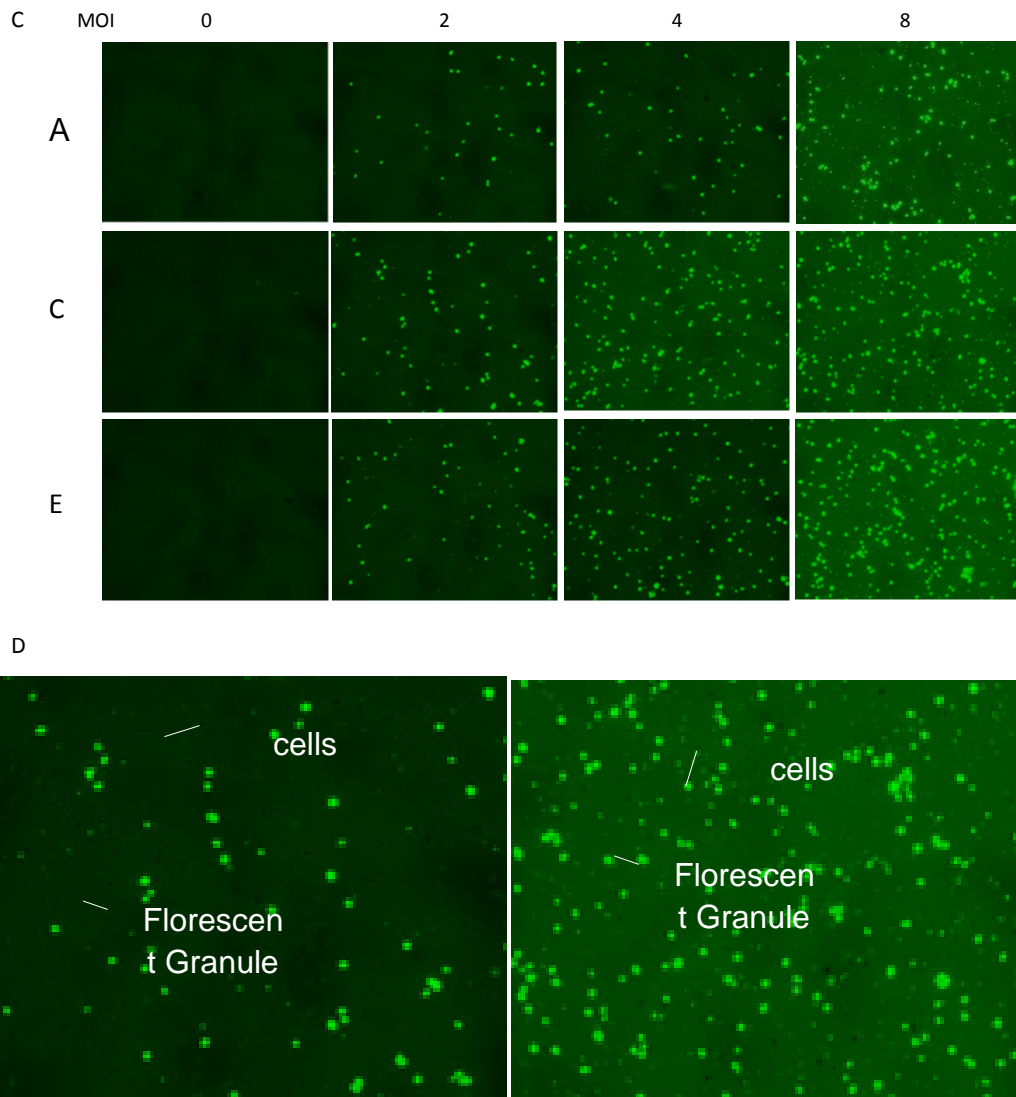


Figure A1. hTERTp-E1A, WTp-E1A Δ 24 and E2F1p-E1A Δ 24 viruses replication in A549 cells

The histograms of A549 infected by virus A 2vp, 4vp, 8vp/cell (A) Fluorescent photos for attached cells before harvesting (B) Fluorescent photos for suspended cells after harvesting (C) Zoon-in presentation of C 4vp/cell and 8vp/cell of suspended cell fluorescent photos (D)

2. Co-infection experiments

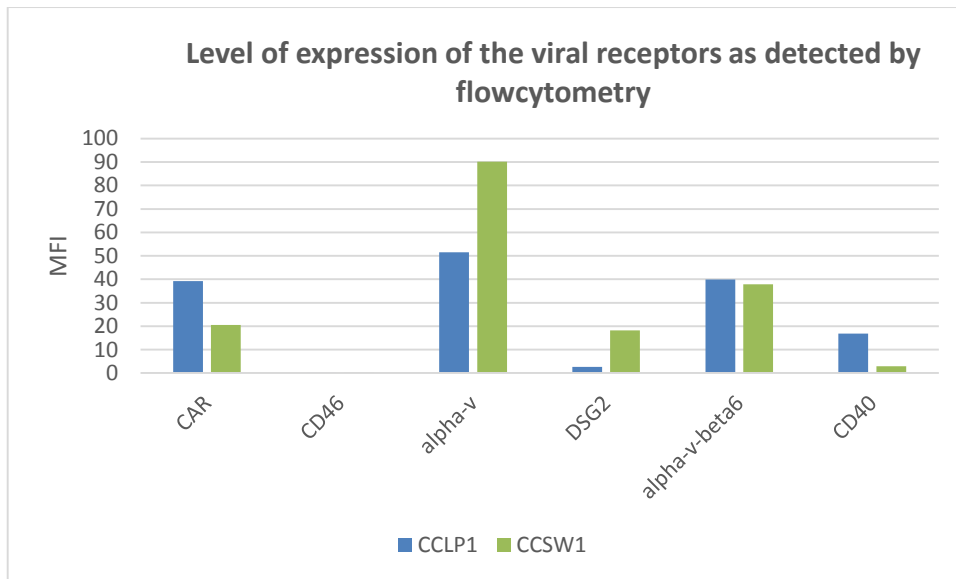


Figure A2. The expression level of receptors on cell surface

3. MTT assays

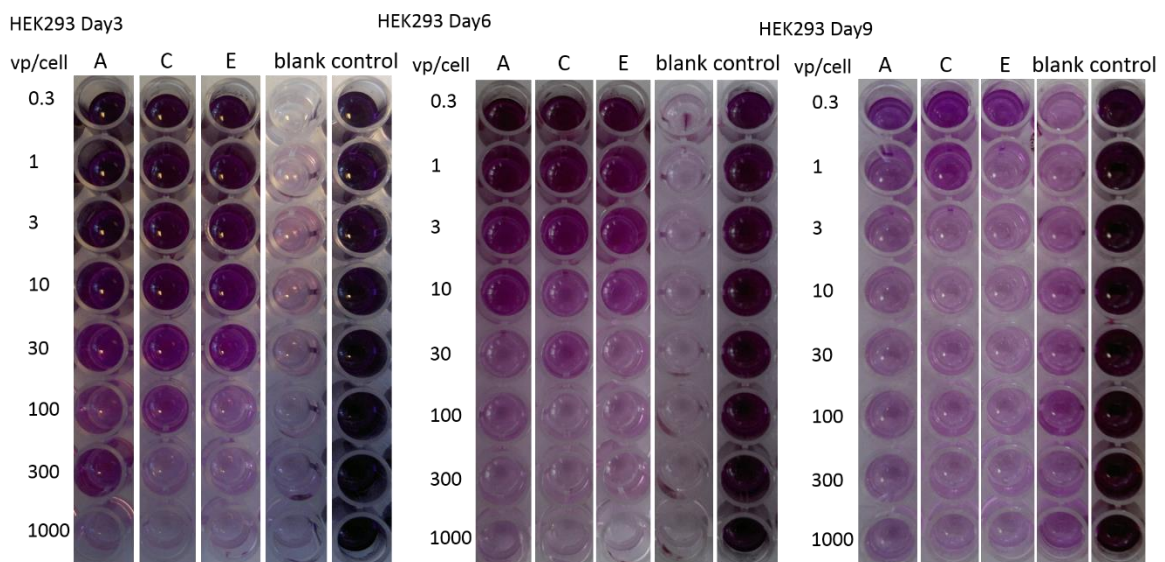


Figure A3. MTT assay for CCLP cells

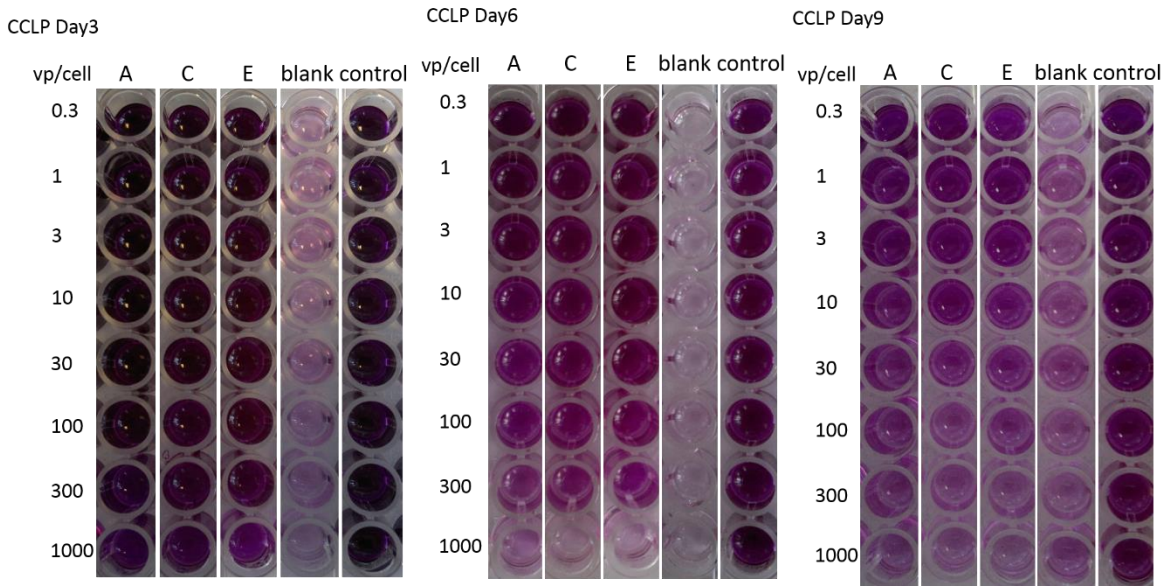


Figure A4. The MTT assay for CCLP cells

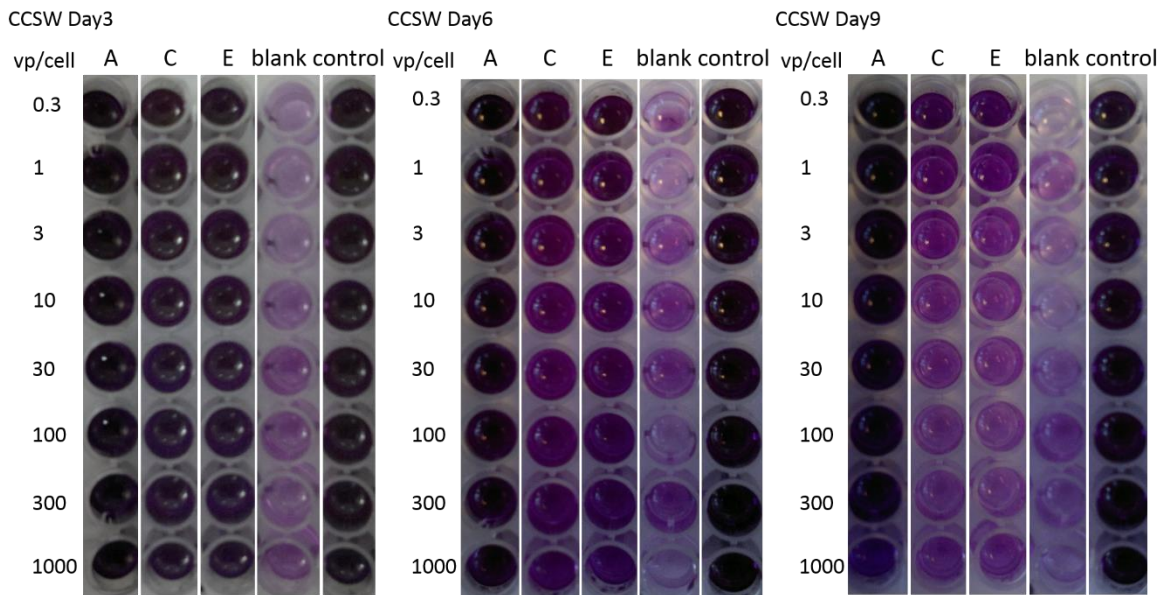


Figure A5. MTT assay for CCSW cells

4. Coinfection experiment

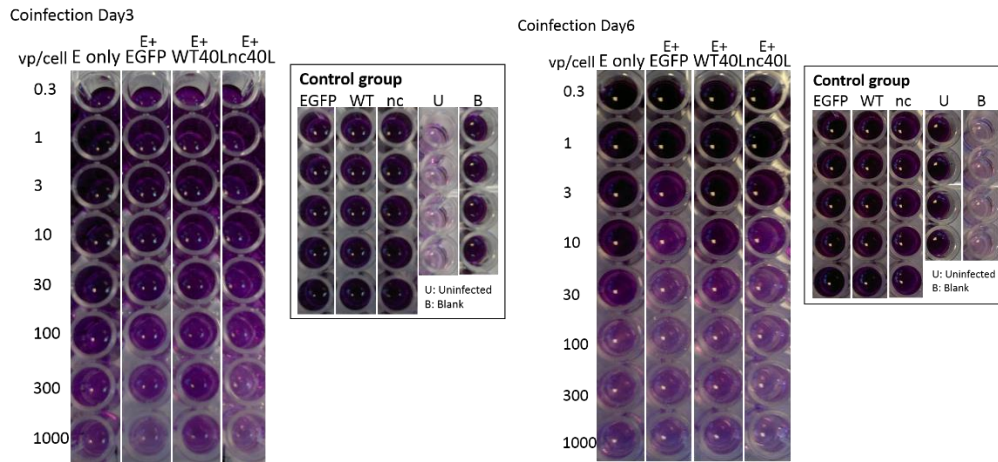
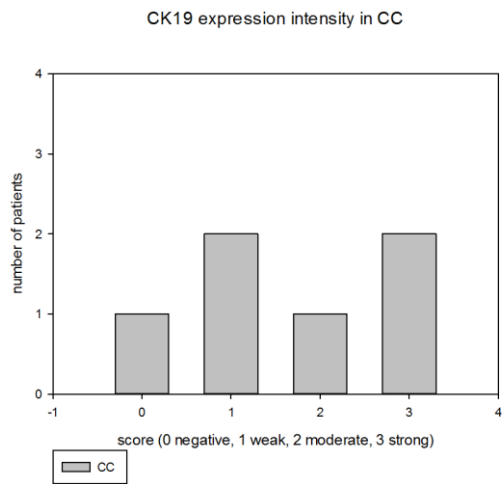


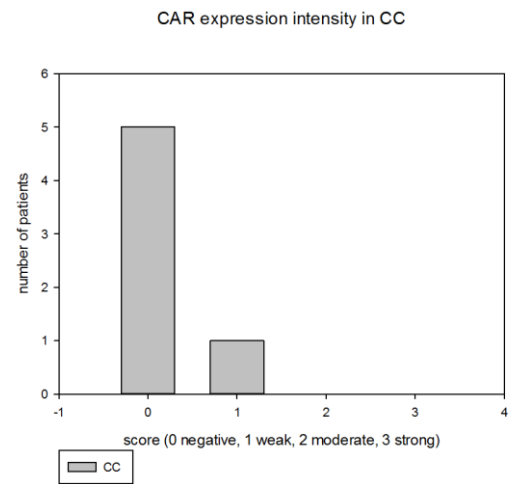
Figure A6. The MTT assay of co-infection experiment

5. Immunohistochemistry staining

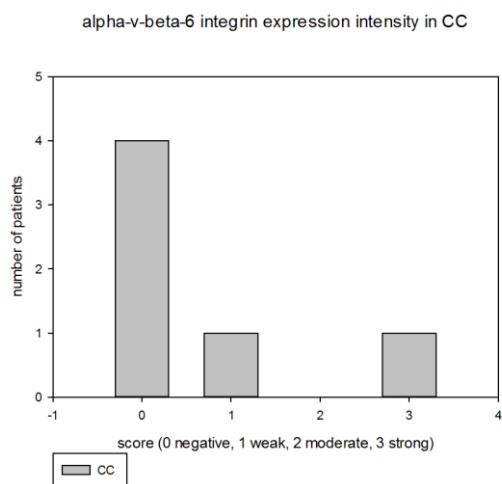
A



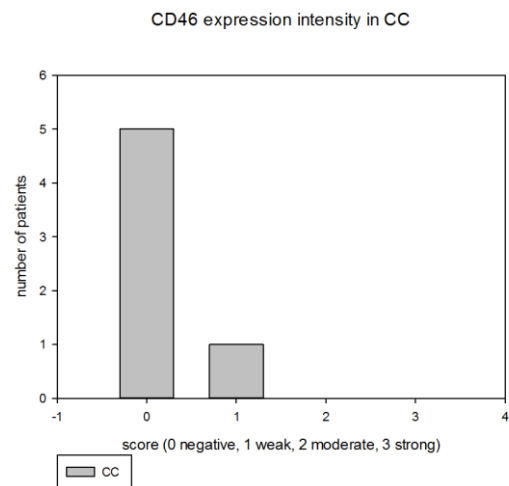
B



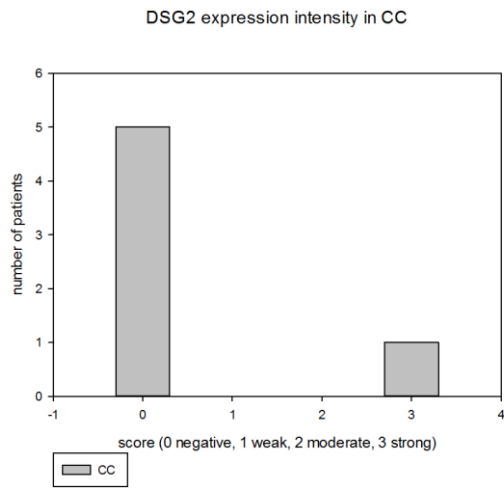
C



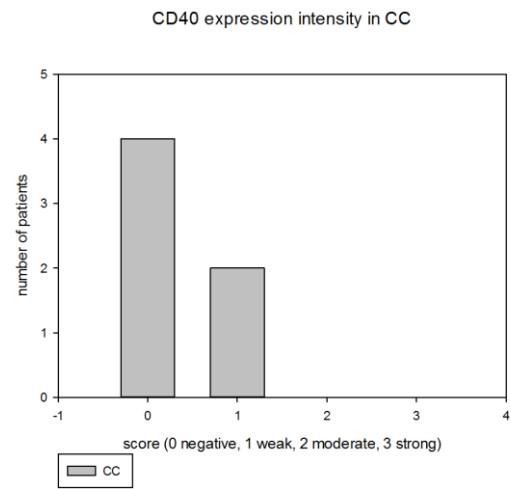
D



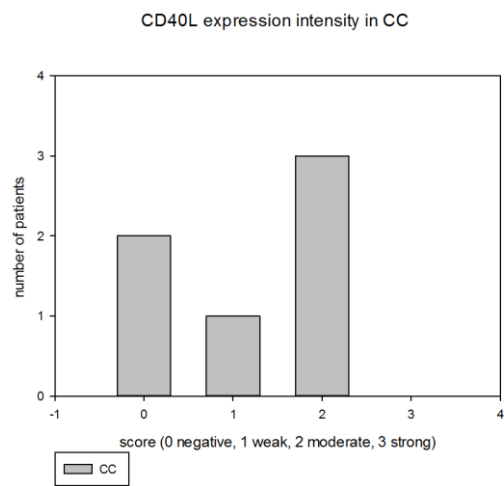
E



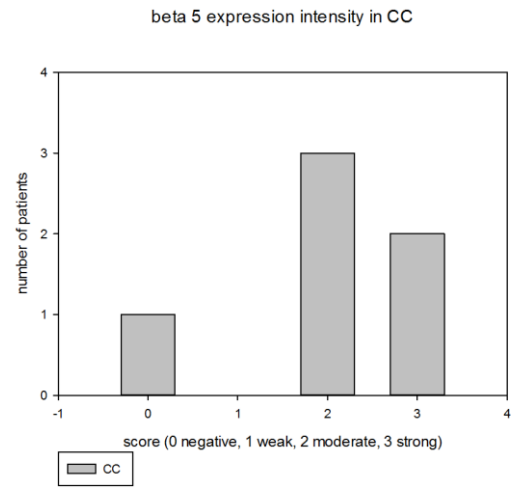
F



G



H



I

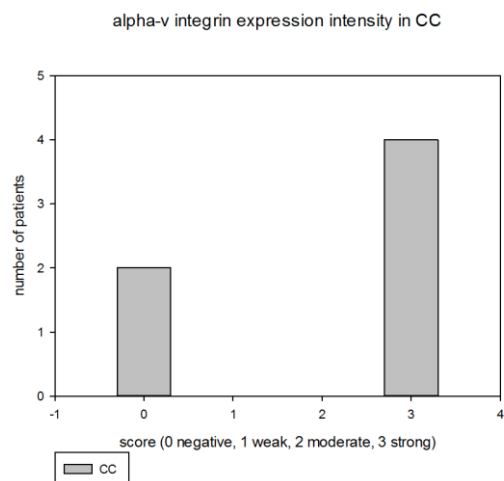


Figure A7. The expression level of receptors in cholangiocarcinoma patients

(A) CK19 (B) CAR (C) $\alpha\beta 6$ (D) CD46 (E) DSG2 (F) CD40 (G) CD40L (H) $\beta 5$ (I) αv
 X axis represents the strength of the signal (scores: 0 negative, 1 weak, 2 moderate, 3 strong), and Y axis symbolizes the number of CC patients.